Lola

Development of a smart knee-wearable for osteoarthritis patients

Detecting acoustic emissions and temperature changes

M.M. (Manon) van der Stap
Master's Thesis
Integrated Product Design, TU Delft
March 2026

Author

M.M. (Manon) van der Stap

Master thesis

Delft University of Technology

Faculty of Industrial Design Engineering

MSc Integrated Product Design

March 31st, 2026

Supervisory team

Chair

Prof.dr.ir. K.M.B. (Kaspar) Jansen

Department Sustainable Design Engineering,

Section Emerging Materials

Mentor

Ir. S.H. (Stephanie) Gieles

Department Human-Centered Design

Section Design Aesthetics

Preface

Dear reader,

This report presents the research I've conducted over the past seven months, which I've pursued with great enthusiasm. During this project, I've learned a great deal about textiles, electronics, osteoarthritis, and more, bringing these together in a smart knee-wearable called Lola, short for Long-term Osteoarthritis Logging Assistant.

Thanks to Kaspar Jansen and Stephanie Gieles for guiding me through this project and for their helpful feedback and insightful comments along the way. I also want to thank everyone at Applied Labs for always being willing to answer my questions about electrical or textile-related topics. Marienke van Middelkoop, an expert in osteoarthritis, and Jérôme Paul Rémy Thevenot, who focuses on wearables for osteoarthritis, also contributed substantially through their expertise.

Lastly, thank you to all my family and friends for their support and for offering fresh perspectives throughout the process.

Manon

Abstract

Osteoarthritis (OA) is a joint disease that causes cartilage degeneration, stiffness, and unpredictable, painful flare-ups. Current diagnostic methods provide only clinical snapshots. This leaves a lack of continuous insight into symptom changes in daily life. This project was driven by the hypothesis that elevated localised skin temperature and more frequent or intense acoustic joint emissions (crepitus) could indicate a flare-up and increased pain. To test this, a non-invasive smart wearable needed to be developed. By continuously measuring thermal and acoustic signals in daily life, this smart knee-wearable aims to objectively detect flare-ups and, in the future, bridge the gap between subjective pain and objective clinical data.

To achieve this goal, the Double Diamond design methodology was applied. After a discovery phase of literature research and expert interviews, a Programme of Requirements was established in the define phase. An iterative design process was followed for the development phase. Ideas were explored in Virtual Reality, and physical prototypes were made. These iterations were tested for technological feasibility and comfort, with input from both healthy individuals and OA patients.

The resulting prototype is a comfortable, breathable knee sleeve made of a spandex-like material. The design has an open kneecap and knee hollow for optimal freedom of movement. With silicone anti-slip elastic to keep it in place. Integrated technology includes a XIAO ESP32-S3 microcontroller, SD card module, MEMS microphone, and several NTC temperature sensors. Conductive yarn, stitched in a zigzag stitch, enables seamless, flexible integration of components.

The validation showed that the wearable effectively records the desired data. During controlled movements, the acoustic algorithm distinguished a healthy knee from an OA knee, but continuous walking and friction from long trousers caused mechanical noise in the sound data. The temperature sensors also accurately recorded physiological heat changes. Furthermore, the wearable scored highly for comfort. Test subjects reported forgetting they wore it within 30 minutes. However, patients also reported that a wraparound model would be easier to put on and is an area for improvement.

In conclusion, developing a non-invasive wearable to measure crepitus and temperature for patients with OA is feasible. Although it is not a market-ready medical product, and noise-reduction software still needs refinement, this proof-of-concept shows that continuous, objective monitoring of osteoarthritis in daily practice is possible and valuable, provided that several aspects of the wearable are further investigated and optimised.

Disclosure of AI: Google Gemini was used throughout this project to correct grammar and improve sentence structure, without altering the study's focus or intent. It also supported the coding work for this project.

Reading Guide

"This is a remark of an expert" [1]

[1] M. van Middelkoop, PhD

[2] J.P.R. Thevenot, PhD

This is a requirement

This section discusses the conclusions and the relevance for the wearable.

Throughout the project, requirements and wishes are organised into 4 categories. These categories are referred to in short via the shortcuts below:

(UR-1)	User Requirement 1
(TW-1)	User Wish 1
(TR-1)	Technical Requirement 1
(TW-1)	Technical Wish 1

Abbreviations

BLE: Bluetooth Low Energy

GS: Gravity Sketch

IRT: Infrared thermography

KL: Kellgren and Lawrence

Lateral: Further from the body's midline

Medial: Closer to the body's centreline

MEMS: Microelectromechanical systems

MRI: Magnetic Resonance Imaging

OA: Osteoarthritis

PCB: Printed Circuit Board

PoC: Proof-of-concept

UI: User Interface

UX: User Experience

VAG: Vibroarthrography

VR: Virtual Reality

XIAO: Small processor

Table of contents

Project outline

In this phase, an introduction to the project is given. The context of the wearable for knee osteoarthritis (OA) is introduced, the stakeholders involved in its development and users are identified. By clarifying who is involved and who will benefit from the wearable, better design choices can be made in later stages.

Furthermore, the core problem is framed: understanding what makes flare-ups difficult to detect and why a wearable could contribute to both research and patient well-being. From this problem, the project's main goals and ambitions are outlined.

Finally, this phase explains how the project will be approached. The design process is mapped out using the double diamond methodology, and the research and development methods relevant to this project are introduced. The purpose of this phase is therefore not to solve the problem yet, but to establish the project so that the following steps are meaningful, well-grounded, and feasible within the given timeframe.

---

1 Project introduction

This chapter provides an introduction to osteoarthritis (OA) and its need for a smart wearable. Also, the stakeholders will be introduced.

1.1 Introduction

This project focuses on the design of a smart wearable for individuals with osteoarthritis (OA). OA is a degenerative joint disease characterised by the progressive erosion of joint cartilage. This wear leads to pain, stiffness, and difficulty in movement (Artrose Gezond, 2025; World Health Organisation, 2022). OA affects a significant proportion of the population in 2023; 8 people per 100 had OA (GBD Compare, n.d.).

A common symptom of OA is the occurrence of flare-ups, periods in which the patient experiences increased pain and discomfort (Queiroga et al., 2023). Queiroga et al. (2023) reported that patients with OA experience symptoms in five areas during a flare-up. These are shown in Figure 1.

Pain, swelling, and stiffness appear to be direct observations, whereas psychological aspects and symptom impact are more likely to be consequences. Patients have reported these domains; therefore, they are subjective.

In osteoarthritis, increased temperature and crepitus (a crackling or grinding sound caused by joint movement) are also observed in and around the joint (Kovats et al., 2024; Denoble et al., 2010). These are two variables that could be measured with sensors.

These two different aspects of OA come together in a hypothesis:

"Flare-ups described by the patient may be accompanied by increased knee temperature and crepitus." [1]

Pain during flare-ups	A distinct change in pain, that is more severe and lasts longer, that is particularly heightened with physical activity and persists with rest.
Swelling during flare-ups	A new increase in size or feeling of fullness of the joint.
Stiffness during flare-ups	Increased or prolonged stiffness of the joint that does not resolve with movement.
Psychological aspects during flare-ups	Alterations in mood, including depressive symptoms, greater anxiety, greater irritability, and/or low morale that are consequences of the symptoms during flare.
Impact of symptoms	A change in the ability to perform daily activities, requiring new adaptation and strategies due to the increase in pain, swelling, stiffness, fatigue and sleep disturbance related to the flare.

Figure 1: Symptoms of flare-ups (Queiroga et al., 2023)

To measure this, a wearable could be used to monitor temperature increases and crepitus around the joint. Since flare-ups are difficult to predict (Thomas et al., 2022; Queiroga et al., 2023), it is important that the wearable is non-invasive and can be worn every day.

This wearable will be designed in this report. The aim is to support prospective research that links patients' subjective observations of OA to objective measurements.

Gap

Currently, no projects or products have developed a knee-wearable specifically designed to detect flare-ups in knee OA for everyday use by patients. The company Sensemodi has created a similar wearable, but it is relatively bulky, making it less suitable for everyday use. This highlights the need for a non-invasive, lightweight solution that can be worn comfortably throughout the day.

Future outcomes

A potential outcome is that the wearable can detect flare-ups before the patient experiences pain, allowing them to take their medication on time and preventing flare-ups early and causing less damage. For this, there is also a hypothesis:

"Flare-ups can be suppressed and cause less damage if medication is administered earlier." [1]

The rationale is that intenser flare-ups damages more tissue in the joint, requiring more energy and longer to restore the tissue to its original state. If flare-ups could be detected earlier, patients would be able to initiate medication sooner, reducing damage.

This is supported by Thomas et al. (2019), who recognise that the early signs of a flare-up could help patients take medication in time to suppress the flare-up, potentially reducing symptom severity and improving quality of life.

1.2 Goal

The goal of this project is to develop a proof-of-concept, non-invasive knee-wearable for OA patients that can detect temperature and crepitus. This prototype will be tested in simulated situations. And validated by a panel of OA patients. The wearable will include sensors to monitor both crepitus sound and knee skin temperature.

Focus

The focus of this project will be on developing a knee-wearable that can detect knee sounds (crepitus) and temperature changes in the knee for OA patients.

An additional focus is the integration of conductive yarns to connect sensors and assess their ability to detect temperature changes.

Deliverable

The deliverable will include the final report, a works-like prototype with integrated acoustic and temperature sensors, a feels-like prototype for comfort testing, and a looks-like render.

Market and planning

This project focuses on smart textiles in the health sector. It addresses the initiation of a larger research project. Using this wearable, the hypotheses can be tested. If the outcome is positive, further research can be conducted to determine whether the wearable can detect flare-ups beforehand.

1.3 Stakeholders

This project involves multiple stakeholders (Figure 2). At the core are OA patients, who will directly use the wearable to monitor knee crepitus sounds and skin temperature in daily life. With this wearable, further research on OA can be conducted, and patients will ultimately benefit from the resulting findings. If research on the hypothesis yields interesting insights, flare-ups may be detected early, medication can be started early, and the pain will not be as long or as severe as when no flare-up is detected.

Researchers are close to the core, since they need a wearable that can be used in investigating their hypothesis. In the long term, they can collect data to inform treatment decisions and track disease progression. So, they learn more about OA and develop optimised treatment plans for the patient.

Since this project is still in the proof-of-concept phase, these two stakeholders have been the primary focus. Some other stakeholders are out of scope but warrant brief mention.

At the secondary level, if the hypothesis is true, doctors will also be involved; they can prescribe medication to the patient if the wearable data indicates a flare-up. Family members and caregivers benefit from early warnings and improved patient independence. Health insurers may use the wearables results to assess cost savings by preventing complications and reducing treatment intensity.

Finally, at the external level, sensor manufacturers and MedTech companies play a role in developing reliable, wearable technology, while regulators and policymakers ensure patient safety, data privacy, and compliance with medical standards.

To conclude, as the designer, I am also a stakeholder who will develop this smart knee-wearable, bringing all stakeholders together to deliver a functional proof-of-concept.

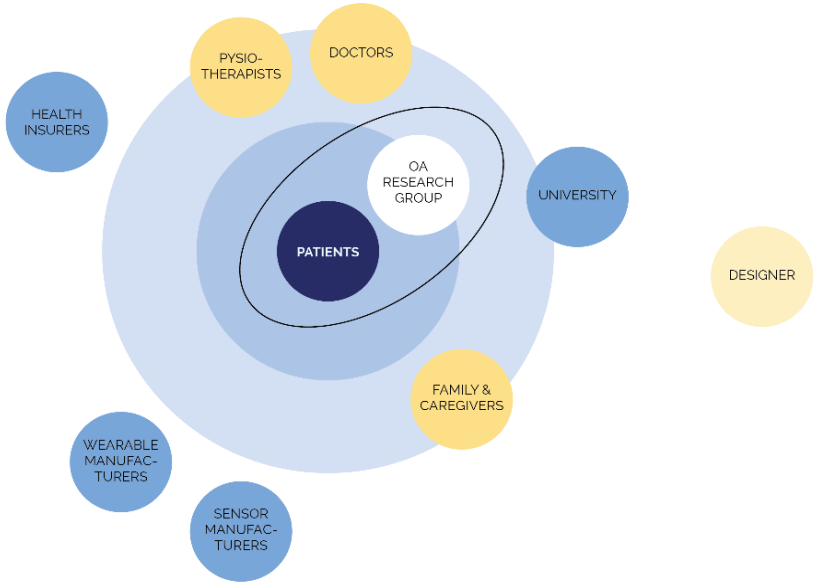

Figure 2: Stakeholders

2 Project approach

2.1 Project overview

This project was done in 100 working days. Most of the work was done at the TU Delft, and some visits were made to Erasmus MC. Feedback sessions with the coaches were held every other week.

In this project, there are 14 chapters divided into 5 main stages: The Outline, Discover, Define, Develop, and Deliver, shown in Figure 3, p. 15. These steps are based on the double diamond methodology, as described in the Delft Design Guide (Van Boeijen et al., 2020).

In this project, the process is presented in chronological order to enhance readability; however, it was iterative and not always as straightforward as it appears.

Phase 1, Outline: establishes the assignment, explains it, and discusses key factors. It also provides information on the structure of this report and the timeframe for project completion.

Phase 2, Discover: The research phase begins. Here, all project-relevant prior knowledge is addressed. Questions will be answered, including: what is osteoarthritis; what are flare-ups; how are crepitations measured; what is the difference in skin temperature; and how could this be measured?

Phase 3, Define: Phase 3 is about framing the project. Insights from phase 2 will guide the project. The project's context will be determined, and the focus will be narrowed to specific challenges, objectives, and requirements.

Phase 4, Develop: Here, the prototype and iteration process is reviewed, choices are made, and research is conducted. The iterations will be tested and developed further.

Phase 5, Deliver: In this phase, the project will be completed, and deliverables will be finalised to produce the final product. The final concept will be validated, described, the project will be presented, and recommendations will be made.

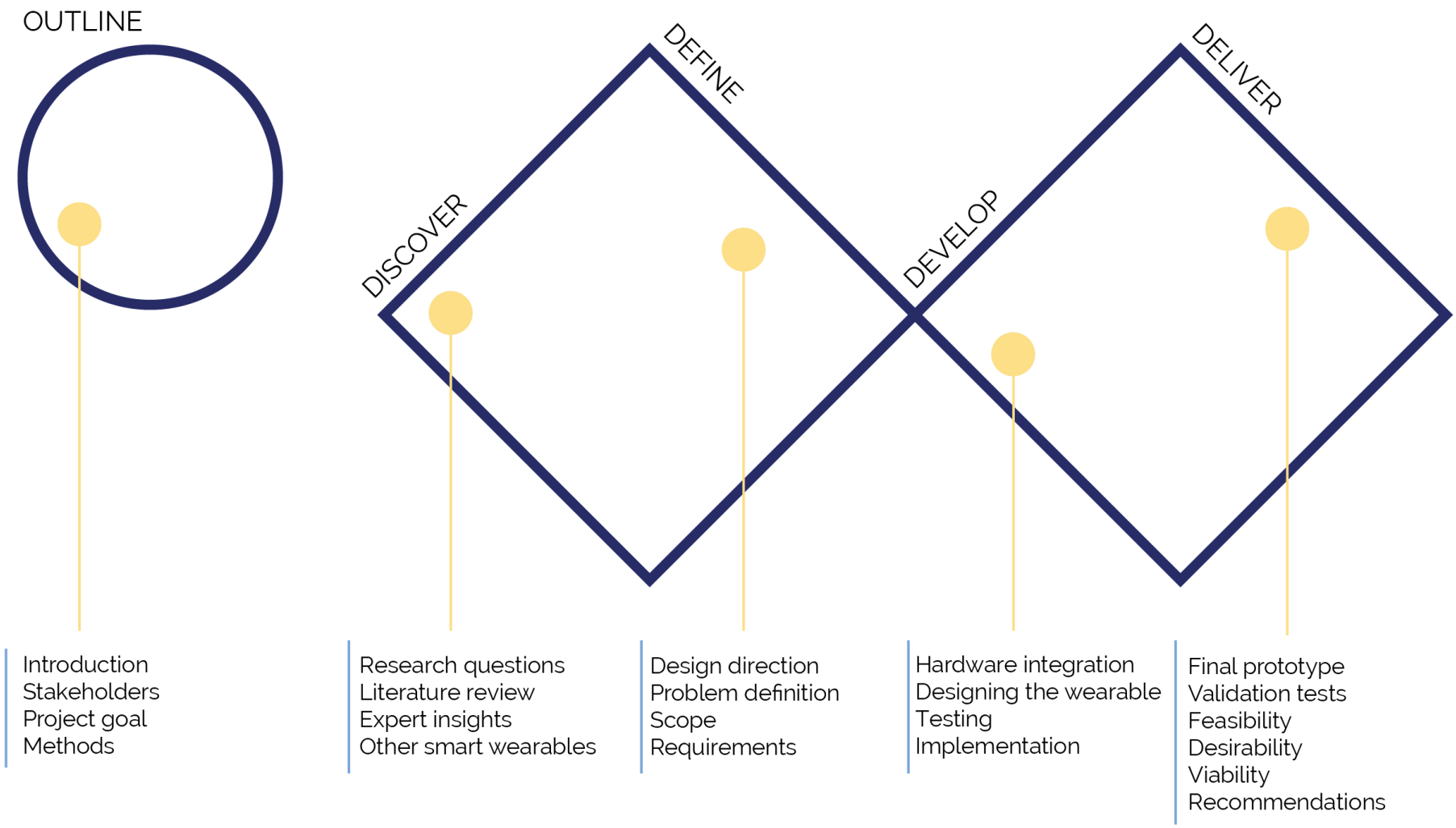

Figure 3: Project overview

2.2 Methods

The overarching method, as mentioned before, is the double diamond methodology. This is a method that first diverges in the Discovery phase, then converges and frames in the Define phase, then again diverges in the Development phase, where new ideas can bloom, and finally brings it all together in the Deliver phase.

In each phase, methods are used; they are described here.

Discover

For the Discover phase, a literature review was done, and experts were interviewed.

Define

To Define the project, a problem statement was formulated, the project scope was defined, the target group was identified, and the wearables functions were listed.

Additionally, a list of requirements was developed to guide the wearables development.

Develop

During the Development phase, various prototyping methods were employed, including VR sketching, iterative design, feedback integration, and coding.

Deliver

In the Delivery phase, the final prototypes were shown, tested, and the measured data were evaluated. Multiple participants were asked to share their thoughts on the design and the concept of a wearable for monitoring crepitus and temperature. Finally, recommendations were made for further development of the wearable.

Discover

The Discover phase begins with research questions that the literature review will answer. In the literature review, the symptoms, diagnosis, and treatment of OA are discussed. Subsequently, temperature and sound are discussed as measurable signals of OA.

Finally, other smart knee-wearables have been studied for research purposes. By gathering this knowledge, a general understanding of the situation now provides an overview of OA research, enabling better-informed decisions in the future and clarifying why the development of this wearable is so important.

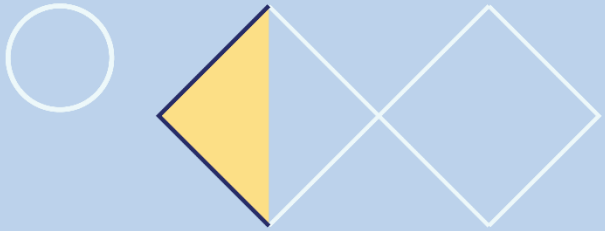

3 Research questions

To establish a foundation for the design process, a literature review was conducted. The primary objective of this review is to gain an understanding of OA and to identify the necessary design parameters for the wearable. The insights gathered in this chapter inform technical specifications, which in turn serve as the basis for the design requirements.

To guide this investigation and ensure all relevant aspects of the disease and sensing technology are covered, the following research questions were formulated:

About osteoarthritis (OA)

- What is OA, and which symptoms are associated with it?
- How is OA currently diagnosed and treated?
- How is a flare-up described, and what are its characteristics?

Measurements and sensing

- How can a flare-up be measured objectively?
- How is crepitus measured in patients with OA?
- How is skin temperature measured in patients with OA?

Technical implementation

- What specifications do sound and temperature sensors need in a knee-wearable to detect OA?
- What is the optimal placement of temperature and sound sensors on the knee for maximum signal quality and minimal artefacts?
- How do external factors such as movement and ambient temperature affect the reliability of skin temperature measurements around the knee?

The insights and specifications derived from answering these research questions form the foundation for the Development phase. Together, they provide the necessary context to further develop the wearable. In the deliver phase, the final design question will be answered, which is as follows:

Can a wearable proof-of-concept be designed to technically validate non-invasive acoustic and temperature sensing at the knee for osteoarthritis patients?

4 Literature review

4.1 Rheumatic diseases

There are many different rheumatic diseases. Many types are characterised by inflammation and degeneration of the joints, muscles, blood vessels, and organs. Rheumatism can be genetically transmitted, but environmental factors can also contribute to its development (Okada et al., 2017). There are different types of rheumatic diseases (Korzelius, 2013). A few types are shown in Figure 4.

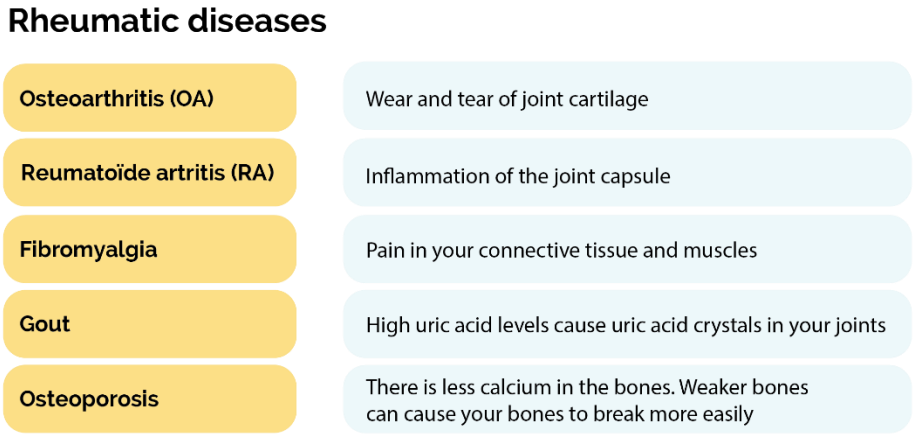

Figure 4: Common rheumatic diseases (Korzelius, 2013)

There are already many treatment options for various rheumatic diseases. However, there is no single treatment for OA that can slow disease progression (Osteoarthritis | ReumaNederland, n.d.). Currently, pharmacological treatments primarily aim to relieve the OA symptoms associated with inflammation and pain. There is no cure or disease-modifying drug for OA (Cho et al., 2021). Partly because it is not clear how the disease begins and progresses over time (Yao et al., 2023).

This is also what M. van Middelkoop confirms and what her research group is working towards: a better understanding of OA through research, thereby improving treatment. There are already many treatment methods for RA, which is why the focus on OA is so important. [1]

Because there remains considerable uncertainty surrounding OA, much research is being conducted on it. The knee-wearable was designed for these studies to provide researchers with new insight into OA development.

4.2 Osteoarthritis

This part of the Discover phase provides the medical and diagnostic rationale for designing a non-invasive wearable to monitor sound and temperature at the knee, without going into the technical specifications. It is important to note that most of this subchapter is prior knowledge, so a general view of OA could be developed.

4.2.1 What is osteoarthritis (OA)?

OA is the most common form of rheumatic disease. OA affects the joints, and cartilage within the joint changes. Cartilage becomes thinner and eventually may break down; as a result, the bones begin to rub against each other. When bones rub against each other, the bone beneath the cartilage can change. Bumps can develop at the edges; these bumps are called osteophytes. This process leads to pain, stiffness, and swelling in the affected joints (Artrose | Reuma Nederland, n.d.). In Figure 5, a healthy knee is compared to an OA knee.

OA is not only the breakdown of cartilage, but it also involves the joint structure surrounding the joint. Changes occur in the subchondral bone, synovium, ligaments, and periarticular muscles. As a result, OA is a complex, multifactorial condition (Loeser, 2009). Inflammatory processes in the joint also contribute to pain and disease progression (Hunter & Bierma-Zeinstra, 2019).

Certain patient groups are at increased risk of developing OA. These include individuals with a history of knee injuries, people with obesity, and those whose occupations involve prolonged sitting or standing. Such factors place additional mechanical or metabolic stress on the joints, accelerating the degenerative process (Karpiński et al., 2024).

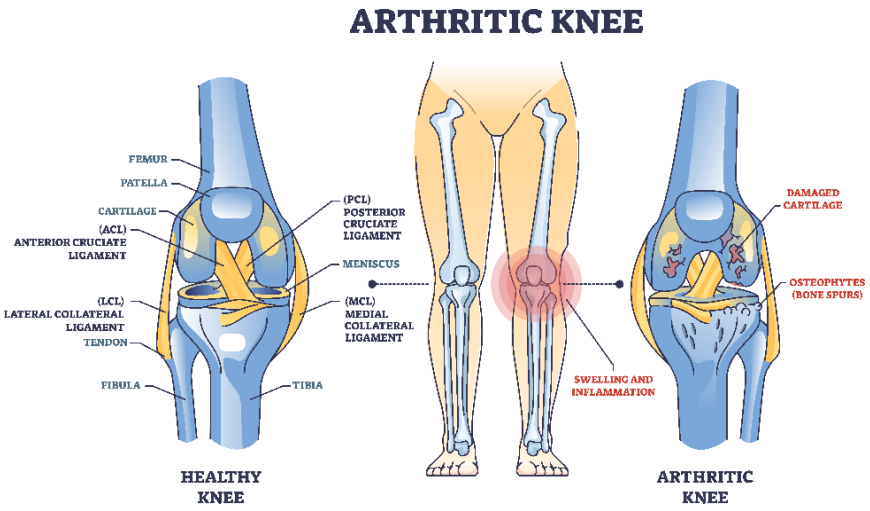

Figure 5: Healthy knee vs OA knee

4.2.2 Symptoms

Symptoms of OA are joint pain, stiffness, reduced mobility, and functional limitations. These symptoms can worsen over time and can differ in intensity. There may be periods with less or no pain, or periods of increased pain (flare-ups). Pain in OA not only results from cartilage loss but also from changes in the surrounding structures (Hunter et al., 2008).

Pain in OA arises from both peripheral and central sensitisation. Peripheral sensitisation occurs around the joint, where, through inflammation and tissue damage, nociceptors respond faster than usual. As a result, normal stimuli may cause pain. Central sensitisation increases the sensitivity of the central nervous system. If pain persists or recurs frequently, the nerve pathways become overstimulated, amplifying the pain signals. Someone can feel pain even without a stimulus. As a result, the measured severity of OA may not correspond to the patient's subjective experience (Hunter et al., 2008).

Other symptoms of OA are crepitus and a rise in temperature around the joint. These symptoms will be discussed in greater detail later.

4.2.3 Diagnosis of OA

The diagnosis is based on a combination of clinical symptoms, physical examination, and imaging techniques. X-rays, for example, can detect joint space narrowing, osteophyte formation, and changes in the subchondral bone (Hunter & Bierma-Zeinstra, 2019). For diagnosis, imaging alone is insufficient, as symptoms and radiographic changes do not always align (Katz et al., 2021).

Karpiński et al. (2024) compares various imaging techniques and diagnostic methods for knee OA, and describe their advantages, disadvantages, and limitations. An overview of the methods is provided in Table 1, p. 22. Examples include X-ray, ultrasound, and MRI. Additionally, vibroarthrography (VAG), a new, relatively inexpensive, non-invasive tool, has been examined. All methods differ in sensitivity, cost, accessibility, and suitability for early-stage detection.

"Different diagnostic methods have different criteria to consider." [1]

Table 1: Imagining techniques (Karpiński et al., 2024)

Method	Cost	Availability	Detection of the early stage	What is measured	Qualification	Advantage	Disadvantage
Radiography (X-ray)	Low	High	No	Joint space narrowing.	-	Time.	(Low) Exposure to ionising radiation. Unable to diagnose small cartilage changes.
Computed Tomography (CT)	High	-	No	Estimating signs of its damage based on bone changes.	-	High resolution (detailed).	Time. Can not detect early stages. Dose ionising radiation. Allergic reactions.
Ultrasound	Low	High	-	Visualise the structure of the knee joint detects soft tissue.	Quality depends on the sonographer's experience.	Lack of radiation. Dynamic examination. Ability to assess inflammation.	No high-quality image. Can not go through bones.
Magnetic Resonance Imaging (MRI)	High	Low	It is most effective to detect OA.	Thickness of the cartilage repair layer. Structure of the repaired cartilage with the sub-chondral bone. Presence of cysts or fibrosis.	Required specialised equipment and personnel.	High resolution 3d imaging. Detection of damage to cartilage. Menisci ligaments.	Time-consuming. Complex.
Vibroarthrography (VAG)	Low	-	Can detect micro-damage before it is visible on MRI.	Elements moving relative to each other emit oscillations and vibrations caused by friction.	-	Provides information about the condition of the moving joint. Repeatability. Speed. No radiation.	No detected equipment. No test protocols.

OA can occur at different grades, as defined by the imaging technique. For radiographic findings, the Kellgren & Lawrence (KL) grading system is most used. This system helps physicians assess the severity of joint degeneration and guide treatment decisions (Kohn et al., 2016). The KL system defines five grades:

- Grade 0: No OA.
- Grade 1: Doubtful narrowing of joint space and possible osteophyte formation.
- Grade 2: Definite osteophytes and possible narrowing of the joint space.
- Grade 3: Moderate multiple osteophytes, definite narrowing of joint space, some sclerosis, and possible deformity of bone ends.
- Grade 4: Large osteophytes, marked narrowing of joint space, severe sclerosis, and definite deformity of bone ends.

The KL classification is used in both clinical and research settings to indicate OA progression and evaluate treatment outcomes. In knee OA, radiographic imaging has an important role in diagnosis and monitoring. An example of X-ray images with different KL-grades is shown in Figure 6.

For MRI, the most widely used system is MOAKS. MOAKS is the most widely accepted semi-quantitative scoring system for knee OA (Halmandge et al., 2024). MOAKS is divided into subregions, such as medial and lateral. Each of these sub-regions receives a separate score from 0 to 3. The total score reflects the severity of OA spread in the knee (Knipe, 2020). An example of MRI images from a person with OA and from a person without OA is shown in Figure 6, the yellow line marks the outline of the bone, indicating the difference.

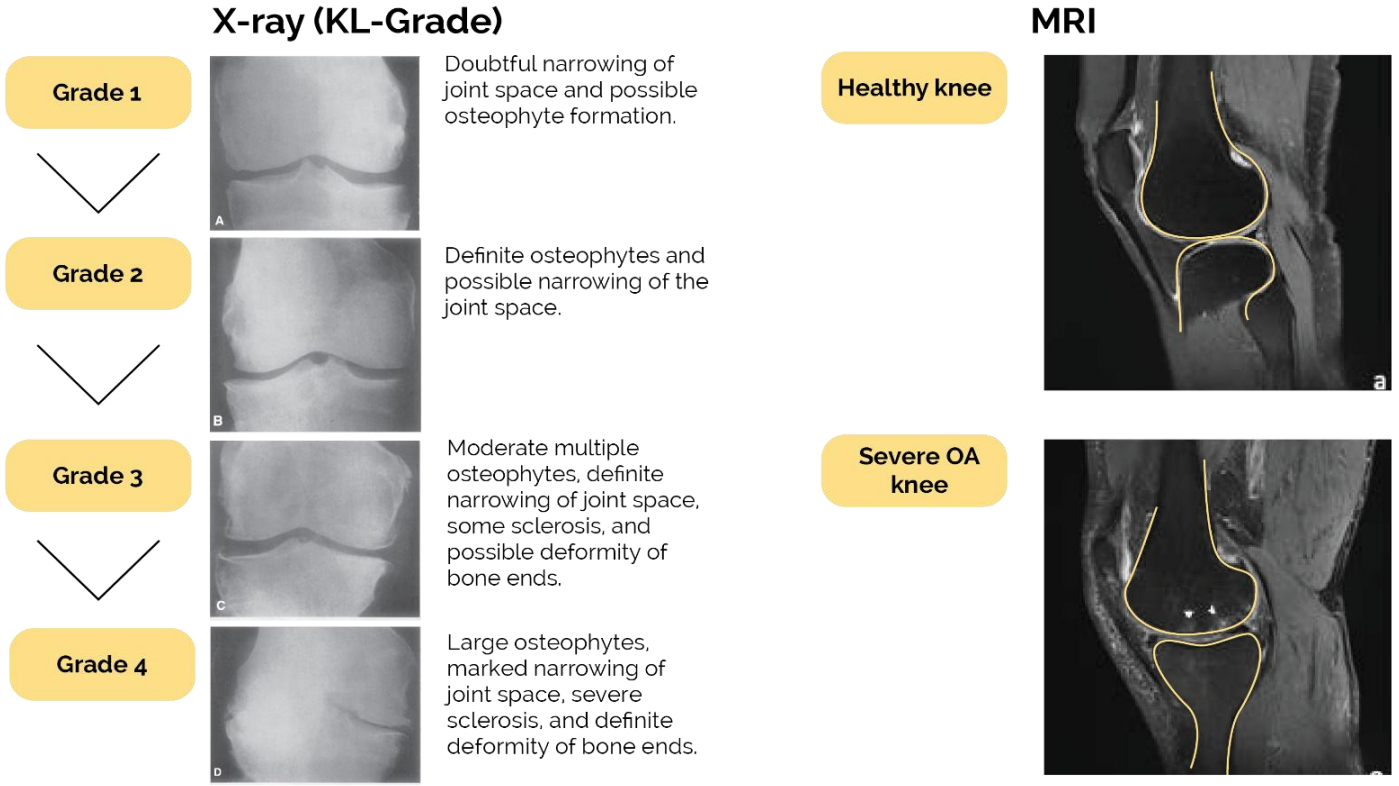

Figure 6: KL grades and MRI images (Ehmig et al., 2023; Kohn et al., 2016)

The UK National Institute for health and Care Excellence (NICE, 2022) has issued guidelines on clinical symptoms and physical examination. These guidelines provide a clinically focused approach to diagnosing and treating OA in adults. Diagnosis is based on symptoms, and treatment begins with non-pharmacological interventions. These guidelines are visualised in Figure 7.

They advise diagnosing OA based on clinical symptoms alone, without imaging. The symptoms that NICE mentions are:

- Pain during loading
- Morning stiffness lasting <30 minutes
- Reduced joint function

These symptoms are sufficient for a clinical diagnosis, particularly in individuals aged 45 years or older.

The physical examination supports the diagnosis. The following are assessed:

- Limited movement
- Crepitus
- Joint line tenderness
- Inflammation

NICE (2022) states that these signs help recognise OA and that X-rays are not standard, because they often do not correlate well with symptom severity.

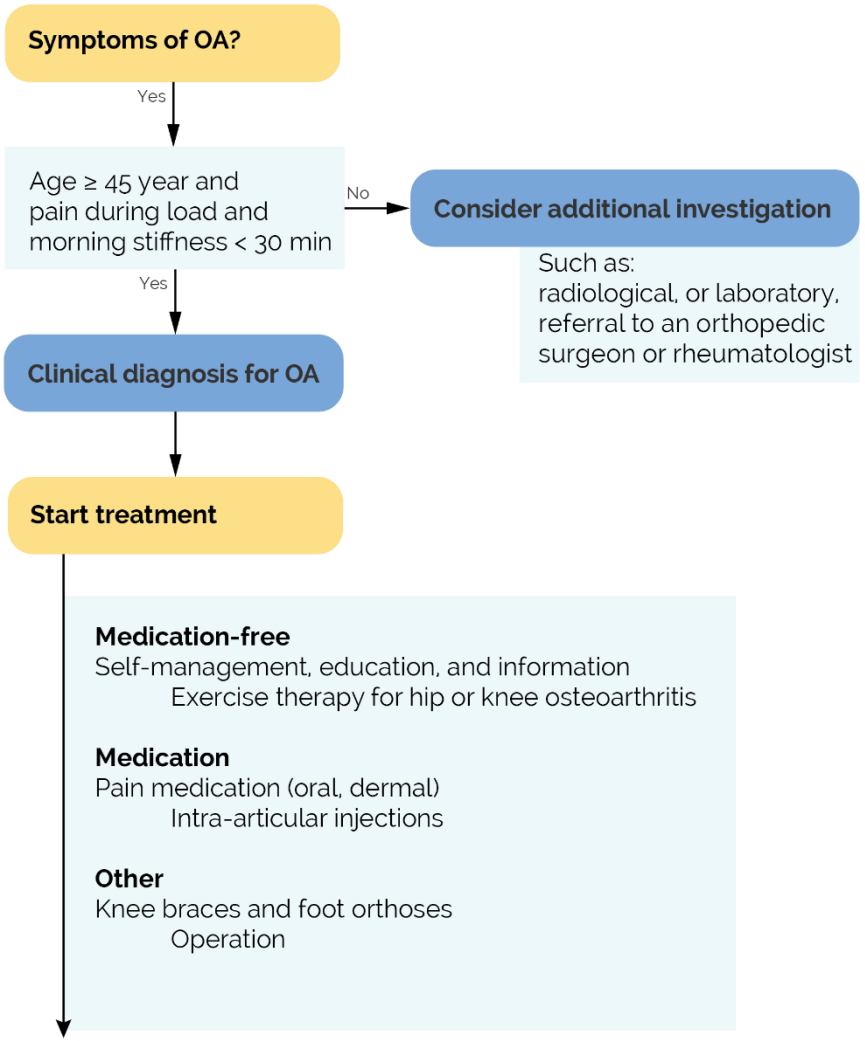

Figure 7: NICE step by step (NICE, 2022)

4.2.4 Treatment

The treatment of OA aims to reduce symptoms and improve joint function. Non-pharmacological approaches, such as weight management, exercise, and physical therapy, are implemented first. Pharmacological treatments, including pain relief and anti-inflammatory medication, are used when necessary. In some cases, a brace is prescribed to give support. Finally, in severe cases, surgical interventions such as joint replacement may be required (Katz et al., 2021; Hunter & Bierma-Zeinstra, 2019; NICE, 2022).

"The wearable that is designed does not need to have any additional supportive function; if it did, you would immediately start looking at a specific patient group." [1]

4.2.5 Flare-ups

Flare-ups are symptoms of OA (Queiroga et al., 2023). Flare-ups are sudden-onset increases in signs and symptoms that occur periodically. For the patient, this can be distressing and disabling. What triggers flare-ups can vary from patient to patient. The same applies for the impact of the flare-up and how long the flare-up persists (Thomas et al., 2022).

From a patient perspective, flare-ups in OA are experienced as discrete episodes of increased pain, often with rapid onset, that interfere with their daily activities. Despite its clinical relevance, there is currently no consensus on what constitutes a flare (Thomas et al., 2022).

The duration of a flare varies from a single day to several consecutive days. According to Thomas et al. (2022) and Queiroga et al. (2023), flare-ups involve changes across five domains: pain, swelling, stiffness, psychological distress, and overall symptom impact (Figure 8). However, flare-ups are not consistently observed across all domains, and patients experience different types of flare-ups.

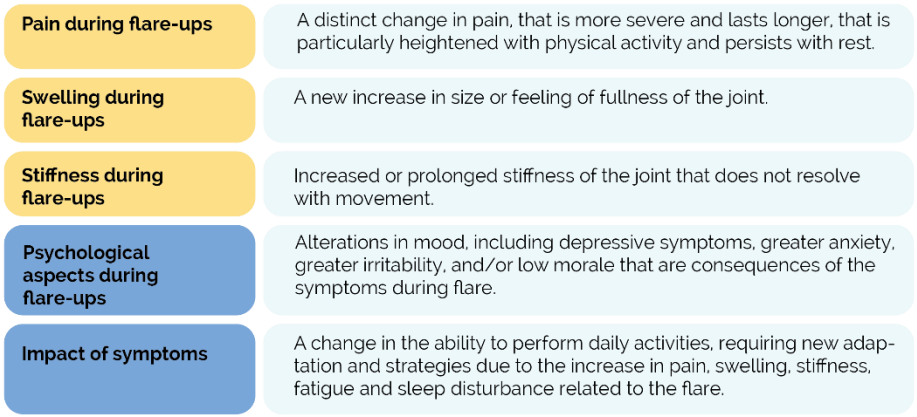

Figure 8: Symptoms of a flare-up in OA (Queiroga et al., 2023)

Parry et al. (2019) found that flare-ups are often triggered by high-intensity physical activity and typically last approximately one week. Swelling is a distinguishing feature, occurring in approximately 50% of flare days compared to 35% of non-flare days. This illustrates how OA symptoms can vary from day to day, emphasising the need for continuous non-invasive monitoring to capture these changes.

"The product would be a wearable, non-invasive device that allows you to monitor the patient throughout the day." [1]

Thomas et al. (2019) demonstrated that early pharmacological intervention, such as the timely use of anti-inflammatory painkillers, can reduce pain intensity during a flare. However, this does not work for everyone.

"Early intervention of an OA flare would be best, so less damage to the surrounding tissue can be done." [1]

OA flare management can be divided into two approaches:

Short-term management

Goal: Rapid response to flare-ups to temporarily reduce pain and functional limitations.

Examples:

- Short-term use of medication
- Temporary reduction in physical activity
- Fast access to care via digital platforms
- Patient education for self-management

Focus: Symptom control and minimising the impact of acute episodes (Thomas et al., 2022).

Long-term management

Goal: Optimise chronic care and reduce flare-up frequency.

Examples:

- Education about OA and flare-up mechanisms
- Weight loss (if applicable)
- Regular physical activity and exercise therapy
- Social support and cognitive strategies to avoid catastrophising

Focus: Lifestyle change, flare-up prevention, and long-term mobility preservation (Thomas et al., 2022).

Hypothesis

Increased crepitus and temperature are also observed in and around the joint (Kovats et al., 2024; Denoble et al., 2010). These two parameters are objective symptoms that can be measured.

"These physiological parameters (acoustic emissions and temperature changes) could serve as objective indicators of a flare-up." [1]

Although subjective flare-ups in OA are well documented and patients clearly experience periods of increased pain, stiffness and swelling (Queiroga et al., 2023), it has not yet been proven that these objective physiological markers are precisely synchronised with these flare-ups.

"The hypothesis is that changes in knee temperature and crepitus may be associated with a subjective flare-up (Figure 9)." [1]

However, it is important to emphasise that the relationship between crepitus, temperature and subjective symptoms has not yet been scientifically confirmed. This means that the so-called "objective flare-ups" in this project are an exploratory concept: they may co-occur with subjective flare-ups, but this remains to be investigated. This could be the next step after the wearable is designed in this project.

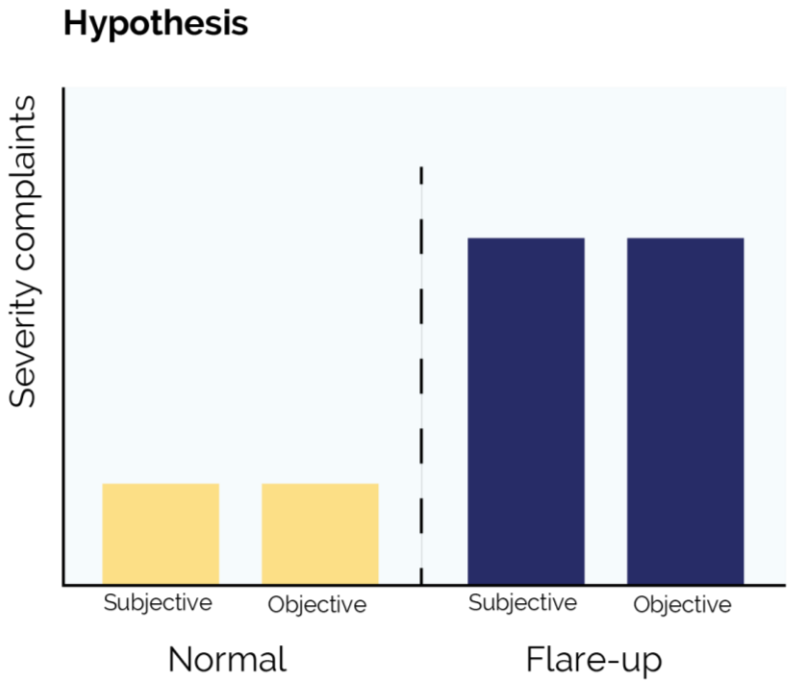

Figure 9: Hypothesis

Relevance for the wearable

From this part of the Discover phase, several implications for the project become clear:

1. Need for objective daily-life monitoring

Because symptoms fluctuate day to day, they do not consistently align with imaging results, which are snapshots. Flare-ups are now described by subjective observations (Parry et al, 2019; Hunter et al., 2008; Queiroga et al., 2023). There is a clear need for continuous, objective monitoring of physiological parameters during daily life. For this, the wearable will (in the end) be worn daily (16 hours per day, when 8 hours are for sleeping).

UI Requirement A: For prospective research, it is necessary that objective data can be visualised and that subjective symptoms can be indicated when pain occurs.

Technical Requirement A: For daily monitoring, robustness of the hardware is essential. Bumping your knee into a table should be possible without breaking the hardware.

2. Focus on flare-up detection

Flare-ups are subjective, variable, and poorly defined (Thomas et al., 2022). A wearable that records physiological changes may help researchers better understand flare-up mechanisms and, in the future, support earlier intervention for patients.

Technical Requirement B: An increase in physiological activity (crepitus and temperature) needs to be detectable.

3. Non-invasiveness is essential

Flare-ups are unpredictable (Thomas et al., 2022), so the wearable must be comfortable and unobtrusive enough to be worn all day.

User Requirements A: The wearable needs to be non-invasive and comfortable. It can be worn for at least 16 hours per day, with 8 hours reserved for sleep; it is not worn during sleep.

Technical Requirement C: To make sure the wearable is as non-invasive as possible, the hardware integrated into the wearable must be as compact as possible.

4. No additional support is needed for OA monitoring

Not in all cases is a supportive brace required for OA complaints. If the designed wearable is supportive, fewer people would be able to wear it [1].

User Requirements B: The wearable should not have supportive properties.

4.3 Physiological parameters

In this section, the focus shifts to the roles of acoustic emissions and temperature changes in understanding knee OA. The physiological background of these signals is explored, along with current diagnostic applications, sensor technologies, filtering techniques, and considerations for wearable integration.

4.3.1 Acoustic signals in knee OA

A symptom of OA is crepitus. Crepitus is the perception of grating, cracking, or popping sounds during joint movement. Also defined as a hearable grinding noise and or palpable vibrations in the knee. It results from friction between degenerated cartilage surfaces, gas bubbles in the synovial fluid, or joint instability. In a large cohort study, 44.2% of individuals with OA reported experiencing crepitus, highlighting its prevalence among symptomatic patients (Schiphof et al., 2014).

Self-reported crepitus is a simple and effective assessment tool for predicting the development of OA (Lo et al., 2017). Pazzinatto et al. (2018) demonstrated that in individuals with KL grades 1-3, the presence of crepitus was associated with an 80% likelihood of OA diagnosis.

Kovats et al. (2024) describe crepitus as a primary symptom of knee OA, underscoring its diagnostic relevance. And Teague et al. (2016) demonstrated that knees affected by OA produce distinct acoustic signatures compared to healthy joints.

These findings support the integration of acoustic monitoring into smart wearables for early OA detection and flare-up monitoring.

Vibroarthrography (VAG) as a diagnostic tool

In addition to subjective crepitus, VAG provides a quantitative method for assessing joint health. VAG involves recording and analysing the vibrations and sounds emitted by the knee joint during movement, such as flexion and extension. These signals are influenced by changes in mechanical properties, such as nodules, cracks, and cartilage defects, that occur during OA progression (Karpiński et al., 2024).

OA-affected knees emit more acoustic events with higher amplitudes and longer durations than healthy knees. This makes VAG a promising tool for early, non-invasive screening, particularly in wearable applications. Table 1 on p. 22, in Karpiński et al. (2024) compares different diagnostic methods, showing that VAG offers high diagnostic accuracy while remaining minimally invasive.

Technical implementation

Detecting VAG-signals involves three steps:

- Recording: using sensors such as accelerometers, contact microphones, or stethoscopes.
- Processing and filtering: applying band-pass filters to isolate relevant frequencies. This depends on the type of sensor you chose.
- Feature extraction: identifying patterns linked to cartilage damage or joint instability.

Filtering techniques include fixed filters (e.g., Butterworth band-pass) and adaptive filters that adjust to signal variability over time. These methods help isolate the vibroacoustic signature of OA from background noise and physiological variability (Karpiński et al., 2024).

Current placement

Karpiński et al. (2024) provided a visual of all current sensor placements in Figure 10. They also state that the medial compartment below the midline of the patella is where joint surfaces interact most directly (blue triangle, medial side). This is considered the optimal location according to Karpinski et al. (2024) because the size of the contact area between the moving surfaces of the knee joint increases sensitivity. This area provides stable contact and is less affected by motion artefacts than the lateral or posterior regions. This will be taken into account when placing the sound sensor for this project.

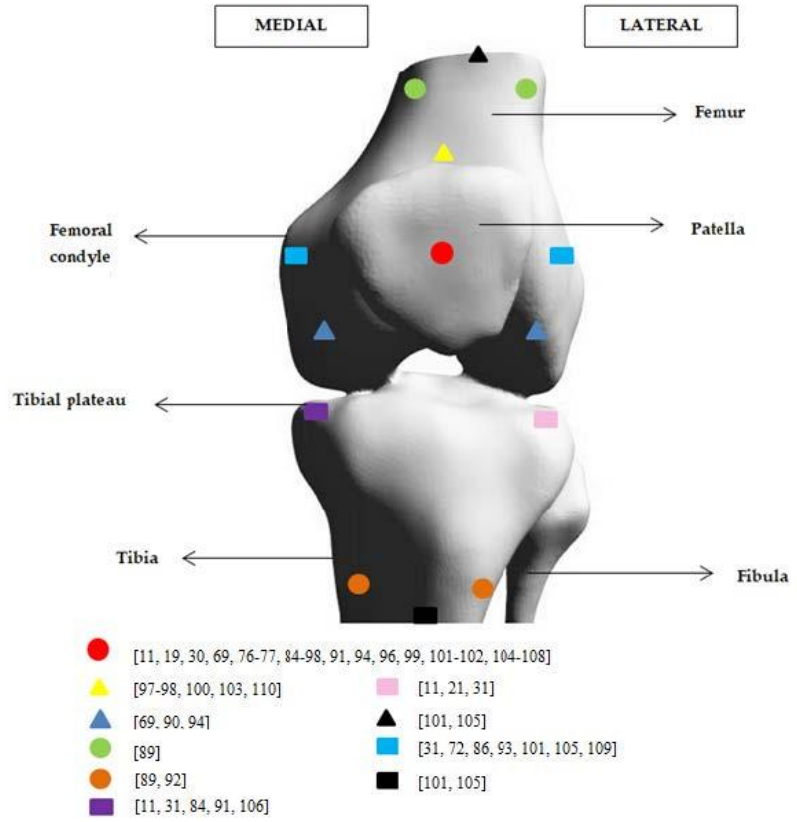

Figure 10: Placement of acoustic sensors in different research projects as referenced in Karpiński et al. (2024)

Sensors used now

To record VAG-signals, the most used sensors are accelerometers, contact microphones, and airborne microphones (Karpiński et al., 2024).

Contact microphones detect mechanical vibrations. They are characterised by the ability to record low-frequency sounds, enabling detection of microdamage in the knee. The costs are low, but they are less resistant to movement and are more easily influenced by ambient noise (Karpiński et al., 2024). Teague et al. (2016) further note that, theoretically, contact microphones yield the highest quality because they capture the original signal. However, when activity is present during practice, it can fall off the skin, and no proper signal will be detected. In their proof-of-concept, they integrated airborne microphones for this reason.

Accelerometers also detect mechanical vibrations. They are known for their accurate recording of vibrations across wide frequency ranges. Accelerometers are also resistant to mechanical interference, which can originate from the environment or from body motion (Karpiński et al., 2024). For accelerometers, sensitivity and frequency response are important. The typical bandwidth used is 10 kHz, as this is sufficient to capture relevant joint sounds (Karpiński et al., 2024).

Airborne microphones were introduced by Teague et al. (2016) in a proof-of-concept study that integrated 1 contact microphone and 2 airborne microphones. Airborne microphones capture acoustic emissions in the air. Airborne microphones do not require direct skin contact; however, the distance between the skin and the sensor should be considered. A disadvantage is that they are more sensitive to background noise. Despite this, they still recommend airborne microphones for wearables over contact microphones.

Toreyin et al. (2016) published an article about quantifying the consistency of wearable knee acoustical emission measurements during complex motions. This article was recommended by J.P.R. Thevenot as a methodology to follow. He also sent two datasheets for the sensors they used in the Sensemodi wearable, both of which were airborne microphones. [2]

Toreyin et al. (2016) used MEMS (Microelectromechanical systems) as microphones. In this article, they interpret various noises that are unwanted:

- First background noise, where most of its power is limited to 10 kHz
- Second, a stepping noise, when the patient is stepping on the floor. 90 % of this power is limited to 1.5 kHz.
- Also, rubbing noise occurs when the microphone rubs on the skin during exercise. This sound is limited to <5 kHz.

Because stepping and rubbing noises are more variable, it is difficult to universally filter them. For these reasons, a bandpass filter is recommended from 10-20 kHz, not because crepitus is only present between these frequencies, but because this zone is most ‘free’ from variable mechanical noise of background, stepping and rubbing sounds.

Teague et al. (2016) further investigated the sensing of acoustic emissions from the knee, specifically addressing the difficulties introduced by interface friction. To reliably identify short-duration, high-frequency crepitus bursts that emit continuous mechanical noise, their methodology emphasises extracting the signal's amplitude envelope. By applying envelope detection after initial bandpass filtering, transient acoustic events can be quantified and separated from the baseline noise floor. This two-step approach, frequency isolation followed by envelope extraction, forms a critical foundation for accurately processing airborne microphone data in wearable joint-health applications.

For accelerometer microphones used, the bandpass filter is much lower (1-10 kHz), whereas for airborne microphones, it is much higher (10-20 kHz). This is because accelerometers measure mechanical vibration, whereas airborne microphones measure sound waves.

An important factor in audio detection is the sampling rate. Sampling rate is the rate at which samples come in. For this, the formula of $f = \frac{1}{T}$ is given. So, if there is a sample rate of 1 sample per 1 ms (1 s = 1,000 ms), the formula would be:

$$\frac{1}{1} \times 10^{-3} = \frac{1{,}000}{1} = 1{,}000\ Hz$$

Equally important is the Nyquist frequency. This is defined as half of the sampling rate:

$$f_N = \frac{1}{2 \times \Delta t}$$

For a sampling rate of 1,000 Hz (1 ms), the Nyquist frequency is 500 Hz. This means that only frequencies up to 500 Hz can be correctly reconstructed from the sampled data. Higher frequencies will be misrepresented as lower ones, a phenomenon known as aliasing (Onajite, 2013).

If a bandpass filter with a 10 Hz-10 kHz bandwidth is used, a reliable sampling rate of 20 kHz is required. For a sample rate between 10 kHz and 20 kHz (as recommended by Toreyin et al. (2016)), a reliable 40 kHz sample rate is required.

Relevance for the wearable

From this section, several implications emerge for designing the acoustic component of the wearable:

1. Crepitus is measurable and diagnostically meaningful

This supports the integration of an acoustic sensor to monitor changes in joint function relevant to OA and potential flare-up activity (Toreyin et al., 2016).

2. VAG aligns well with wearable-based monitoring

VAG is non-invasive and suitable for daily use when small acoustic sensors are used, such as airborne microphones (Karpiński et al., 2024; Toreyin et al., 2016).

3. Sensor placement must follow clinical evidence

Placing the sensor on the medial or lateral side, just below the centre of the patella, increases sensitivity and reduces motion artefacts, improving data reliability.

Technical Requirement D: The acoustic sensor must be placed on the medial or lateral side, just below the centre of the patella.

4. Airborne microphones are a good fit for textile integration

They do not require firm skin contact, are lightweight, and have been used successfully in similar wearable OA studies (Teague et al., 2016; Toreyin et al., 2016).

5. The signal pipeline is technically feasible

With filtering in the 10-20 kHz range and a sampling rate of at least 40 kHz, airborne microphones can capture clinically relevant acoustic emissions. With filtering centred at 10-10 kHz, an accelerometer microphone should operate at a sampling rate of 20 kHz.

Technical Requirement E: The sampling rate of the acoustic sensor needs to be doubled, depending on the signal filtration, which will vary with the chosen sensor.

4.3.2 Skin temperature monitoring in knee OA

Increased knee skin temperature is another symptom of OA. Multiple studies have shown that patients with OA may have higher skin temperatures around the joint, particularly during inflammation. These are associated with flare-ups (Denoble et al., 2010; Arfaoui et al., 2012).

Petrigna et al. (2024) summarise temperature findings from various sources. While some studies report differences of 1 °C or more, others report much smaller differences of up to 0.1 °C. This supports the need for high-resolution sensing.

Temperature as a diagnostic tool

Infrared thermography (IRT) has been used to assess joint inflammation and detect thermal asymmetries in patients with OA. It is a non-invasive tool and provides clear temperature maps. In Figure 11, you can see a symptomatic knee for OA on the left and a non-symptomatic knee with OA on the right (De Marziani et al., 2024). You can see that a symptomatic knee has higher temperature measurements. **(See scale on the right of the figure, as the first impression can be misleading!)**

A disadvantage of IRT is its use in wearable applications. This is limited due to cost, bulkiness, and sensitivity to ambient conditions (Petrigna et al., 2024). Instead, contact-based

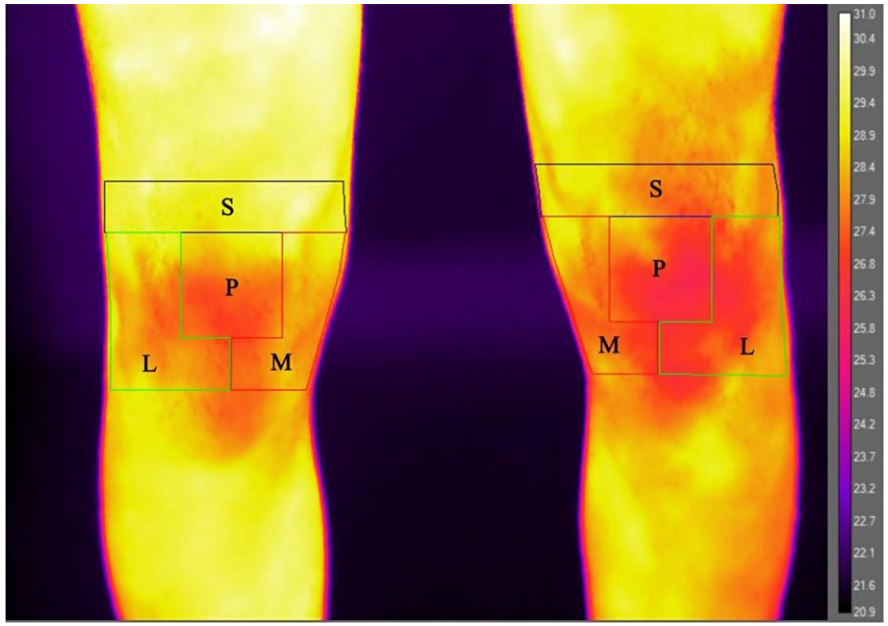

Figure 11: IRT image of OA knee (Left) and healthy knee (Right) (De Marziani et al., 2024)

sensors would be more suitable for continuous monitoring in wearables.

Technical implementation

For a contact-based sensor, key parameters such as accuracy and sensitivity must be determined. Body temperature was considered within the operating range of the sensor.

The core temperature of a body is around 36-37.5 °C. This can vary by a few degrees due to environmental influences, diseases,

or physical activity. However, skin temperature can differ from core body temperature by up to 2.5 °C (Togawa, 1985). Majumder et al. (2017) state that a range of 35-40 °C would cover the body's core temperature. However, the knee is not the body's core. Selfe et al. (2007) report a baseline skin surface temperature of the knee of 29.4 °C. Additionally, in other studies, the temperature of the control group's knee is below 35 °C (Denoble et al., 2010; Alfieri et al., 2020; Arfaoui et al., 2012; Brito et al., 2021).

As a result, the sensor's temperature range in this project has been set to 25-40 °C. According to Niedermann et al. (2013), an accuracy of 0.1 °C of the sensor is desirable for clinical relevance, especially since the temperature difference between OA and healthy patients could be as small as 0.1 °C (De Oliveira Vargas E Silva et al., 2020), though larger differences have also been reported, such as 1 °C (Arfaoui et al., 2012).

Studies have shown that skin temperature increases during exercise and is influenced by external factors such as clothing, ambient temperature, and movement artefacts (Billings et al., 2024; De Marziani, Boffa, Orazi, et al., 2023). For instance, a study using wearable sensors has confirmed that physical activity significantly alters thermal patterns around the knee, as evidenced by increased temperature. These variables must be considered when interpreting temperature data in daily lives (Pugliese et al., 2013).

Current placement

The placement of temperature sensors is important for accurate and consistent measurement of skin temperature. De Marziani et al. (2024) identify different regions of the knee joint that could serve as guidelines. These are the L, lateral; M, medial; P, patella; S, suprapatellar (Figure 11, p. 34). Other studies have explored placements such as the suprapatellar region or directly over the patellar tendon, but these are more prone to environmental interference and may yield less consistent readings during movement (Majumder et al., 2017; Brito et al., 2021).

Sensors used now

In wearables designed for skin temperature monitoring, Negative Temperature Coefficient (NTC) thermistors are frequently used. They offer high sensitivity, compact size, and low power consumption, making them suitable for integration into textiles (Majumder et al., 2017). Majumder et al. (2017) provide an overview of sensors used in health-monitoring wearables, noting that NTCs are preferred for skin applications due to their responsiveness and affordability. Other sensors, such as infrared sensors and thermocouples, are less common in wearables due to bulkiness or lower skin-contact reliability. Recent studies have explored flexible printed sensors and microfluidic temperature sensors, but these technologies remain in early stages of development and are not widely adopted for skin temperature sensing applications (Billings et al., 2024; Chen et al., 2010).

Relevance for the wearable

From this section, several implications emerge for designing the temperature-monitoring component of the wearable:

1. Skin temperature is a relevant indicator of inflammation

OA-related temperature increases are small but measurable, supporting the inclusion of a precise temperature sensor to detect flare-up related physiological changes.

2. Continuous, contact-based monitoring is feasible

Infrared imaging is unsuitable for wearables, but contact sensors (NTC thermistors) offer stable, low-power, and accurate real-time monitoring.

3. A specific sensing range is required

Baseline knee skin temperature typically falls between 29-35 °C; therefore, the wearable must operate reliably within 25-40 °C to capture both normal and elevated states.

Technical Requirement F: The temperature sensor needs to capture temperatures between 25-40 °C.

4. High measurement accuracy is essential

Reported OA-related differences can be as small as 0.1-1 °C. Therefore, for the validation of this prototype, a detection of 1 °C is targeted. Ensuring that the system can identify inflammatory events while distinguishing them from environmental fluctuations.

Technical Requirement G: The accuracy of the temperature sensor needs to be 1 °C to detect meaningful changes accurately.

5. Sensor placement must minimise external influences

Positioning near the patella or medial region improves consistency, while stable skin contact helps reduce the effects of clothing, movement, and ambient temperature on readings.

Technical Requirement H: The temperature sensor will be placed around the patella to map knee skin temperature at different locations, as this can vary.

Technical Requirement I: A temperature sensor needs to measure ambient temperature. So, temperature changes can be explained.

UI Requirement B: A place where you can tell about the sports you played is needed.

6. Integration with textile structures is realistic

NTC thermistors are flexible, small, and energy-efficient, making them suitable for direct embedding in the wearables fabric.

4.4 Other smart knee-wearables for OA

Several smart knee-wearables have been developed in research, each designed for different purposes and using different sensors. Table 2 on p. 38 provides an overview of some relevant wearables.

Existing smart knee-wearables are often designed for rehabilitation, gait analysis, or post-operative monitoring, and rely on rigid sensors or adhesive patches. Majumder et al. (2017) gives an overview of wearable sensors currently available on the market, including their applications and limitations. Another interesting observation, which confirms previously mentioned literature, is that NTCs are commonly used in wearables, such as in Billings et al. (2024). Where an NTC is implemented in a sock, showing its possible unobstructive integration in textiles. Furthermore, airborne microphones are mentioned and used in other wearables, indicating their potential for utilisation as crepitus detectors.

The only knee-wearable specifically for OA monitoring is one developed by Sensemodi, which captures acoustic, thermal, and kinematic data; however, its relative bulk makes it less suitable for everyday use (Figure 12). This is not optimal for non-invasive, continuous use, particularly outside clinical settings. Which, as shown previously, is essential for the unpredictable flare-ups. This highlights the need for a non-invasive, lightweight solution that can be worn comfortably throughout the day.

This project addresses this gap by developing a wearable for OA monitoring that integrates acoustic sensing and temperature in a non-invasive way. The goal is to enable long-term data collection without interfering with daily activities and to support clinical research into flare-up dynamics and disease progression.

Figure 12: Sensemodi wearable ("Home | Sensemodi," n.d.)

Table 2: Different smart wearables

Picture	Reference	What is measured?	Technical details	Relevance
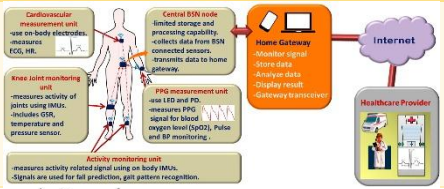	(Majumder et al., 2017)	Gives an overview of all wearable sensors		All sorts of wearable sensors
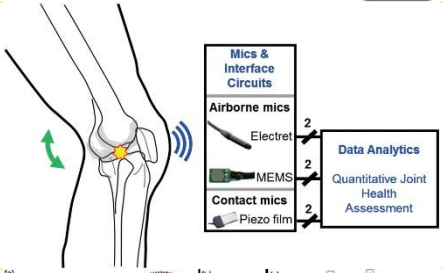	(Teague et al., 2016)	Gives an overview of methods for sensing acoustical emissions	Airborne microphones (Electret, MEMS), contact microphones (Piezo film). Recommends using air microphones for wearable joint sound sensing	Crepitations analysis
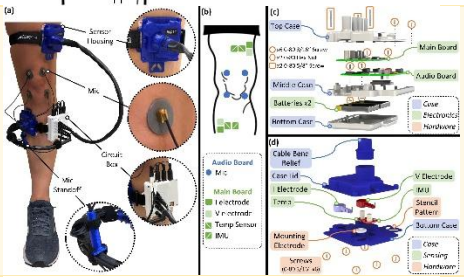	(Teague et al., 2020)	Monitor knee joint health	Contact microphones, temperature sensor, IMU	Crepitations analysis
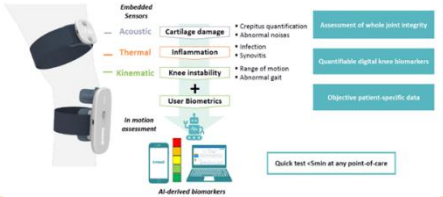	(Home | SenseModi, n.d.)	Monitoring OA	Acoustic I2S or PDM, temperature sensor, IMU	Wearable for OA
	(Billings et al., 2024)	Early detection of diabetic foot ulcers	Thin film NTC	Use of NTC temperature sensor

4.5 Conductive yarns in smart textiles

Conductive yarns are essential in the development of smart textiles. They can be directly integrated into fabrics using various manufacturing techniques, such as sewing, embroidery, weaving, and knitting, without compromising comfort or wearability (Bekaert, n.d.). With electrical resistance ranging from 5 Ω/m to several kΩ/m, most conductive yarns are not insulated. These yarns are produced by blending or coating traditional fibres with conductive materials such as stainless steel (McKnight et al., 2018).

These yarns can serve as the basis for a wide range of textile-integrated sensors and systems, including stretch and pressure sensors, wearable antennas, and stretchable interconnections (Stoppa & Chiolerio, 2014). Chen et al. (2010) further demonstrated that conductive yarns can successfully replace copper wire, enabling the seamless embedding of sensors into a garment. This greatly improves flexibility, durability, and user comfort compared to rigid wiring.

Building on these advantages, other studies have focused specifically on temperature sensing. Amers et al. (2023) showed that textile-based sensors can provide accurate and comfortable measurements without direct skin contact. Similarly, Polanský et al. (2017) introduced a large-area embroidered temperature sensor using a hybrid resistive thread, which proved its durability under washing and thermal cycling while maintaining a linear resistance-temperature relationship. Soukup et al. (2014) extended this approach by presenting embroidered textile-based temperature and humidity sensors specifically designed for healthcare applications. Their research emphasised washability, flexibility, and comfort as critical factors for clinical adoption. Together, these studies show that using conductive yarns as sensors is not only mechanically and electrically viable, but also clinically relevant for long-term wearable health monitoring. Their integration into textiles offers a path to reliable, comfortable, and non-invasive sensing that can support the early detection and management of conditions such as osteoarthritis.

In recent years, conductive yarn sensors have emerged as a promising solution for integrating this temperature sensing directly into textiles. Unlike conventional sensors attached to the fabric surface, these sensors are embedded within the yarn itself. Lugoda et al. (2020) describe three industrial techniques used to achieve this: knit braiding, braiding, and double covering. Knit braiding involves wrapping the sensor with multiple yarns using a knitting machine. While this offers mechanical protection, it results in thicker yarns (±3.4 mm) and reduced sensitivity. Braiding places the sensor in the core and surrounds it with 24 yarns, producing a flatter structure with improved aesthetics but slightly lower responsiveness. Finally, double covering sandwiches the sensor between two yarn layers with different twist-per-meter settings. This method yields the thinnest and

most flexible yarns (±0.5 mm) and preserves signal quality, making it ideal for wearable applications (Lugoda et al., 2020).

However, these specific integration methods are unconventional as they require complex industrial fabrication steps. If this process could be simplified, conductive yarn sensors would offer a unique and accessible pathway towards fully textile-integrated temperature monitoring. Inspired by the potential of seamless integration described by Lugoda et al. (2020) and the embroidered sensor concepts presented by Soukup et al. (2014), a study will be conducted in this project's development phase (8.4.2 Conductive yarn as a temperature sensor p. 81) to explore these conductive yarns as a pathway for temperature sensors in this wearable. Investigating whether commercially available, conductive yarns could function directly as reliable temperature sensors.

Relevance for the wearable

From this section, several implications emerge for designing the OA-monitoring wearable:

1. A gap exists for OA-specific daily-life monitoring

Current smart wearables do not support non-invasive flare-up detection or long-term inflammatory monitoring, underscoring the need for their development. Showing this project's relevance.

2. Conductive yarns enable a fully textile-integrated system

Conductive yarns enable the direct incorporation of sensor paths or sensing elements into the fabric, thereby enhancing comfort, flexibility, and aesthetics.

4.6 Conclusions

What is OA

The literature indicates that OA is a complex, degenerative joint disease involving surrounding tissues (Loeser, 2009; Hunter & Bierma-Zeinstra, 2019). Symptoms such as pain, stiffness, reduced mobility, crepitus, increased skin temperature and swelling fluctuate over time and do not always correspond to radiographic severity (Hunter et al., 2008; Katz et al., 2021). This highlights the difficulty of assessing OA based solely on imaging.

Current diagnostic methods vary. X-ray (KL scale) and MRI (MOAKS) are commonly used in research settings, whereas NICE guidelines emphasise clinical diagnosis without imaging, as findings often do not match symptom severity (NICE, 2022; Kohn et al., 2016; Knipe, 2020). This mismatch highlights the need for additional, non-invasive objective forms of daily monitoring.

Flare-ups are recognised as a sudden increase in symptoms (Thomas et al., 2022; Queiroga et al., 2023). They are unpredictable, vary from patient to patient, and currently lack a universal clinical definition. Swelling occurs more frequently on flare-up days (Parry et al., 2019), and early medication initiation can reduce flare-up severity for some patients (Thomas et al., 2019). However, flare-ups are still poorly understood, and current assessments rely on subjective reporting. The literature does not confirm a link between flare-ups and increases in joint temperature or crepitus, however, clinical experts suggest that inflammatory episodes may influence both physiological parameters (M. van Middelkoop, PhD).

Acoustic signals in knee OA

The literature shows that crepitus is a common and diagnostically relevant symptom of knee OA, occurring in over 40% of patients and showing predictive value for OA development (Schiphof et al., 2014; Lo et al., 2017). OA-affected knees produce distinct acoustic VAG-signals, making VAG a suitable non-invasive method for assessing mechanical joint changes (Teague et al., 2016; Karpiński et al., 2024).

For wearable integration, the medial or lateral side below the patella is considered the most effective placement due to its proximity to the interacting joint surfaces and reduced motion artefacts (Karpiński et al., 2024).

Airborne microphones appear most practical for a textile-based wearable, as they do not require direct skin contact and have previously been successfully applied to OA wearables (Teague et al., 2016; Toreyin et al., 2016). To reliably capture high-frequency joint sounds, filtering between 10-20 kHz and a minimum sampling rate of 40 kHz are required to ensure sufficient bandwidth and prevent aliasing (Onajite, 2013; Toreyin et al., 2016).

Skin temperature in knee OA

The literature indicates that skin temperature around the knee increases during inflammation in OA, although the magnitude of these temperature differences varies across studies (Denoble et al., 2010; Arfaoui et al., 2012). As some reported differences are as small as 0.1 °C, high-resolution sensing is required (De Oliveira Vargas E Silva et al., 2020; Niedermann et al., 2013). Infrared thermography (IRT) reliably visualises temperature asymmetries in symptomatic knees but is impractical for wearable use due to size, sensitivity to ambient conditions, and cost (Petrigna et al., 2024). This makes contact-based sensors more suitable for continuous monitoring.

Skin temperature at the knee is typically lower than core temperature, with baseline values around 29-35 °C in healthy individuals (Selfe et al., 2007; Denoble et al., 2010). Based on this, a sensing range of 25-40 °C is thought appropriate for monitoring OA-related changes. Furthermore, knee temperature is influenced by environmental factors, clothing, and activity (Billings et al., 2024).

Multiple anatomical locations can be used to measure knee temperature, including the medial, lateral, patellar, and suprapatellar regions (De Marziani et al., 2024). Placements closer to the patella tend to provide more consistent readings during movement (Majumder et al., 2017; Brito et al., 2021).

For wearable integration, NTC thermistors remain the most practical option due to their high sensitivity, small form factor, low power use, and suitability for textile-based applications (Majumder et al., 2017).

Other wearables and conductive yarns

Existing smart knee-wearables are primarily designed for rehabilitation, gait analysis, or post-operative monitoring. These systems are often bulky and not optimised for continuous, non-invasive monitoring of OA symptoms in daily life.

Conductive yarns offer a promising solution for wearable integration, providing a mechanically and electrically viable platform that can be embedded directly into textiles without compromising comfort or flexibility.

Textile-based temperature sensors using conductive yarns demonstrate that it is possible to integrate sensing elements seamlessly into garments, although challenges such as fabrication complexity remain.

This literature review has provided the fundamental physiological and technical parameters required for acoustic and thermal joint monitoring. These insights will now be carried over into the Define phase, where they will be translated into concrete user and technical requirements for the wearable design.

Define

The Define phase marks the transition from theoretical exploration to concrete specification. Drawing on insights from the OA literature and the limitations of current diagnostic tools, this chapter establishes the framework for the design process.

It begins by describing the precise problem definition and delimiting the design scope to ensure a feasible proof-of-concept. Subsequently, the foundational elements are translated into a Program of Requirements. By categorising these requirements into User and Technical, criteria and wishes, a clear set of benchmarks is created to guide the Development phase.

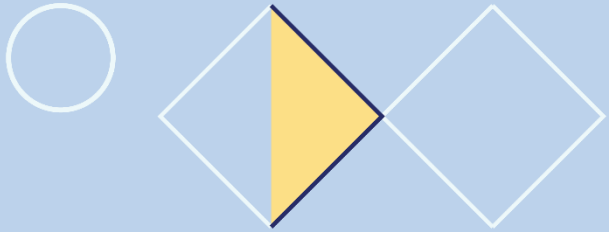

5 Design direction

This project aims to develop a proof-of-concept wearable for the knee that continuously measures acoustic activity (crepitus) and skin temperature for patients with OA. The literature indicates that both increased joint sound and elevated skin temperature are associated with OA (Denoble et al., 2010; Arfaoui et al., 2012; Petrigna et al., 2024). These parameters are therefore hypothesised to change during flare-ups as described by the patient (M. van Middelkoop, PhD; Queiroga et al., 2023).

Although the wearable is in its early stages, it is primarily intended as a research tool for collecting data to verify the hypothesis. Its potential long-term application lies in daily-life use by OA patients, who will be the end users of the wearable. For this reason, the patient perspective is important in the early design stage. By considering the patient's needs and preferences, this project ensures that future development is not constrained by wearability or usability issues, thus supporting a smoother transition from experimental research to real-world application.

OA patients are, therefore, in this project, the end users of the wearable, while researchers and clinicians are the primary users of the collected data.

5.1 Problem definition

OA is a joint disease characterised by pain, stiffness, inflammation, and functional limitations, which often occur in flare-ups (Queiroga et al., 2023). These flare-ups are typically identified from subjective patient reports, but it remains unclear whether they are accompanied by measurable physiological changes, such as increased temperature or increased acoustic activity (Denoble et al., 2010; Arfaoui et al., 2012; Petrigna et al., 2024; De Marziani et al., 2024).

Current OA monitoring and diagnostic methods, such as imaging or clinical assessment, have limitations: they provide only momentary snapshots, can be costly, and are unsuitable for continuous monitoring in daily life (Majumder et al., 2017). Existing smart knee-wearables are primarily designed for rehabilitation or gait analysis, rely on rigid sensors or adhesive patches, and are not optimised for non-invasive, long-term use for patients with OA. Consequently, patients rely on subjective reporting and infrequent consultations, which limit early intervention and real-time understanding of flare-up dynamics.

Problem statement

Osteoarthritis causes pain, inflammation, and functional limitations, described by patients as subjective flare-ups. Objective OA-related physiological symptoms include increased skin temperature and elevated acoustic activity (crepitus). To investigate whether these objective signals can support or complement subjective flare-up reporting, a non-invasive wearable is required to detect these parameters at the knee.

Currently, such objective measurements are not collected continuously in daily life, which limits understanding of whether and how physiological changes occur in response to patient-reported flare-ups. This gap restricts scientific understanding of flare-up mechanisms and limits the potential for timely intervention.

Key aspects addressed by this project:

- Enabling continuous measurement of OA-related physiological signals.
- Ensure comfort and wearability for daily use of the wearable.
- Developing a proof-of-concept for future studies.

By defining this problem, the project addresses current gaps in OA research, the technical feasibility of a wearable, and the future goal of patient-centred, non-invasive, everyday monitoring.

5.2 Design scope

The scope of this project is defined by its focus on the first development phase of a wearable for knee OA. This first proof-of-concept demonstrates the technical feasibility of non-invasive (crepitus) acoustic and temperature sensing at the knee.

The goal is not to test or validate the hypothesis that flare-ups coincide with changes in crepitus or temperature. Instead, the project aims to determine whether these physiological signals can be measured reliably and continuously using a wearable suitable for daily use. In Figure 13, a broader view is visualised; the stakeholders are included as well to provide a comprehensive overview, and the scope is outlined.

OA patients will be the end users in the long term; this project focuses on incorporating the patient perspective at a conceptual level. User and non-user opinions are considered to inform comfort, wearability, and acceptance, ensuring that future iterations are not limited by fundamental design choices. If a wearable is not acceptable to users, it has no practical value.

The wearable will be designed to be worn all day, enabling long-term data collection. As a result, the design prioritises non-invasiveness and comfort. For this proof-of-concept, the hardware's operating time is limited to a minimum of two hours. This duration is sufficient to technically validate that the sensors

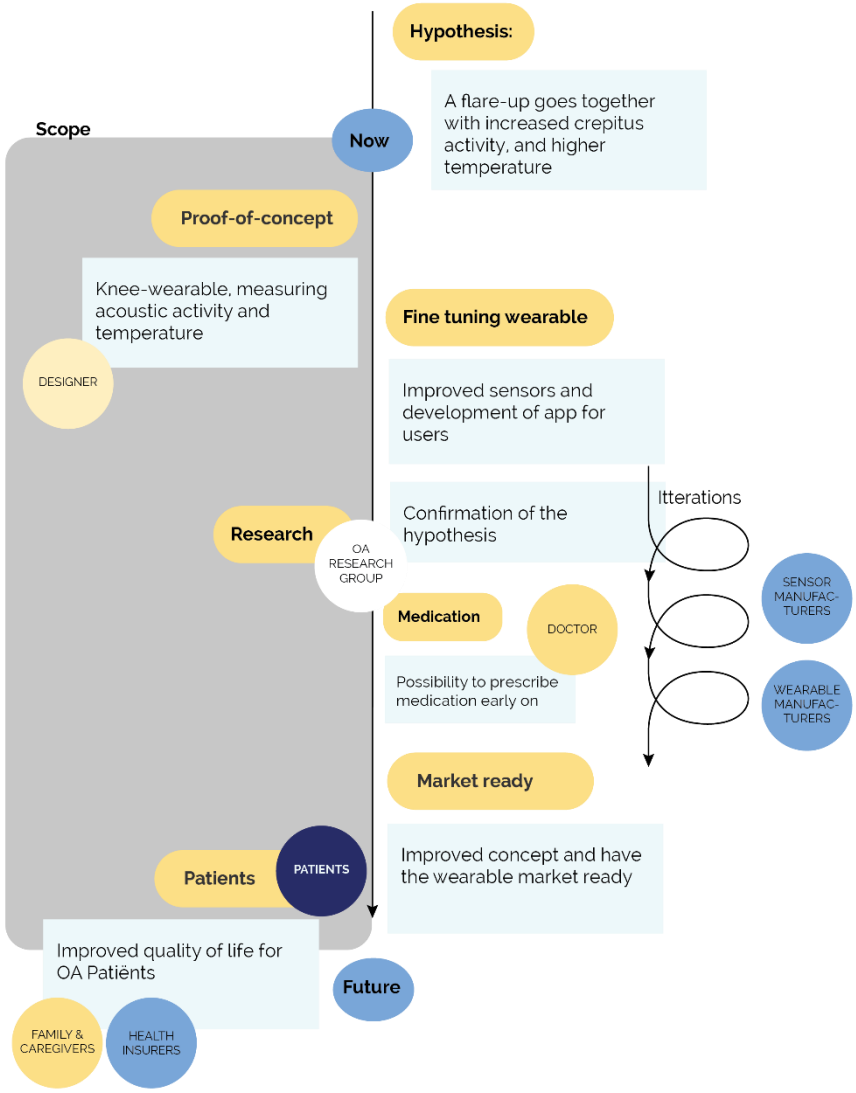

Figure 13: Project overview, with scope and placed stakeholders

function correctly and to ensure that temperature and sound can be measured continuously.

Testing within this project is limited because formal testing with diagnosed OA patients was not permitted. Consequently, the technical validation of sensor data was conducted with a healthy individual (the researcher) and a non-diagnosed individual who had audible knee crepitus. Furthermore, wearability and general usability aspects are explored through testing with a healthy individual (the researcher) and validated with 5 fellow students. To obtain general feedback during the process, a panel with 8 healthy volunteers was held, and to reflect the intended user group, feedback from 2 OA patients was used to assess the relevance and acceptability of the final proof-of-concept.

Several aspects are explicitly out of scope, as the project does not aim to deliver a fully developed product. These include:

- Clinical validation or hypothesis testing involving OA patients.
- Real-life testing in medical settings, which is excluded due to ethical requirements and time constraints within the 100-day project period.
- As the prototype is designed for short-term validation (2 hours), the washability and moisture resistance of the electronics and textiles are not addressed in this iteration.
- Since data collection can be specific to each study, in this wearable design process, only the sensor's function is confirmed. Refining how data is delivered is necessary before conducting initial research on flare-ups.
- Hardware optimisation beyond the chosen microcontroller, the XIAO microcontroller used in this project imposes certain technical limitations, and while personalised PCBs are available, their integration is outside the scope of this project.
- Full development of a user interface or optimisation of prototype software.

In summary, this project establishes a technical and design foundation for future research into objective flare-up monitoring in knee OA, without making clinical claims or testing disease-related hypotheses.

6 Requirements

The proof-of-concept requirements and wishes are categorised into four groups: user requirements, user wishes, technical requirements, and technical wishes. During the literature review, several requirements were identified. These are compiled into the list.

A distinction is made between requirements (must-haves) and wishes (should-haves). While requirements define the hard boundaries of the design, the wishes are guides for the design. Furthermore, because this project focuses on developing a functional prototype, a 'Scope' column has been added to the tables. This explicitly distinguishes between the criteria the current proof-of-concept (PoC) must meet and the requirements for a final, market-ready wearable. If a criteria is labelled exclusively as 'PoC', it indicates that this specification is tailored for the current testing phase and must be refined or expanded in the final design.

In the development phase, different requirements and wishes are referenced using an abbreviation consisting of a U for user or T for technical, combined with an R for requirement or W for wish, followed by a number. For example:

UR-1 User Requirement 1

TR-1 Technical Requirement 1

UW-1 User Wish 1

TW-1 Technical Wish 1

6.1 User requirements

In the literature, two primary requirements emerged: the wearable must be non-invasive and comfortable for at least 16 hours, and it should not provide mechanical support.

Consequently, although the ultimate target is 16 hours of wear, the requirement for this proof-of-concept has been reduced to 4 hours. This duration is seen as a valid predictor of long-term physical comfort in this project. Gefen (2008) demonstrates that sustained pressure on the skin restricts local blood flow, leading to observable skin damage, such as persistent redness or pressure sores. Within 1 to 2 hours of continuous loading (Gefen, 2008). Furthermore, ergonomic assessments (Knight & Baber, 2005) indicate that a user's subjective perception of tactile discomfort, friction, and movement restriction stabilises rapidly during early use. Therefore, if the wearable remains comfortable during this initial period, it provides a strong indication of its suitability for extended daily use.

Furthermore, the general requirement for the wearable to be non-invasive and comfortable is too broad to be directly testable and therefore requires further specification. Knight and Baber (2005)

define comfort not as the presence of a positive sensation, but rather as the absence of negative sensations experienced by the user. To operationalise this concept, Knight and Baber developed the Comfort Rating Scale, which structures comfort into six distinct dimensions: emotion, attachment, harm, perceived change, movement, and anxiety. By dividing comfort into these components, the scale enables a more systematic evaluation of a wearables comfort.

To ensure a comprehensive comfort profile for this wearable, the user requirements and wishes defined in this project are categorised into the six dimensions of the Comfort Rating Scale proposed by Knight and Baber (2005). The full list can be found in Table 3, p. 51.

6.2 Technical requirements

In addition to user-related requirements, the literature review identified several key technical requirements for the wearables sensor and hardware. The battery life for this proof-of-concept is limited to 2 hours, as the primary goal of this proof-of-concept is to capture and analyse relatively short, focused measurement sessions of around 30 min to validate sensor performance, so a 2-hour window is sufficient. The full list of technical requirements and wishes is presented in Table 4, p. 52.

Table 3: User requirements and wishes (UR-1 to UR-14, UW-1 to UW-15)

Category (Knight & Baber, 2005)	User requirement (must)	Scope	Rationale	Wish (nice to have)
Movement *The wearable affects my mobility. My movement is restricted.*	**UR-1** **Freedom:** The design allows for full functional knee flexion (up to 120°). With no mechanical support.	**PoC** **Final**	According to Pinskerova et al. (2019), knee mechanics change completely beyond 120 degrees; therefore, the focus is on the primary flexion phase, which covers standard daily activities.	**UW-1** **Effort:** Minimise the additional physical effort required for daily tasks (e.g., stair climbing, sitting, walking). **UW-2** **Flexibility:** Maximise conformance to the dynamic curvature of the knee during the full range of motion.
Attachment *I can feel the device on my body. I can feel the device moving (slipping/bouncing).*	**UR-2** **Adaptation**: The user is unaware of the wearables physical presence after 60 minutes of wear.	**PoC** **Final**	If the wearable remains noticeable after an hour, it may irritate and reduce compliance (researchers' assumption).	**UW-3** **Adaptation time:** Minimise the time required for the user to become unaware of the wearable.
	UR-3 **Stability**: The wearable shifts vertically by less than 1 cm after 4 hours of wear.	**PoC** **Final**	Consistent placement is crucial for accurate sensor data. A 4-hour period is a realistic interval between natural readjustment moments, such as toilet breaks.	**UW-4** **Absolute stability:** Minimise vertical shifting during use. **UW-5** **Sizing and fit:** The wearable accommodates a variety of leg circumferences. Essential to ensure the stability and comfort requirements can be met across different body types (Final).
	UR-4 **Weight**: The wearable total weight does not exceed 100g.	**PoC** **Final**	Reference wrist wearables weigh ~50g (Garmin, n.d.). While the leg can carry more weight, keeping it under 100g minimises downward pull, thereby improving stability and comfort.	**UW-6** **Lightweight:** Minimise the wearables total weight.
Harm *The wearable is causing me harm (pain, heat, scratching, itching).*	**UR-5** **Skin integrity**: No visual redness or tissue damage after 4 hours of wear.	**PoC** (For the Final, this will be 16 hours)	Tissue damage from sustained pressure starts within 1-2 hours (Gefen, 2008). A 4-hour PoC test doubles this critical window, serving as a practical and reliable predictor for the Final 16-hour wear requirement.	**UW-7** **Pressure distribution:** Maximise even mechanical pressure across the skin, with no localised pressure peaks.
	UR-6 **Thermal**: Skin temperature under the wearable does not exceed the surrounding skin temperature by more than 2 °C at rest.	**PoC** (For the Final, this needs to be reconsidered)	A localised increase in temperature leads to sweating and discomfort. Also, temperature data will not be reliable (researchers' assumption).	**UW-8** **Breathability:** Maximise the moisture-wicking and air-permeability of the textile components.
	UR-7 **Biocompatibility**: All skin-contact materials are hypoallergenic and do not cause skin reactions.	**Final** (No research will be conducted on allergic reactions)	Essential safety requirement to prevent allergic reactions.	-
	UR-8 **Hygiene/washability:** The textile component of the wearable is machine-washable at 30°C without loss of structural integrity, provided the electronic module is removed.	**Final** (For now, out of scope)	A wearable worn daily on the leg will collect sweat and dirt; washability is needed for hygiene and long-term use.	-
Perceived change *Wearing the wearable makes me feel physically different. I feel strange wearing the wearable.*	**UR-9** **Independence:** An individual can correctly don the wearable independently, without external assistance, within 2 attempts.	**PoC** (For the Final, this requirement should focus on OA patients)	The end-user group (often elderly or with restricted mobility) must be self-sufficient to ensure adoption and daily use.	**UW-9** **Low dexterity fastening:** Minimise the fine motor skills required to secure the wearable.
	UR-10 **Donning/doffing:** The wearable can be put on correctly in 60 seconds and taken off in 30 seconds.	**PoC** **Final**	Fast and correct donning/doffing prevents user frustration and ensures the wearable is positioned correctly for reliable data collection.	**UW-10** **Foolproof orientation:** Maximise intuitive donning by using physical or visual cues.
Emotion *I am worried about how I look while wearing this wearable.*	**UR-11** **Concealability:** The wearable fits under loose-fitting trousers.	**PoC** (For the Final, it should fit under all sorts of trousers)	To facilitate daily, non-invasive monitoring in public spaces, the wearable must integrate seamlessly with standard clothing.	**UW-11** **Aesthetics:** Maximise aesthetic appeal by adopting a neutral, athletic, or premium consumer product look. **UW-12** **Invisibility:** Minimise the wearable visual footprint so it is as unnoticeable as possible under loose-fit trousers. **UW-13** **Compactness:** Keep overall volume and footprint as compact as possible.
Anxiety *Not feeling secure wearing the wearable. I feel tense/on edge.*	**UR-12** **Discretion**: The wearable makes no audible noise during walking. Also, no light goes through the trousers.	**PoC** **Final**	To prevent stigmatisation, users should not feel self-conscious or fear that others notice they are wearing a medical wearable.	**UW-14** **Feedback/reassurance:** Provide subtle, non-invasive confirmation that the wearable is correctly positioned and functioning.
	UR-13 **Shape retention**: Materials do not deform or lose elasticity for 30 usage cycles.	**PoC** (For the Final, more cycles must be achieved)	Required for testing validity and ensuring the wearable remains reliable and secure over its intended lifespan.	
Cumulative effect (extra) *Long-term comfort and durability of the wearable.*	**UR-14** **Duration**: Overall comfort remains valid for at least 4 hours of continuous wear.	**PoC** (For Final comfort remains valid for 16 hours)	A 4-hour continuous test is a valid and feasible predictor of 16-hour (all-day) wear comfort in this project context.	**UW-15** **Longevity:** Maximise the durability of the textile and elastic components beyond the baseline requirements.

Table 4: Technical requirements (TR-1 to TRO-14, TW-1 to TW-10)

Category	Technical requirement (must)		Scope	Rationale	Wishes	
Hardware and mechanics	**TR-1**	**Continuous operation:** The hardware module operates reliably for a continuous 2-hour period during standard daily activities without failure.	**PoC** (Final: continuous operation)	Ensures basic mechanical durability during the initial testing phases.	TW-1	**Robustness:** Maximise impact resistance so the housing withstands low-impact collisions (e.g., bumping into a table) without structural failure or sensor displacement.
	TR-2	**Assembly**: Electronic components and PCB footprints are suitable for manual soldering and handling.	**PoC** (Final: this is not needed as automated fabrication is available)	Required for rapid prototyping with standard lab equipment.		
	TR-3	**Wiring flexibility:** Internal wiring connecting the PCB to the distributed sensors can withstand bending up to 120° without signal loss.	**PoC Final**	Required to survive continuous knee flexion without breaking the circuit.	TW-2	**Integration:** Maximise seamless integration of wiring into the textile.
Data and connectivity	**TR-4**	**Data export:** Raw acoustic and thermal data can be analysed.	**PoC Final**	Required for the researcher to run data analysis.	TW-3	**Wireless:** Implementation of wireless data transfer.
					TW-4	**Filtering:** Apply data filtering to smooth raw signals and highlight trends.
	TR-5	**Data reliability and storage:** Data is accurate, reliable, and stored without loss.	**PoC Final**	Crucial for aligning acoustic and thermal events during data analysis.	TW-5	**Precision syncing:** Maximise synchronisation precision by ensuring acoustic and thermal timestamps align.
Acoustic sensor	**TR-6**	**Acoustic placement:** The acoustic sensor is positioned below the centre of the patella on the medial or lateral side.	**PoC Final**	Karpiński et al. (2024) identify this as the optimal location for capturing joint crepitus.	TW-6	**Noise:** Minimise mechanical friction noise from materials near the microphone.
	TR-7	**Sampling rate:** For reliable data, the acoustic sampling frequency is at least 44.1 kHz.	**PoC Final**	Required to prevent aliasing for the 20 kHz maximum frequency of interest (Nyquist) (Onajite, 2013).		
Thermal sensors	**TR-8**	**Thermal range & accuracy:** The sensor captures 25-40 °C with a 1 °C resolution/accuracy.	**PoC Final**	Necessary to detect subtle inflammatory temperature changes on the skin (Petrigna et al., 2024).	TW-7	**High Resolution:** Maximise thermal resolution for even more precise tracking of inflammation.
	TR-9	**Physical fit:** For reliable data, the wearable provides a tight, skin-fit around the temperature sensors.	**PoC Final**	Prevents air gaps and stops ambient air from cooling the skin sensor. Which could result in unreliable data.	TW-8	**Thermal mapping:** Expand to a multi-node sensor array to map the complete temperature distribution around the patella.
	TR-10	**Insulation:** Thermal insulation is required over the temperature sensors.	**PoC Final**	Ensures more accurate skin temperature measurement and reduced influence of ambient air.		
	TR-11	**Ambient reference:** An outward-facing, uninsulated external sensor continuously measures the ambient environmental temperature.	**PoC Final**	Required to compensate for environmental changes.		
Power and autonomy	**TR-12**	**Battery life:** The battery supports at least 2 hours of continuous data logging.	**PoC** (Final: 16-20 hours)	Sufficient for analysing short, targeted PoC measurement sessions.	TW-9	**Efficiency:** Maximise power efficiency to enable smaller battery capacities while maintaining logging time (Final).
	TR-13	**Safety**: The battery is enclosed in a rigid, puncture-resistant casing and includes a Battery Management System for overcharge and thermal protection	**PoC Final**	Prevents overcharging and overheating near the skin. And possible explosions due to sharp external impacts (CM Batteries, 2025).		
System status indicators	**TR-14**	**Recording feedback:** It must be explicitly clear to the user when the wearable is active and logging data.	**PoC Final**	Users need confirmation that the test is running successfully.	TW-10	**Connection status**: Provide detailed, non-intrusive status feedback (e.g., recording, charging, errors, connection status) via a companion app or discrete haptics, without violating the "no visible light" rule.

Develop

The Develop phase implements the theoretical definition to physical prototypes. In this chapter, the concept established in the previous phases is developed into a tangible wearable. The process follows an iterative approach, in which distinct categories, ranging from hardware selection and sensor integration to casing and design, are developed, tested, and refined individually.

Design choices made throughout this phase are based on the Program of Requirements, insights from the literature review, and observations gathered from preliminary user tests. By systematically addressing the technical and ergonomic challenges, this phase aims to provide a comprehensive answer to the main design question:

Can a wearable proof-of-concept be designed to technically validate non-invasive acoustic and temperature sensing at the knee for osteoarthritis patients?

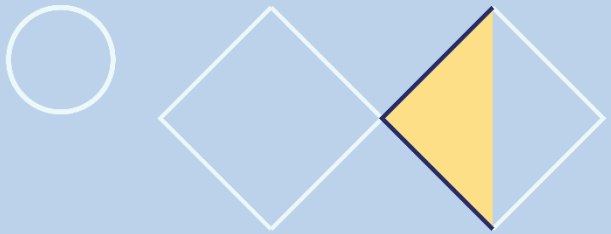

---

7 Design of the wearable

This chapter describes the design development of the knee-wearable, focusing on the textile layout, material selection, wiring integration, and electronic component connection. The design process was iterative and driven by wearability, comfort, and sensor placement, aligned with the literature review findings and the defined requirements.

Key aspects addressed in this chapter include:

- Textile placement and overall form of the wearable.
- Selection of fabrics for the final design.
- Integration of wiring using conductive yarns.
- Placement, connection and integration of the hardware.
- Additional components, such as non-slip elastic, to improve stability.

Furthermore, tests of various concepts were conducted with a healthy individual (the researcher) to enable rapid iteration and to more quickly consider different wishes and requirements. Midway through the development process, a panel session with 8 healthy individuals from 20 to 58 years was conducted to gather input on several design-related questions. These insights informed design decisions throughout this chapter (Appendix 2). Where relevant, this panel's feedback is referenced when making specific choices.

Also, a stability and comfort test was conducted with one healthy individual (the researcher) to confirm the panel results and evaluate the improved design.

Finally, a comfort test was done with one other healthy individual, and a possible addition was tested with five individuals.

7.1 Initial placement of sensors

A critical constraint in the design of this wearable is the positioning of the temperature sensors. To create a comprehensive thermal view of the knee, multiple temperature sensors will be spread around the patella. Measurement locations were identified in the four quadrants surrounding the superior (North), Medial, Lateral, and Inferior (South) regions.

This layout, illustrated in Figure 14, aims to provide a heat map-like view, enabling the wearable to pinpoint localised inflammation (TW-8).

It is important to note that this placement served as the starting point. While the primary goal was to measure temperature differences across multiple locations, the final placement was revised throughout the process. Modifications are based on optimal skin contact (TR-9) and user comfort. In addition to the skin-contact sensors, an environmental reference sensor is required (TR-11). This specific temperature sensor is positioned on the exterior of the wearable. So, temperature changes when going from inside to outside can be recognised and later compensated for.

Furthermore, regarding the acoustic sensor, the initial exploration identified two potentially optimal placements (TR-6). For now, both locations are maintained as valid options, as it was assumed that the specific choice between them would not significantly impact the overall mechanical and textile design of the wearable. The definitive selection between these two positions will be determined through acoustic testing later in the development process (8.3.3 Placement acoustic sensor p. 75).

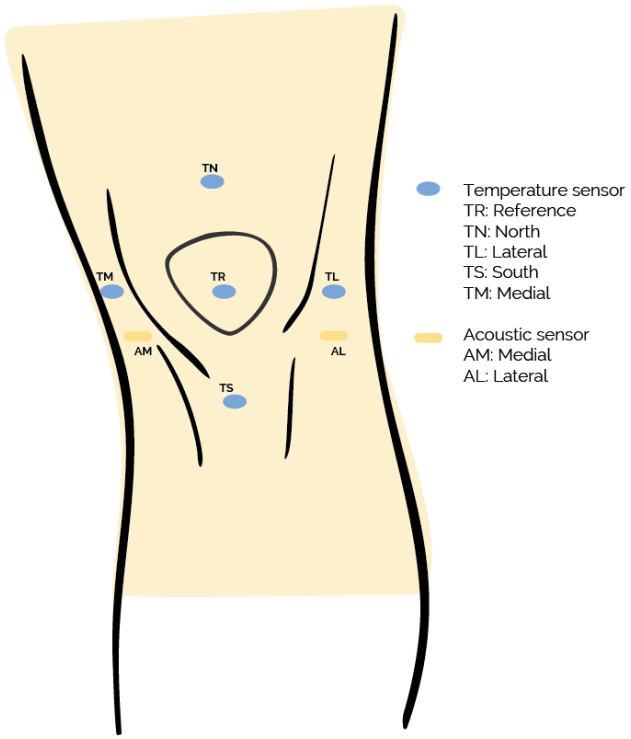

Figure 14: Initial placement of temperature and acoustic sensors

7.2 Design exploration

To explore different design options, Virtual Reality (VR) was used during the early concept phase. The software Gravity Sketch was used to sketch and iterate on 3D wearable concepts. This approach enabled rapid evaluation of shape, coverage, and material distribution prior to physical prototyping (Figure 15).

A key starting point for the concepts was a sock-like structure around the knee, based on the assumption that circumferential contact would support stable sensor-skin interaction (TR-9). However, this iteration had some undesirable aspects, such as heat accumulation (UR-6) and improved physical movement (UW-1). From this starting point, inspiration was drawn from topology-optimised design that uses as little material as possible for a breathable design (UW-8). With in mind that a continuous textile surface must be present at sensor locations to ensure structural stability and enable continuous wiring using conductive yarns (TR-3).

Four specific iterations (circled in yellow) were selected for further development as they successfully address distinct requirements. VR-Concept 1 utilises a breathable web structure, prioritising thermal comfort (UR-6). VR-Concepts 2, 3 and 4 introduce strategic cut-outs, with improved stability due to the bands around the upper and lower parts of the leg (UR-3), and in VR-Concept 2 it was thought there would be a better range of motion as there was no band in the hollow of the knee (UR-1).

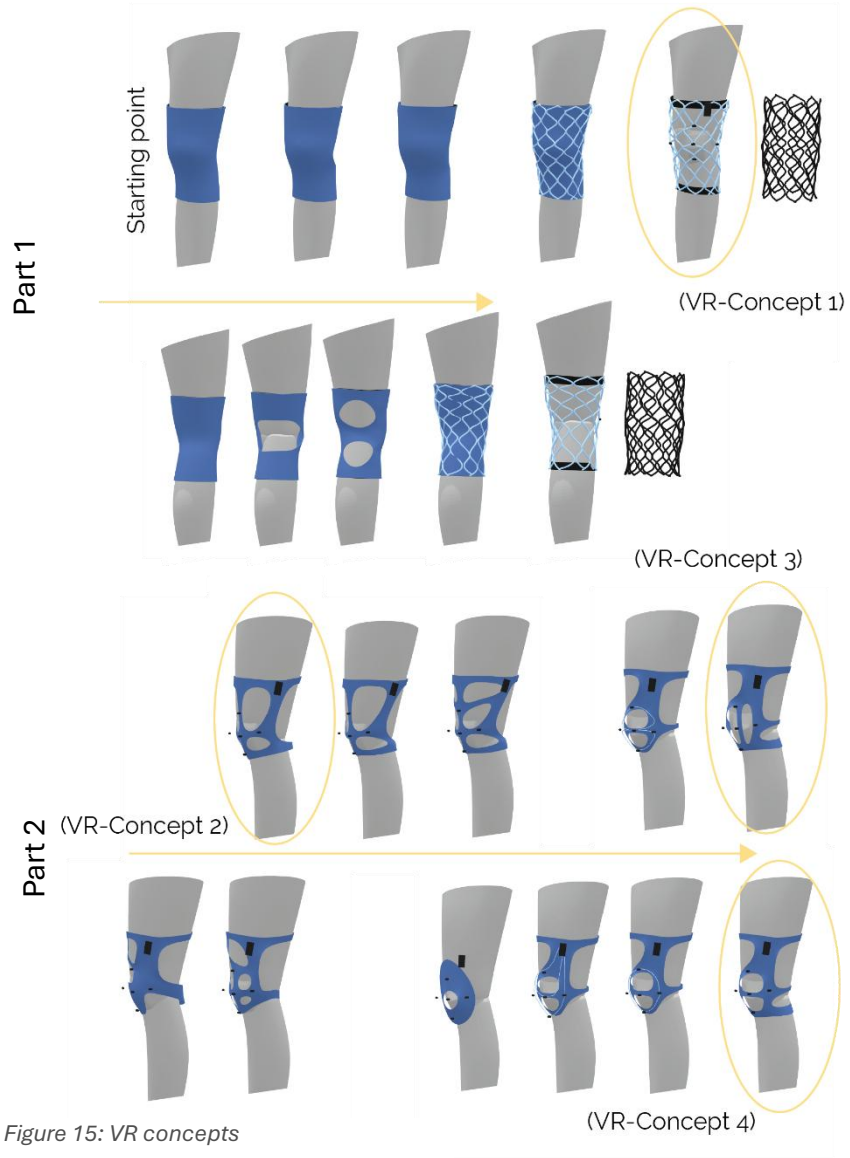

Figure 15: VR concepts

7.3 Physical prototyping

The physical prototypes were produced using a range of textile materials, including T-shirt fabric (90% cotton, 5% elastane, 5% viscose), sports legging fabric (90% polyester, 10% elastane), pantyhose (80% polyamide, 20% elastane), and diamond mesh tights (90% nylon, 10% elastane). In addition, anti-slip elastic was incorporated to improve positional stability (UR-3). The focus was mostly on the following requirements and wishes:

User requirements and wishes as described in Table 3, p. 51

- UR-1 **Freedom:** The design allows for full functional knee flexion (up to 120°). With no mechanical support.
- UR-6 **Thermal**: Skin temperature under the wearable does not exceed the surrounding skin temperature by more than 2 °C at rest.
- UW-4 **Absolute stability:** Minimise vertical shifting during use.

Technical requirements and wishes as described in Table 4, p. 52:

- TR-9 **Physical fit:** For reliable data, the wearable provides a tight, skin-fit around the temperature sensors.
- TW-1 **Robustness:** Maximise impact resistance so the housing withstands low-impact collisions (e.g., bumping into a table) without structural failure or sensor displacement.

Other requirements are applicable to all concepts or are not yet relevant at this stage.

The physical prototyping consists of 2 rounds. In the first round, the VR-Concepts are explored as physical prototypes. Afterwards, the two most promising concepts were presented to the non-OA panel of 8 individuals aged 20 to 58. Following this panel's feedback, round 2 began.

A full overview of all prototypes is shown in Figure 16 on p. 58.

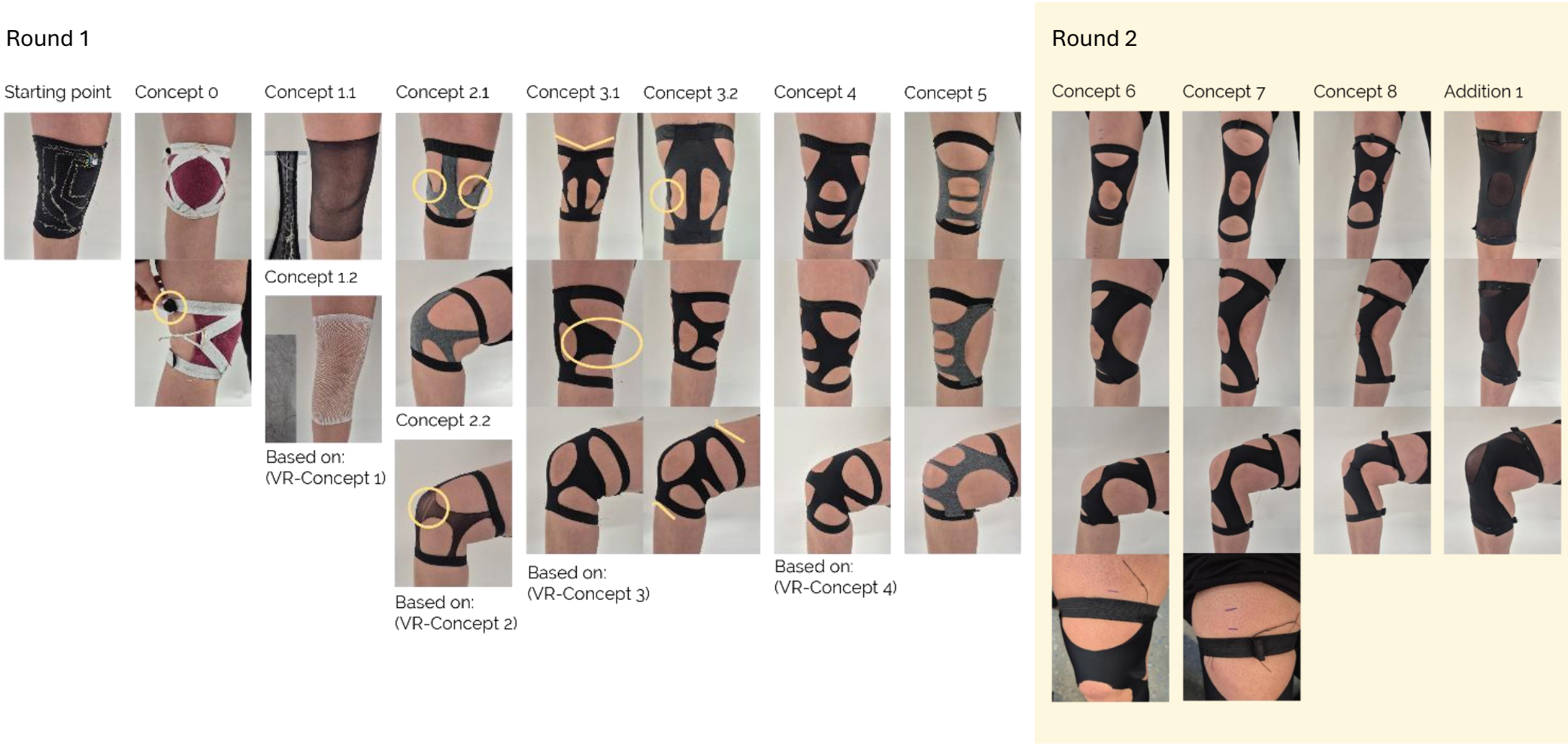

Figure 16: Round 1 and 2 physical prototyping

7.3.1 Round 1

Findings from early concepts

Concept 0 (Figure 17) was created as the first prototype, including NTC temperature sensors. This concept was tested during walking, and a key finding was that the temperature sensors must be in direct contact with the skin to obtain accurate measurements (TR-5, TR-9). Also, for this prototype, velcro was used as a fastening mechanism. This worked quite well, but after this prototype, it was abandoned because this relatively stiff component irritated the skin (UR-5).

Based on VR-Concept 1 (Figure 17), concepts 1.1 and 1.2 were made. It quickly became clear that sewing into the pantyhose (80% polyamide, 20% elastane) and diamond mesh tights (90% nylon, 10% elastane) damaged the material. The material scrunched and lost its elasticity during stitching (UW-2), rendering this material unsuitable for a comfortable knee-wearable in which the conductive yarns are sewn. As elasticity is essential for comfort and mobility, these concepts were discarded. Another limitation of these fabrics was the lack of shape retention, as they are relatively fragile (UR-13).

However, these early concepts demonstrated that lightweight, breathable designs significantly reduced bulk and heat retention, both of which are desirable for long-term wear (UR-6, UR-11).

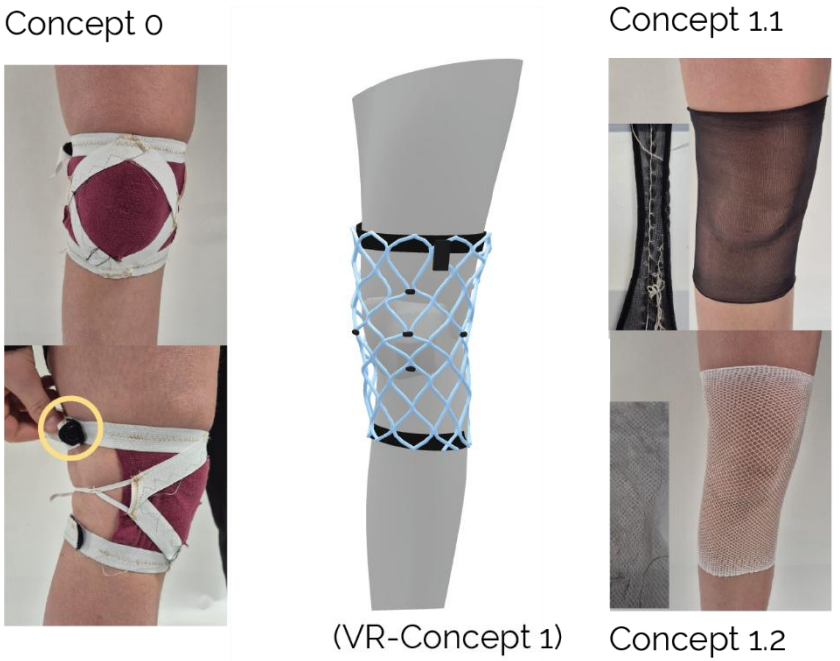

Figure 17: Early concept 0, 1.1, 1.2, VR-Concept 1

Concept 2: Reduced textile design

For concept 2, T-shirt fabric (90% cotton, 5% elastane, 5% viscose) was used, and excess material was removed in accordance with the VR-Concept 2 (Figure 18).

This fabric allowed for zigzag stitching, preserving elasticity and improving comfort (UW-2). A major advantage of this concept was the absence of fabric in the knee hollow, which significantly increased comfort during knee flexion (UW-1). Due to the reduced amount of material, the wearable also did not trap excessive heat around the knee (UR-6).

Initial testing with concept 0 showed that good skin contact is crucial for reliable sensing; however, this concept had a gap at the location of the 2 NTCs when the muscles were tensed. As a result, skin contact was not always maintained (TR-9).

As an additional exploration, this concept was also produced using the pantyhose fabric (Concept 2.2 in Figure 18). However, this material (again) proved difficult to sew and was prone to tearing, indicating insufficient robustness for this application, where the conductive yarns are sewn to the fabric (UW-2, UR-13).

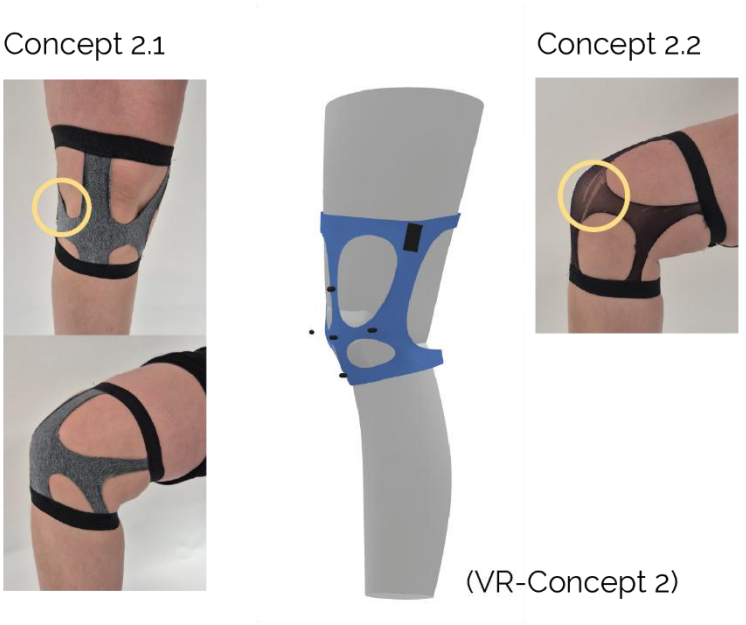

Figure 18: Concept 2.1, 2.2, based on VR-Concept 2

Concepts 3, 4 and 5: vertical and horizontal band structure

Concept 3 introduced a vertical band-based structure (Figure 19). Concept 3.1 included a third band at the hollow of the back of the knee. However, it was preferred not to have fabric in the knee hollow, so this band was split into two sections, one above and one below the moving area. This modification significantly improved comfort during flexion (UW-1). A drawback of this concept was that the vertical connection between the upper and lower bands pulled the elastic downward during knee flexion, reducing stability (UW-4).

This iteration also prompted a critical reassessment of sensor placement. When the knee is flexed, the same visible gaps appear at the sides of the wearable as concept 2.1, compromising sensor-skin contact (TR-9). As continuous contact during movement is essential, this issue could be addressed by rotating the sensors by approximately 22 degrees (Figure 20), improving conformity to the knee's anatomy while maintaining coverage.

To address the downward pull observed in concept 3, a variation with a fully horizontal band configuration (concept 4, Figure 21) was developed and an iteration with less material around the knee hollow, concept 5. These versions provided improved freedom (UR-1) during movement and reduced displacement of the wearable (UW-4).

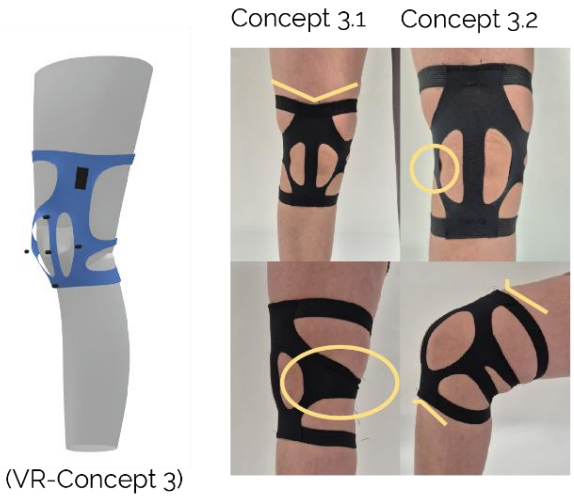

Figure 19: Concept 3.1 and 3.2 based on VR-Concept 3

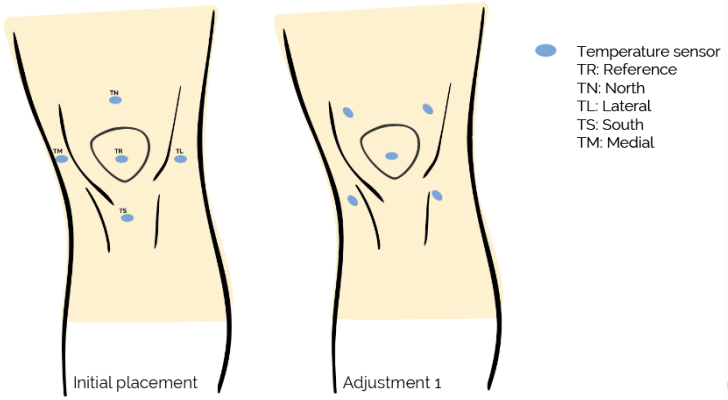

Figure 20: Adjustment 1 placement of temperature sensors

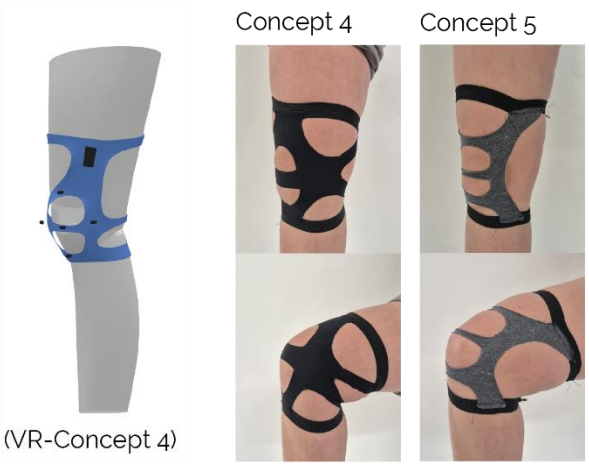

Figure 21: Concept 4, based on VR-Concept 4 and additional concept 5

Presenting concepts 4, 5 and a full sleeve design to users

Concepts 4 and 5 (Figure 22), along with a full-sleeve design, were presented to an 8-person non-OA panel to evaluate general comfort and gather feedback on both designs.

Concept 5 was the preferred choice among 6 of 8 participants. Strengths included the "open" design, which was valued for its breathability (UW-8). Furthermore, leaving the patella free was identified as a major advantage for overall comfort. Concerns were raised about the wearables open structure; users feared their toes might get caught in the gaps when putting the wearable on. The presence of elastic still in the knee hollow was a source of possible discomfort for both concepts 4 and 5.

The full sleeve: Although the concept provided good pressure distribution, it was rejected by 7 of 8 participants. It was considered too warm for daily use and likely to retain odours over time; it was also noted that the freedom of movement might be obstructed (UR-1, UR-6).

Figure 22: Concept 4 and 5 with improvement points from the non-OA panel

7.3.2 Round 2

Building on concept 5's preference, two new iterations were developed (Figure 23): concept 6 (a shorter version) and concept 7 (a longer version). In these two prototypes, the primary change was the removal of the temperature sensor on the patella (Figure 24, Adjustment 2).

Initially, a temperature sensor was also considered for placement directly on the patella as a reference sensor. For which there was fabric on the patella. Literature indicates that the most relevant temperature differences occur around the patella rather than on it (De Marziani et al., 2024). This raised the question of whether patellar placement is necessary, suggesting that sensor reduction could be achieved without loss of meaningful data. The non-OA panel participants noted that the fabric on the patella did not look comfortable in the concepts. For these reasons, the temperature sensor on the patella is eliminated.

Furthermore, the non-OA panel input indicated that no elastic should be positioned around the knee hollow; this was integrated into concept 7 by lengthening it, ensuring the elastic was positioned far above and below. Both prototypes underwent a 15-minute walking test by the researcher to assess overall comfort and stability.

Figure 23: Round 2 physical prototyping

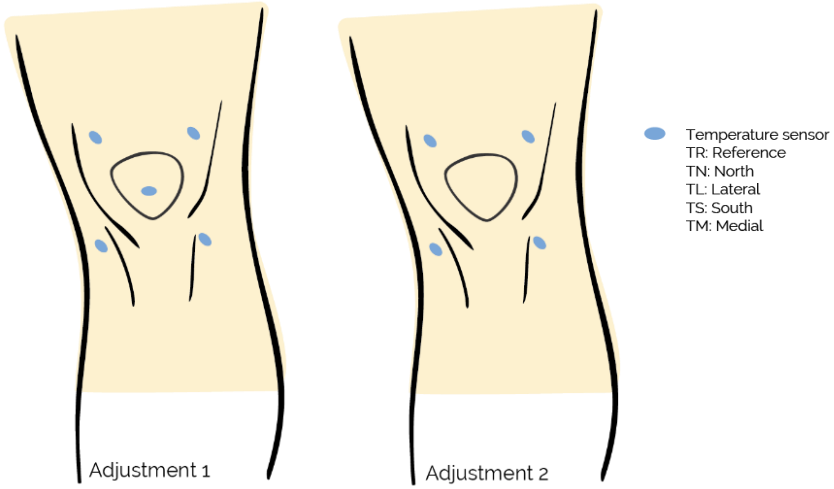

Figure 24: Removal of the temperature sensor on the patella

Results

- **Comfort:** The test confirmed that placing elastic material directly in the knee hollow indeed causes significant discomfort during movement.
- **Stability:** While the bottom band remained secure in both designs, the upper band showed a distinct difference. The longer version (concept 7) slipped significantly, whereas the shorter version (concept 6) remained almost unchanged (Figure 25).

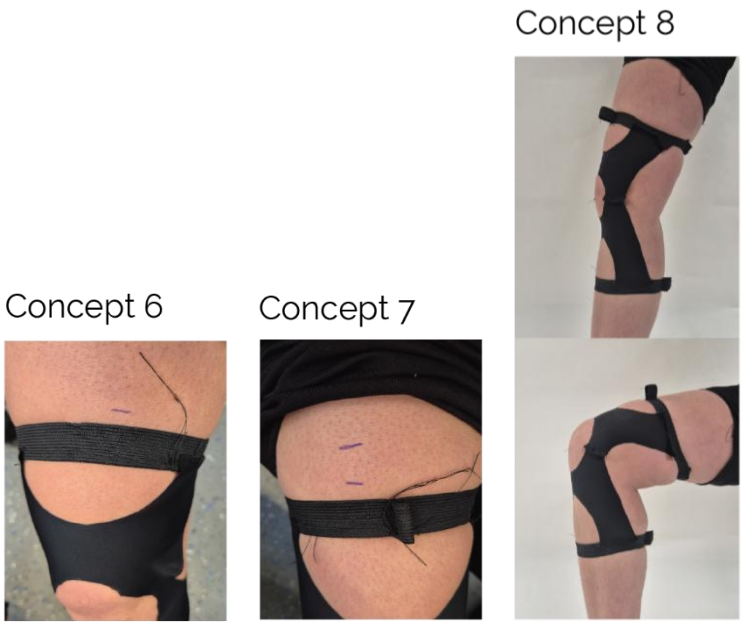

Figure 25: Results stability tests concept 6 and 7, and the merged concept 8

Based on these findings, a merged design was formulated for concept 8 (Figure 25). The bottom band was positioned lower to avoid irritation in the knee hollow, and the top band was lowered as well to prevent the slippage observed in the longer model. This combined approach ensures the wearable remains comfortable and stable (UW-4), which is essential for maintaining consistent sensor contact without requiring the user to constantly adjust it.

This merged design was again tested and worn for 4 hours by a healthy individual. At the end of the wear period, the wearable was tested against the user's comfort requirements (Appendix 3). Some takeaways were:

The wearable is comfortable, and after a period, you no longer notice it. There are enough degrees of freedom, and it fits neatly under your pants. It does not slip off. In total, for 4 hours, only 0.5 cm.

Figure 26: The side of concept 8 that is a bit loose

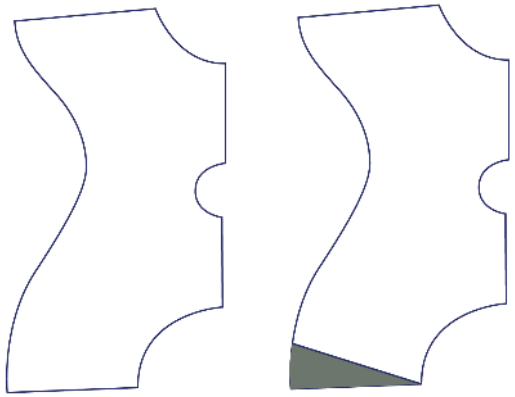

Figure 27: Pattern alteration to reduce loose sides (Gray part will be taken off)

Figure 28: Addition 1, fine mesh lining made with a panty hose

There could be an improvement on the wearables sides, as it was a bit loose (Figure 26). This could be solved by altering the fabric's pattern (Figure 27). Which is considered for the final design.

Some hiccups occurred. While putting on the wearable, the feet became stuck in the holes; however, the test participant resolved the issue themselves. It was noted: ‘’You need to know how to put it on, then this problem will probably not occur. ‘’

To reduce donning time and improve dexterity (UW-9, UR-10), a fine-mesh lining from a pantyhose was added to prevent the foot from snagging on the internal openings (Figure 28). Although this material was previously rejected for insufficient robustness, it was considered suitable here because the outer fabric absorbs mechanical stress. This addition was tested with 5 healthy subjects (fellow students). Participants were asked to don both the open-hole concept (concept 8) and the pantyhose (mesh)-covered iteration, then to qualitatively evaluate comfort and ease of use (Appendix 4). Results of the mesh addition were:

- **Ease of donning (positive):** The mesh prevented the foot from catching, making the application process significantly faster and more intuitive (UR-10).
- **Fit (positive):** The added material tension improved contouring to the leg, providing a secure tactile feel (TR-9).
- **Thermal comfort (negative):** The extra layer trapped heat and severely compromised breathability, failing the thermal management requirements (UR-6).
- **Durability (negative):** The sheer fabric was still susceptible to tearing ("ladders"), lacking the robustness required for daily wear (UR-13).

- **Learning curve:** Participants noted that after practising the donning technique for the open-hole design just once, the mesh's structural guidance became redundant.

Design decision: The addition of the mesh was consequently rejected. The negative impacts on thermal comfort and material robustness outweighed the initial usability benefits. The final design will proceed using the open-hole structure to prioritise breathability (UW-8).

7.4 Material selection

The choice of fabric is an important part of the wearables design. Throughout the prototyping process, a diverse range of materials, including T-shirt fabric (90% cotton, 5% elastane, 5% viscose), athletic textiles (90% polyester, 10% elastane), and two pantyhose structures (80% polyamide, 20% elastane/90% nylon, 10% elastane) was used. The chosen material had to comply with relevant user requirements and wishes: Breathability UW-8, Shape retention UR-13 and Flexibility UW-2.

For fabric selection, the panel was presented with 4 options (Figure 29) to rate based on their preferences and the reasons behind those preferences. The materials included fabric 1: Sports fabric (78% polyamide, 22% elastane), fabric 2: T-shirt-like fabrics (90% cotton, 5% elastane, 5% viscose), fabric 3: Spandex-like fabrics (80% polyamice, 20% elastane), and fabric 4 :Thicker sports fabrics (80% polyamice, 20% elastane).

Figure 29: Fabric options presented to panel

Panel evaluation: The results highlighted a distinct split in preference between Fabric 1 and Fabric 3:

- Fabric 1 (Flexibility): This material was preferred by some for its superior stretch capabilities and lack of skin irritation. However, it felt thicker and warmer to the touch.
- Fabric 2 (Rejected): This material was rated poorly since the sides would curl, which could be uncomfortable when wearing (not so durable for shape retention).
- Fabric 3 (Breathability and flexibility): This option was favoured for being lightweight and thin. However, some participants noted a potential downside: the thinness might make the underlying hardware palpable.
- Fabric 4 (Rejected): This material was rated poorly and subsequently dismissed due to possible skin irritation and its tendency to retain odours since the material was thicker.

Ultimately, Fabric 3 was selected for its breathability, elasticity, accessibility and non-fraying properties, eliminating the need for edge finishing. This significantly reduces bulk and prevents seam-related irritation. The resulting fit offers a smooth, irritation-free experience, comparable to that of seamless underwear.

7.5 Anti-slip elastic selection

To ensure the wearable remains securely in place and does not slide, three distinct anti-slip elastic options were evaluated (Figure 30).

Option 1: An elastic band featuring a silicone layer. This material was available from the project's onset and was utilised in the initial prototypes. Option 2: A thinner elastic with rubber threads woven through in a zigzag pattern. Option 3: A thicker material with woven rubber strands.

Initially, option 2 was favoured for its flexibility, thin profile, and breathability (UW-8). However, during a fitting test, it was observed that the top edge of the wearable tended to curl and roll over (UW-7), cutting into the skin and causing significant discomfort. To address this, the stiffer Option 3 was tested as a reinforcement. This was rejected as the material proved too rigid and uncomfortable against the thigh (UW-2).

To conclude, a hybrid configuration was selected to optimise comfort and stability. For the top edge option, 1 was applied. It provides the necessary structural rigidity to prevent rolling/curling while remaining comfortable against the skin. At the bottom, the lighter woven elastic (option 2) was applied, where curling was not an issue, resulting in a breathable, flexible finish.

Figure 30: Anti-slip elastic options

7.6 Colour and visual design

In addition to the material selection, the panel was shown a range of colour options in a concept to gauge aesthetic preferences (Figure 31). The results from this part were:

- Function over fashion: Participants emphasised that price and comfort are far more critical than a wide colour spectrum.
- Palette preference: There is a demand for neutral options, such as black or grey, to ensure the wearable remains discreet under clothing. However, keeping it away from a medical-like feel (UW-11). Bright colours were suggested only as a potential secondary option, for example, for children.
- Usability: A clear visual indicator distinguishing the top of the wearable from the bottom was recommended to prevent misuse (UW-10).

Based on these insights, the decision was made to exclude further colour exploration and produce the wearable in black.

Selecting black meets the user requirement for aesthetic (UW-11) and simplifies the manufacturing process, keeping costs lower (for later implementation). Furthermore, feedback on the "top/bottom" indicator is a critical design input; a visual marker, such as a small, coloured tag or logo, could be integrated to help the user orient the sleeve correctly, ensuring the sensors are positioned over the correct anatomical landmarks. It is thought that the casing alone could be a sufficient indicator, as could the open circle around the knee.

Figure 31: Colour options presented to panel

Relevance for the wearable

Based on the researcher's iterative design evaluations, non-OA panel feedback, and testing with one other student. The physical form and material composition of the wearable have been finalised (Figure 32). The definitive design choices are as follows:

- **Form factor:** Concept 8 is the structural design.
- **Material and grip:** Fabric 3 has been selected as the primary textile base due to its favourable stretch and comfort properties. To prevent the wearable from sliding down during daily activities (a critical requirement for 16-hour use), Anti-Slip options 1 and 2 will be integrated.
- **Aesthetics:** The colour black was chosen for the exterior. This ensures a sporty, unobtrusive appearance, intentionally moving away from the stigmatising look of traditional, skin-coloured medical devices.

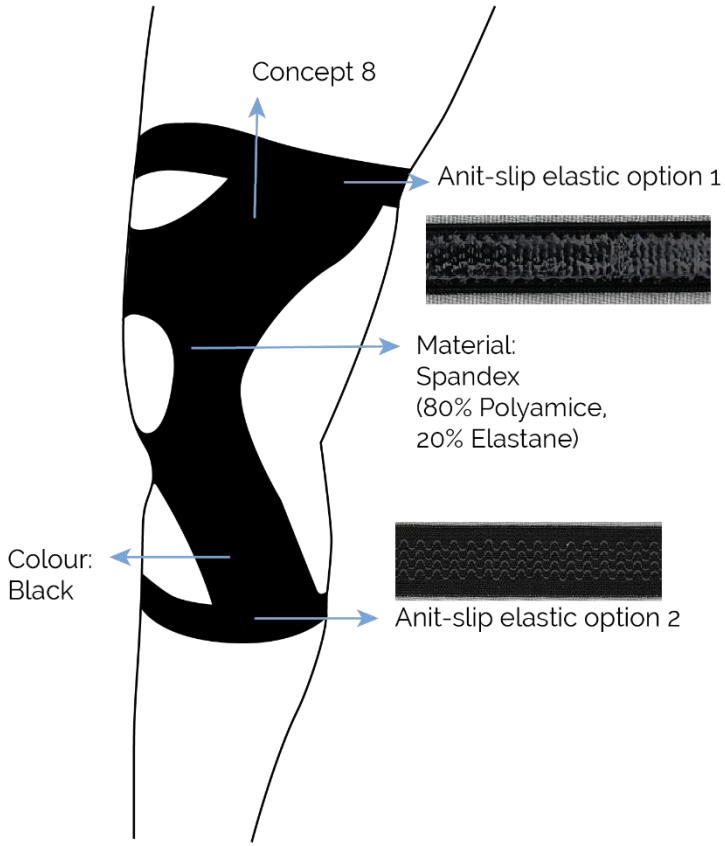

Figure 32: Wearables design

8 Hardware

8.1 Processor

For this wearable, multiple processors were used across different stages of the project. First, an Arduino lotus was used. First codes were tested, and a better understanding of the circuit was gained. Since the Arduino lotus was too large (UW-13) and smaller options were available, the XIAO NRF 2840 sense microcontroller was considered, which was significantly smaller (Figure 33). An advantage of this processor was its Bluetooth Low Energy (BLE) data transmission, and a Pulse-Density Modulation (PDM) microphone was attached, enabling the first tests to detect crepitus. However, this XIAO had some limitations:

- For sending via BLE, the maximum number of bytes per package is 20 bytes, and a maximum of 200 packets could be sent via BLE per second. As a result, not all the required data can be processed for optimal filtering (TR-5).
- The PDM microphone was in a fixed position, and a 16 kHz output sample rate was the maximum; 40 kHz is needed for the airborne microphones (TR-7).
- If an additional airborne microphone will be used, for the optimal placement of the sensor (TR-6), there is no I2S input available on the XIAO NRF 2840 sense.

For these reasons, the switch was made to a XIAO ESP32 S3. This processor included Wi-Fi as a means of sending samples and supported an I2S input, which is essential for connecting a microphone.

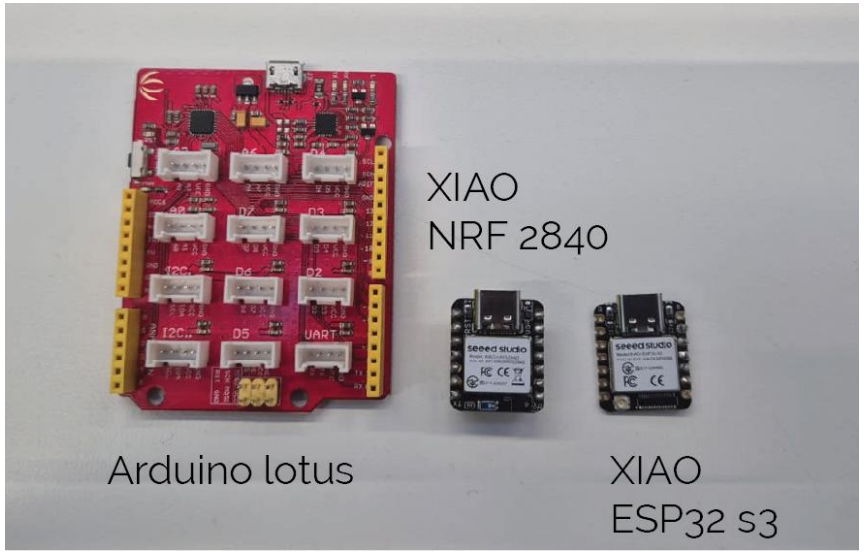

Figure 33: Processor options throughout the project

8.2 Battery and switch

During early testing, an external power bank supplied power to the processor and its sensors. Although suitable for prototyping, this solution was too large and impractical for a wearable application (UW-13). In comparable small-scale wearables, such as smartwatches, lithium-based batteries are commonly used due to their high energy density and compact form factor (Leroux, 2025).

For the proof-of-concept, it was stated that the wearable only needs to operate for two hours (TR-1). For this, a small LiPo battery with sufficient capacity was selected (UW-13). This was a 155 mAh LiPo battery.

To manage the power, a physical switch was integrated into the circuit between the battery and the microcontroller. This addition allows the power supply to be easily turned off and on, enabling the user to turn the wearable on and off without physically disconnecting the battery. There was also an option to use a button to switch the XIAO on and standby; however, this button required a digital pin, and as described later, all pins were used for other, more important sensors, so this option was not implemented.

8.3 Selection of acoustic sensor

Based on the literature review, airborne microphones were identified as the most suitable choice for a textile-based, non-invasive knee-wearable. A primary challenge of designing a wearable for everyday use is that continuous skin contact cannot be guaranteed. Contact microphones are sensitive to this and lose functionality when contact is broken. In contrast, airborne microphones do not rely on direct skin contact, making them significantly more reliable. Furthermore, they are lightweight and have already been successfully validated in prior wearable studies for knee OA (Teague et al., 2016; Toreyin et al., 2016).

In addition to the literature findings, the use of airborne microphones was informed by expert input. J.P.R. Thevenot has implemented airborne microphones in the Sensemodi knee-wearable, further validating this sensor type for real-world wearable applications. Based on both literature evidence and expert experience, the decision was made to proceed with airborne microphones for this project.

8.3.1 Initial sensor testing and limitations

At the start of the development phase, the built-in PDM microphone of the XIAO NRF microcontroller was selected for preliminary testing. This choice was motivated by ease of prototyping and direct compatibility with the development

platform. However, as previously mentioned, early testing revealed some limitations.

According to the literature, airborne acoustic emissions associated with knee crepitus are typically filtered in the higher-frequency range, typically between 10 kHz and 20 kHz (Teague et al., 2016; Toreyin et al., 2016). As a result, the PDM microphone on the XIAO cannot accurately capture the desired frequency range, as a sampling rate of at least 40 kHz is required to meet the Nyquist criteria (TR-7).

An additional limitation of the integrated PDM microphone is its fixed position on the XIAO NRF. Since the optimal placement of the acoustic sensor may differ from that of the microcontroller, this reduces design flexibility and limits wearable integration (TR-6). For these reasons, the built-in PDM microphone was deemed unsuitable for further development beyond initial feasibility testing.

8.3.2 Sensor requirements and selection criteria

The selection of the acoustic sensor was guided by the following key requirements:

- The sensor must be as small as possible to allow integration into a soft, textile-based wearable (UW-13).
- The sensor must support a high sampling rate (at least 40 kHz) to enable filtering in the 10-20 kHz range (TR-7).
- The sensor must be suitable for rapid prototyping, as standalone MEMS microphones are too small for manual soldering (TR-2).

To address these requirements, the use of MEMS microphones on breakout boards was explored. Breakout boards allow reliable prototyping while maintaining a form factor that remains relevant for future miniaturisation. But breakout boards have a limited range of sensors. So, a breakout board with a MEMS and a sampling rate of at least 44.1 kHz (TR-7) was specifically sought: the ICS-43434-FX. For this sensor, three breakout board options were considered (Figure 34):

- **Option 1:** A MEMS microphone on flexible plastic, which aligns well with future wearable integration, but is more challenging to prototype, and it is quite expensive, with a price of € 55,90.

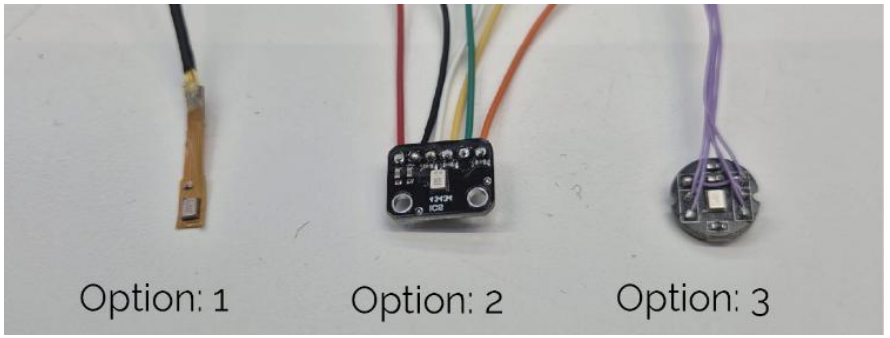

Figure 34: Acoustic sensor housing options

- **Option 2:** A square breakout board, offering good solderability and stability during testing, with a price of € 5,50.
- **Option 3:** A round breakout board, the same as option 2 but round, with a price of € 7,20.

Option 3 was selected for the iterative development process. This option was preferred because it had smooth contours without sharp edges, thereby preventing possible fabric damage and user skin irritation (UR-5). Furthermore, it allowed for rapid prototyping and easy access to components for adjustments (TR-2). Option 1 was rejected for this phase because it proved too fragile for active testing and modifications.

While too delicate for the development phase, option 1 offers a more realistic and compact profile suitable for a finished product. In a mass-manufactured "real-life" setting, the structural weaknesses observed during manual prototyping are minimised by industrial manufacturing methods, making option 1 the best and most realistic choice for the final design. However, price needs to be considered, as this option is quite expensive.

8.3.3 Placement acoustic sensor

The literature shows that in most cases, sensors are placed on both the medial and lateral sides to improve accuracy or to compare results. And for the optimal placement, Karpiński et al. (2024) conclude that the medial compartment below the midline of the patella is the best. To merge these findings, two possible placements for the acoustic sensor have been identified. The medial and lateral compartment blow the midline of the patella Figure 35.

It is important to note that the findings of Karpiński et al. (2024) are based on clinical lab setups. In such controlled environments, practical factors such as noise from clothing are often not considered. However, in real-world scenarios, the friction between trousers and the knee while walking generates significant acoustic noise that can interfere with the signal.

To determine the optimal placement of the acoustic sensor in a real-world setting, a test was conducted. Using a prototype, the sensor was placed on both the lateral and medial sides of the patella, on a healthy individual (the researcher). Acoustic data was recorded for 60 seconds while walking in a figure-of-eight pattern. To measure the impact of fabric friction, this test was performed both with and without long trousers. The data were evaluated using three distinct methods to determine the most suitable sensor placement as described on the next page.

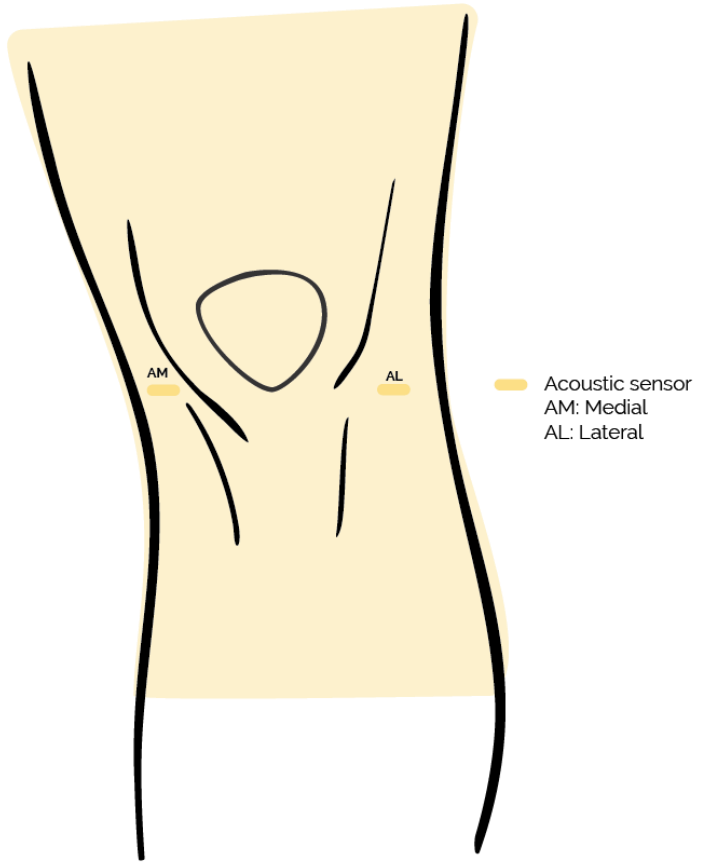

Figure 35: Options placement acoustic sensors

General RMS analysis (broadband)

The first method utilises a standard Root Mean Square (RMS) calculation with a 50 ms window to assess the overall signal energy across the full frequency spectrum. This approach provides a "big picture" view of the acoustic environment, making it easy to identify how clothing interference (trousers) significantly increases the noise floor relative to skin-only measurements. The results are displayed for 2 distinct locations: the medial and lateral sides of both the left and right knee, with and without trousers (Figure 36), however no big differences could be found between the lateral and the medial placement.

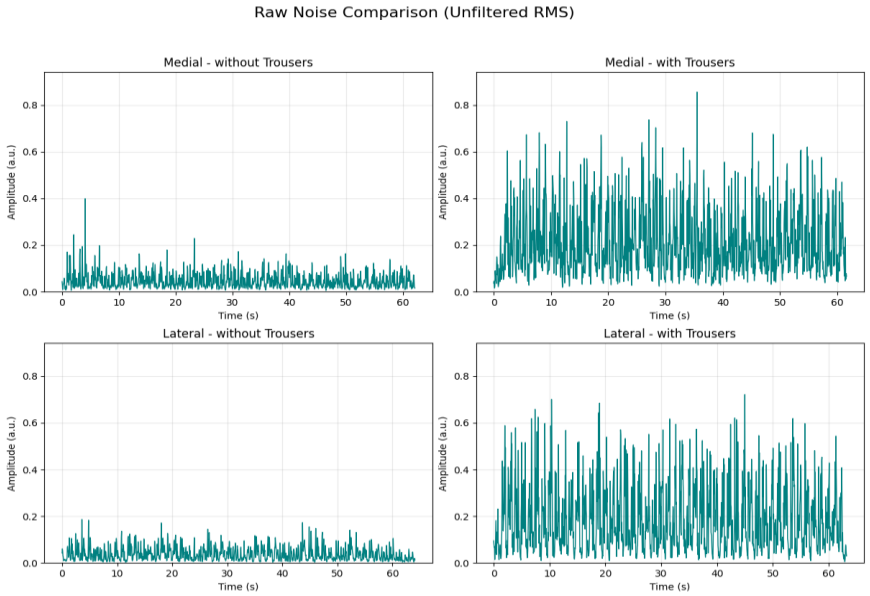

Figure 36: RSM Analysis, with and without trousers, medial vs lateral. Showing that walking with trousers generates more acoustic energy

Hilbert envelope application

The second method uses a Hilbert transform to extract the amplitude envelope of the raw acoustic signal (Figure 37). As demonstrated by Teague et al. (2016) in their work on wearable joint health assessment, it is essential to isolate short-duration, high-frequency joint sounds (crepitus) from continuous background and interface noise, such as fabric friction. Building upon their signal-processing framework, which relies on envelope detection, this project uses the Hilbert transform to achieve the extraction. This mathematical method clarifies the timing of the sounds. It converts the rapid sound waves of the

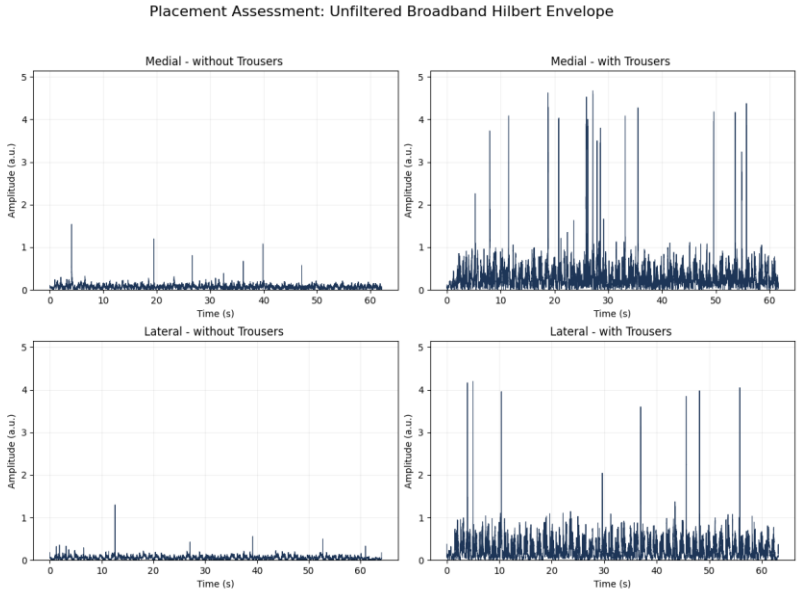

Figure 37: Hilbert envelope. Showing that trousers generate more acoustic energy, and the medial side shows more unpredictable peaks, indicating more noise

joint into a smooth, interpretable curve. This is done by drawing an outline over the loudest points of the sound, ignoring the messy up-and-down movements of the raw audio. As with the RMS analysis, the resulting envelopes are evaluated at two locations on the medial and lateral sides of both the left and right knees under both clothed and unclothed conditions to determine which placement yields the most noise.

Targeted frequency filtering (Toreyin and Teague Method)

The third method combines elements from the methods established by Toreyin et al. (2016) and Teague et al. (2016). The Python script processes the audio through the following specific steps (Figure 38).

- Bandpass filter: The signal is processed by a bandpass filter to isolate frequencies between 10-20 kHz. This removes low-frequency movement artefacts (<1.5 kHz) and skin-sensor rubbing noise (<5 kHz).
- Hilbert Envelope: Instead of using a standard RMS calculation, the code computes the envelope by applying the Hilbert transform to the bandpass-filtered signal (10-20 kHz).

The Hilbert envelope effectively traces the peaks of these rapid vibrations, converting the chaotic audio into a smooth energy curve. This enables precise detection of the timing and magnitude of impulsive crepitus events.

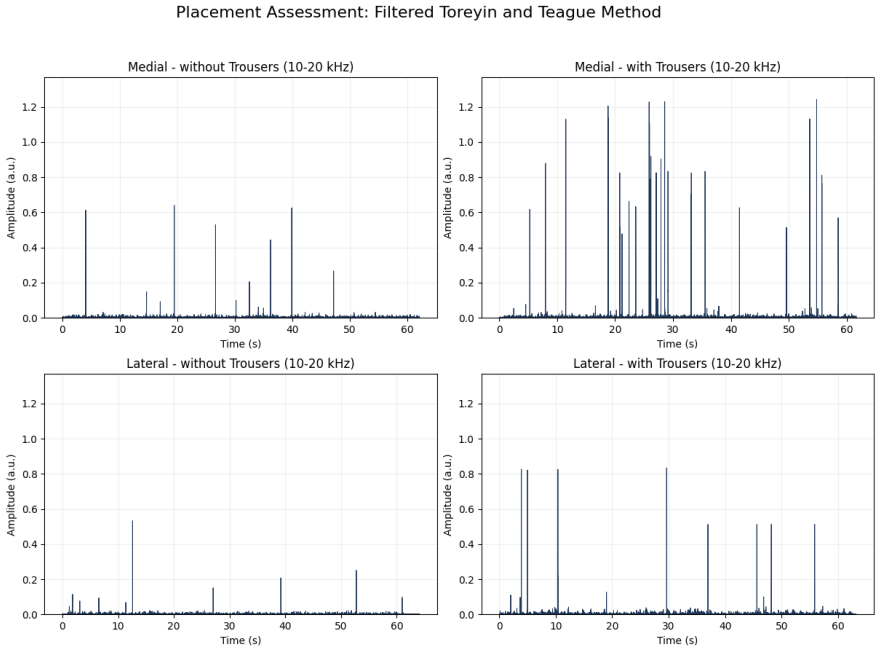

Figure 38: Toreyin and Teague method of filtering, with and without trousers, medial vs lateral. Showing the filtered data, again indicating that the medial side with trousers has the noisiest surroundings as it has the most peaks

Data analysis

The RSM graphs demonstrate that wearing trousers introduces significant background noise. However, the general RMS analysis shows little distinction between the medial and lateral sides, whereas the Hilbert envelope data reveal a clearer contrast between them. Furthermore, adding a bandpass filter to the targeted-frequency filtering method suppresses surrounding

noise; however, not all peaks are suppressed. The medial side shows frequent peaks, confirming that friction, such as mechanical artefacts (ticking on the microphone) and thus noise, is higher on the medial side where the trousers cross when walking, meaning less accurate data can be acquired from this placement. In contrast, the lateral side shows less interference. The code used to generate these graphs can be found in Appendix 5.

Conclusion and relevance to design

Consequently, the lateral side of the knee was selected for the acoustic sensor. This placement minimises noise at the source, ensuring the wearable captures cleaner data and reducing the need for excessive software filtering in the project's final design.

8.4 Selection of temperature sensor

The selection for the temperature sensor is divided into two distinct parts. Preliminary research and measurement reports indicate that conductive yarns (smart textiles) are a viable option for directly integrating temperature measurement into the fabric. However, to ensure reliability, a standard commercial sensor has also been selected, as a fallback solution should the yarns prove insufficiently sensitive for clinical monitoring.

8.4.1 Temperature sensor

For this project, a Negative Temperature Coefficient (NTC) thermistor was selected, as it has been successfully used in similar skin-monitoring applications (Billings et al., 2024; Faisal et al., 2020; Chen et al., 2010).

NTC sensors are small, cost-effective, and offer high sensitivity within the target range (TR-8). They are suitable for textile integration and can be embedded directly into the wearable. Based on the literature, the sensor must detect temperature changes as small as 1 °C, since temperature changes may be minimal.

For the NTC, a 10 kΩ is chosen because it is a usable value at 25 °C. They are relatively inexpensive, compatible with Arduino, and widely available.

At lower resistances (1 kΩ), the sensor draws a large current, which can lead to self-heating and measurement errors. At higher resistances (100 kΩ), the sensor produces very small voltage changes and is more sensitive to noise, which can lead to poor accuracy without stable electronics (Fraden, 2016). 10 kΩ is "in the middle": low self-heating yet still a good signal-to-noise ratio.

For this sensor, a RS PRO Thermistor, 10kΩ Resistance, NTC Type, 2.4 × 63.5mm (RS PRO, n.d) was chosen.

Validation

To verify if the selected RS PRO sensor meets the required thermal range and accuracy (TR-8), a noise analysis was conducted. The sensor was tested over a period of 60 seconds with a high sample rate (not fixed) frequency, resulting in a dataset of over 1 million data points. 8 measurements were done in two rounds, round 1 was on room temperature, and round 2 was on a hotplate in a controlled environment. Both tables with the results of these measurements can be found in Appendix 6.

The validation focused on the standard deviation σ, which quantifies the spread of the data points around the mean temperature. The corresponding code is provided in Appendix 6.

Results

The results highlighted a significant difference between the two conditions. In ambient air (round 1), the signal was noisy, possibly due to air circulation, with a standard deviation of 0.25 °C. When placed on the hotplate (round 2), the stability improved, with the standard deviation dropping to 0.114 °C. Applying the normal distribution rule (3σ) to the contact data (3 × 0.114 = 0.342 °C) confirms that 99.99% of the measurements fall within the project's required accuracy range of ±0.5 °C.

These findings resulted in two technical requirements:

- Physical fit: The instability in open air confirms that consistent skin contact is vital. The wearable must be designed with a tight, compressive fit to eliminate air gaps (TR-9).
- Software filtering: While the data with good contact are statistically reliable, peak-to-peak noise persists. Therefore, software filtering (such as a moving average) is essential to smooth the raw signal before presenting it to the user (TW-4).

8.4.2 Conductive yarn as a temperature sensor

Inspired by the potential of fully textile-integrated temperature monitoring as described by Lugoda et al. (2020) and Soukup et al. (2014), an initial feasibility study was conducted to explore conductive yarns as temperature sensors for the knee-wearable. To bypass the complex industrial fabrication steps typically required, this project investigated whether commercially available, off-the-shelf conductive yarns could function as reliable temperature sensors.

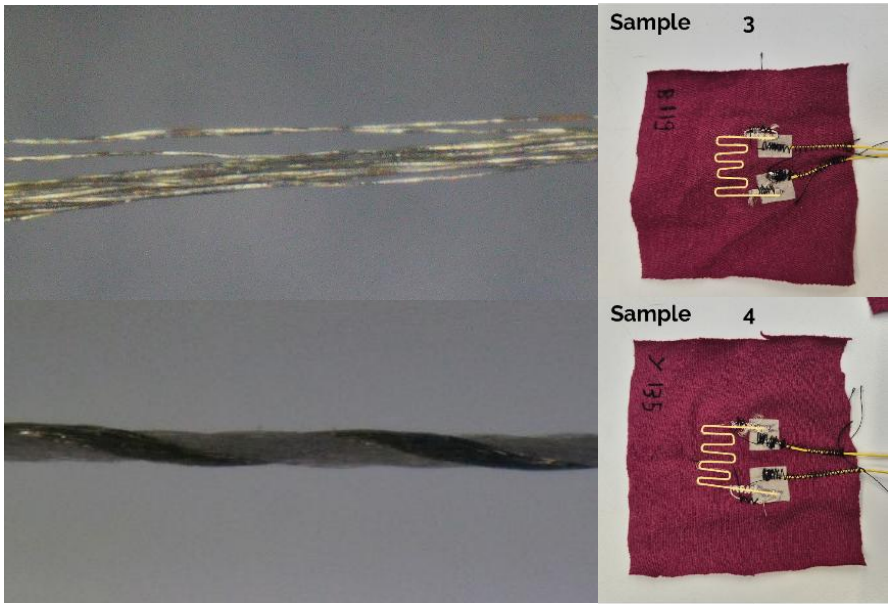

Figure 39: Selected yarns with corresponding sample, up: Shieldex 78f20, down: Silver-Tech RNNT7

According to the literature review, conductive yarns emerged as a promising approach to achieving non-invasive temperature monitoring in textiles. To assess whether the conductive yarns available at TU Delft are sensitive to temperature changes, a series of preliminary measurements was conducted prior to this project. Based on these measurements, two yarns were selected for further research: Shieldex 78f20 and Silver-Tech RNNT7 (Figure 39). These yarns showed the steepest resistance-temperature slope and the most linear response.

The test

Multiple textile integration methods (sewing, twisting, and embroidery) were made and tested on a controlled hotplate. Initial trials quickly revealed that structural manipulations (twisting and embroidery) degraded the electrical predictability of the yarns. Therefore, the primary validation focused on the baseline sewn samples: Sample 3 (Shieldex) and Sample 4 (Silver-Tech). Detailed methodology, setups, and data for the other variations (samples 5-8) are available in Appendix 7.

For samples 3 and 4, 2 relevant tests were conducted on a hotplate: 1 from 25-45 °C with 5 °C increments, and 1 from 25-30 °C with 1 °C increments.

Measurement 1 - Samples 3 and 4

From measurement 1 of samples 3 and 4 (Figure 40, Table 5), it became clear that the Silver-Tech yarn showed a very low slope and poor linearity, making it unsuitable for accurate temperature sensing. The shieldex yarn had a bigger slope, which looked more promising. However, the noise of the resistance is as big as the slope, so no accurate temperature measurements could be taken.

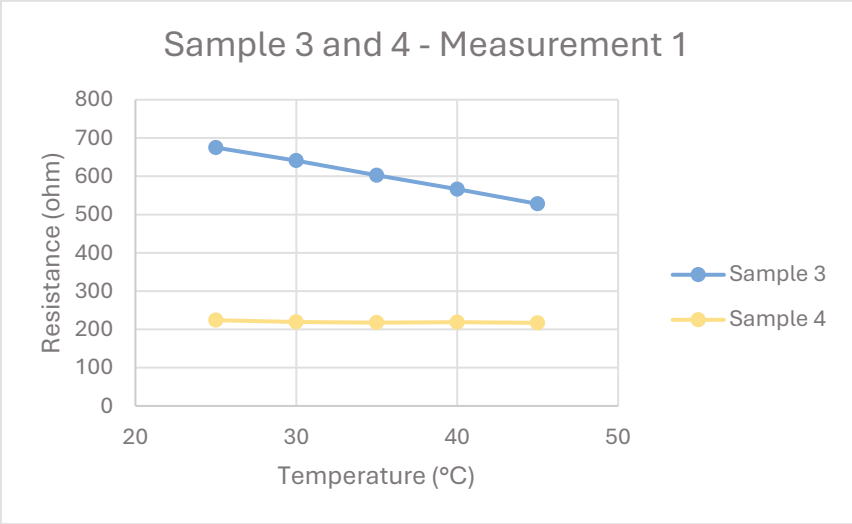

Figure 40: Sample 3 and 4 measurement 1, showing sample 3 has a bigger slope

Table 5: Measurement 1 of samples 3 and 4

M1	Slope (dR/dT) (Ω/°C)	Linearity	Noise at 25 °C (Ω)	Resistance at 25 °C (Ω)
S3 (Shieldex)	7.35	Very	7.6	674.98
S4 (Silver tech)	0.35	Not so linear	5.73	224.04

Measurement 2 - Samples 3 and 4

As shown in Table 6, the second measurement confirms the absence of a linear temperature response for Sample 4 (Silver-Tech), rendering it unusable. Furthermore, while Sample 3 (Shieldex) remained linear, its sensitivity slope unpredictably doubled to 14.62 Ω/°C compared to the first measurement, indicating possible mechanical or electrical instability (Figure 41, p. 83).

Table 7 further highlights the lack of reproducibility in Sample 3 (Shieldex). At a constant temperature of 30 °C, the resistance differed by more than 47 Ω between the two measurement sessions, indicating that the yarn did not have stable resistance readings.

Table 6: Measurement 2 - Samples 3 and 4

M2	Slope (dR/dT) (Ω/°C)	Linearity	Noise at 25 °C (Ω)	Resistance at 25 °C (Ω)
S3	14.62	Very	2.95	666.49
S4	-	Not Linear	3.8	215.63

Table 7: Comparison of resistance at 30 °C - Sample 3

M1 S3 resistance at 30 °C (Ω)	M2 S3 resistance at 30 °C (Ω)
640.88	593.39

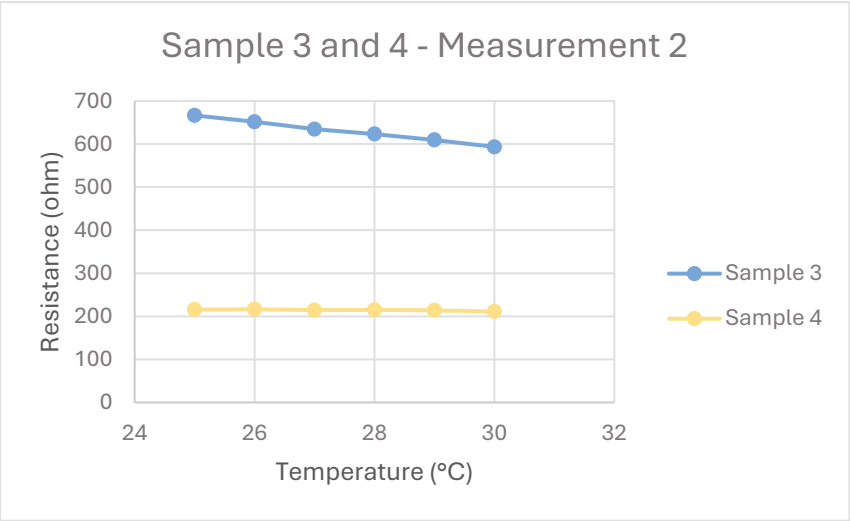

Figure 41: Sample 3 and 4 measurement 2, showing the slope is not as steep as desired for accurate temperature measurements

The results demonstrated critical material instabilities. Sample 4 (Silver-Tech) exhibited poor linearity. While Sample 3 (Shieldex) initially responded to temperature changes, its behaviour proved inconsistent across the two measurements. For example, its sensitivity slope unpredictably doubled from 7.4 Ω/°C to 14.6 Ω/°C between identical tests, and its baseline resistance at a constant 30 °C differed by over 47 Ω.

Conclusion

Consequently, with this measurement setup, the conductive yarns cannot guarantee the required 1 °C precision for this project (TR-8). The concept was therefore rejected for this project. So the selected NTC thermistors will be implemented. Exploring conductive yarns remains recommended for future iterations, pending improvements in material predictability, test setup, and connection stability.

8.5 Addition of SD card module

When sending acoustic data via Wi-Fi, it was decided to add an SD card module because the sensor's high sampling rate exceeded XIAO's internal buffer capacity during brief Wi-Fi interruptions. The SD card module's integration uses specific microcontroller communication pins, which conflicted with the available pins for the NTC sensors. Three solutions were evaluated:

1. Accept data loss (rejected): Missing acoustic data makes the recorded data unusable for accurate filtering (TR-5).
2. Add external hardware (rejected): Adding extra breakout boards increases size and complexity, violating the wish for a compact design (UW-13).
3. Reduce sensor count (selected): One NTC sensor is removed to free up one pin needed for the SD card module.

The decision was made to proceed with four NTC sensors (Figure 42) (when one is for environmental sensing). This choice prioritises acoustic data reliability (TR-5) over the temperature map's maximum resolution. In a future mass-produced version with a custom PCB, this pin limitation could be resolved, thereby enabling the reintroduction of the fourth temperature sensor.

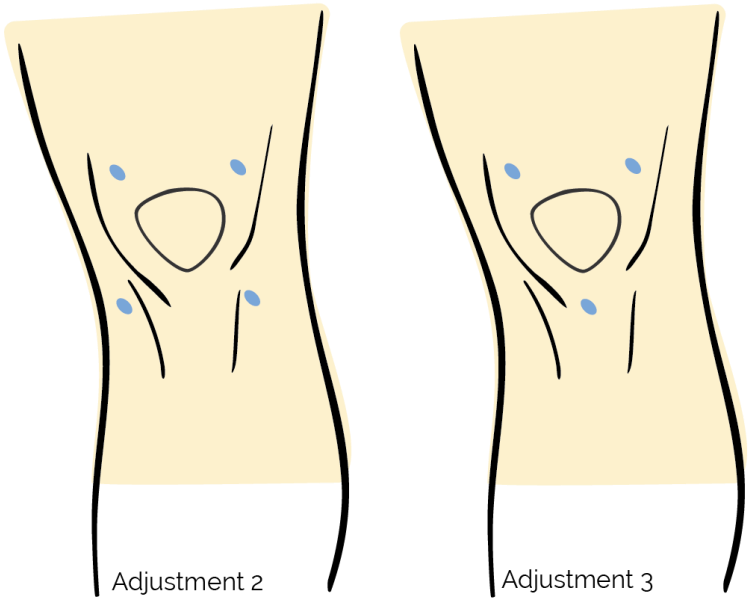

Figure 42: Final adjustment placement temperature sensor

It is important to note that this decision was made only during the visualisation/connection of the data. In the following steps, the SD card module has not yet been integrated. However, during the SD card module integration, no additional issues were encountered with the selected concepts in the development phase. The main change was that the final hardware turned out to be a bit larger than initially thought. For external storage, the

required MicroSD card capacity must be determined to ensure it is sufficient for 2 hours (TR-5). For this the data rate was calculated based on the acoustic sensor's 16-bit recording (1 byte = 8 bits, so 16 bits are 2 bytes), which was deemed sufficient for the ‘’noisy surroundings’’ when worn with trousers.

$$R = f_s \times B_d$$

$$R_{acoustic} = 48{,}000 \frac{samples}{s} \times 2 \ \frac{bytes}{sample} = 96 \frac{kB}{s}$$

$$R_{temperature} = 8 \ \frac{samples}{s} \times 2 \frac{bytes}{sample} = 16 \frac{B}{s}$$

Given that the acoustic data stream is 6,000 times larger than the thermal data stream (96 kB/s vs 16 B/s), the temperature data is excluded from the capacity calculation.

$$V_{volume(hour)} = 96 \frac{kB}{s} \times 3{,}600 \ s = 345.6 \frac{MB}{h} \times 2 = 691.2 \ MB$$

To conclude, a standard 16 GB microSD card is more than sufficient to store the 691.2 MB required for 2 hours of proof-of-concept testing (TR-1). 16 GB is even enough to store 46 hours of data.

8.6 Final placement of sensors

Throughout the project, sensor placement was adjusted in response to specific limitations and insights. These adjustments are briefly described and visualised in Figure 43.

1. Rotation for better contact: During movement tests of the designed wearable, it was observed that when the knee is flexed, gaps appear between the skin and the wearable, compromising sensor-skin contact (TR-9). To address this, the sensors were rotated by approximately 22 degrees. This position aligns with the anatomy of the knee, ensuring continuous contact during movement.
2. Removal of the reference sensor on the patella: Initially, a sensor was placed directly on the centre of the patella. However, literature indicates that the most relevant temperature differences occur around the patella rather than on it (De Marziani et al., 2024). Furthermore, test participants reported that covering the kneecap with fabric and sensors looked uncomfortable. Therefore, the decision was made to remove this sensor.
3. Reduction to 3 NTC sensors around the patella. Finally, a hardware limitation necessitated reducing the number of sensors from four to three. During testing, Wi-Fi instability caused data loss in the acoustic signals. To ensure reliable data analysis, an additional storage buffer was required.

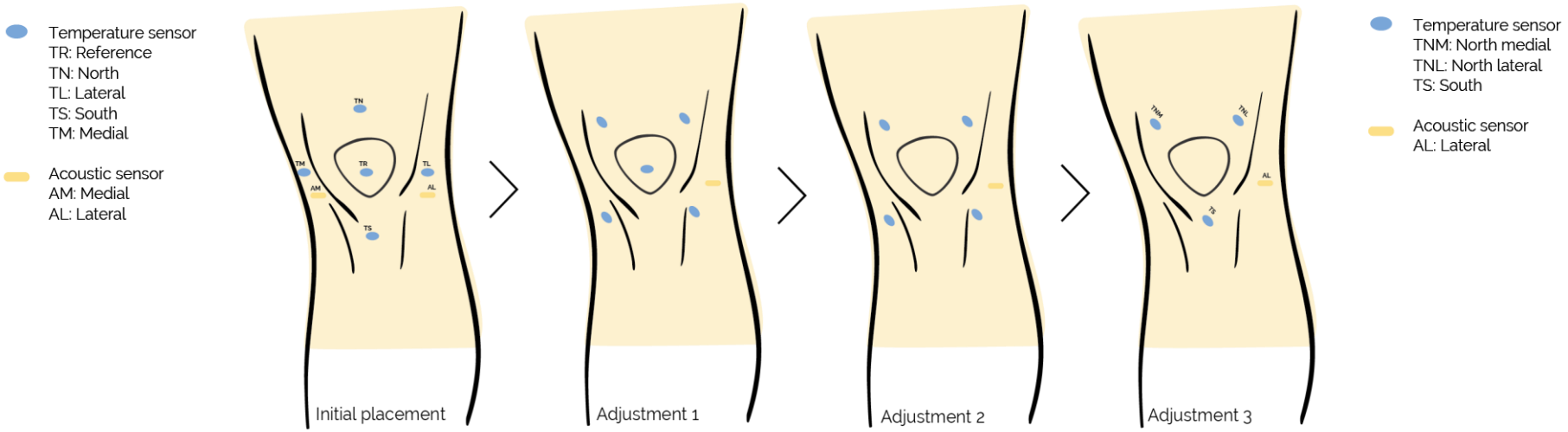

Figure 43: Placement sensors throughout the project

Relevance for the wearable

Based on the evaluations and component tests detailed in this chapter, the definitive hardware for the proof-of-concept has been established. The final system composition and strategic design choices are as follows (Figure 44):

- **Microcontroller and storage:** The XIAO ESP32-S3 was selected as the processor due to its compact form and processing capabilities. To ensure reliable, continuous data logging without data loss, an external MicroSD card module has been added to the system.
- **Power supply & control:** The current prototype will be powered by a 155 mAh (3.7 V) LiPo battery, integrated with a physical hardware switch for direct user control over the power state.
- **Thermal sensor:** The RS PRO 10 kΩ NTC Thermistor is chosen as the primary temperature sensor.
- **Sensor placement:** The anatomical positioning of the sensors has been finalised according to the adjustment 3 configuration on p. 86.
- **Acoustic sensor:** For the prototyping phase (the proof-of-concept), the round breakout board will be utilised. However, for the development of a final, clinical-grade wearable, transitioning to option 1 is recommended.

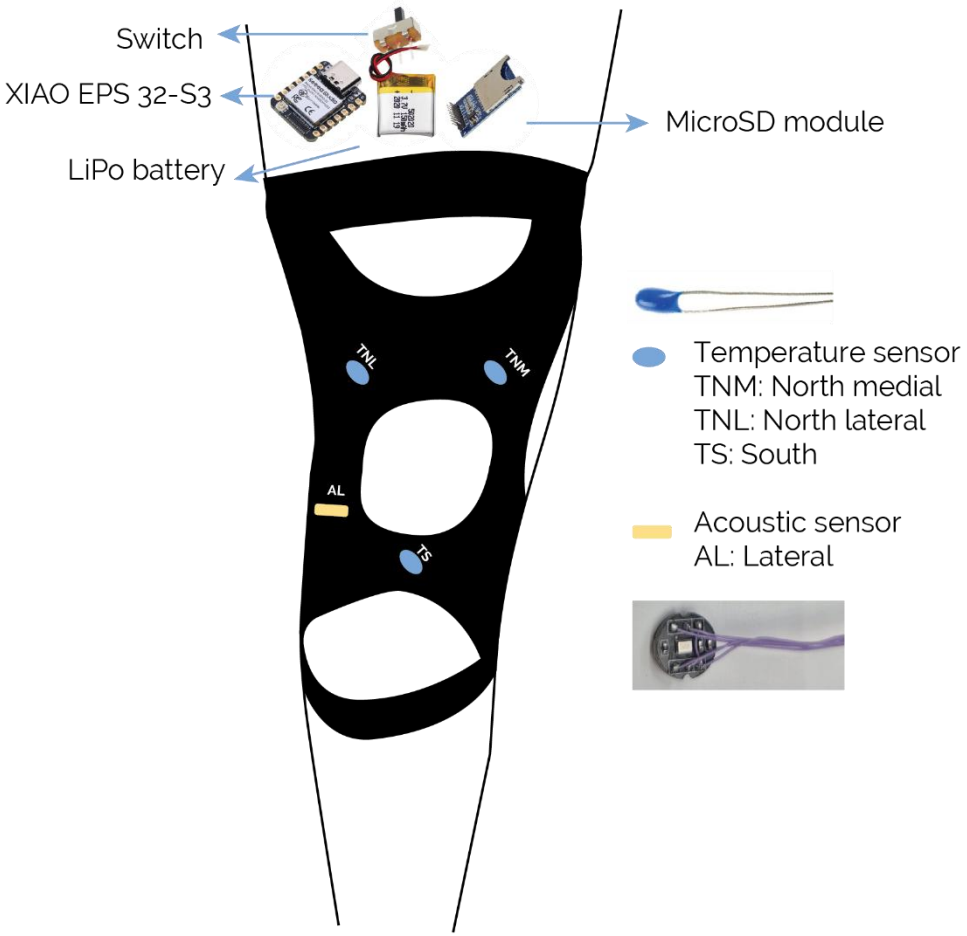

Figure 44: Chosen components and placement

9 Connection hardware to the wearable

In this chapter, the hardware will be integrated into the designed wearable.

9.1 Placement of microcontroller and battery

As the placement of the acoustic sensor and temperature sensors is determined in the previous hardware chapter, only the placement of the microcontroller (XIAO) and the battery needs to be decided. To determine the optimal placement of the XIAO and battery, different positions on the upper and lower legs were evaluated using the user panel (Figure 45). Their responses could be divided into two categories.

Comfort and tissue

Panel participants expressed a strong preference for the upper leg over the lower leg (shin). The upper leg contains more soft tissue (muscle and fat), which acts as a natural cushion. This significantly reduces the sensation of hard components pressing or "poking" against the bones, a common complaint with lower-leg placement.

Stability and mobility

Regarding stability, the upper lateral (outer) side was identified as the most suitable location. This area experiences less intense muscle deformation than the front of the thigh (quadriceps) or the calf, and the placement was not in the way during walking (UR-3). Helping the hardware remain stable during walking.

Based on these findings, the decision was made to position the hardware housing on the upper lateral side of the wearable. This location offers the best balance between wearer comfort (cushioning) and mechanical stability, while keeping the joint itself unobstructed.

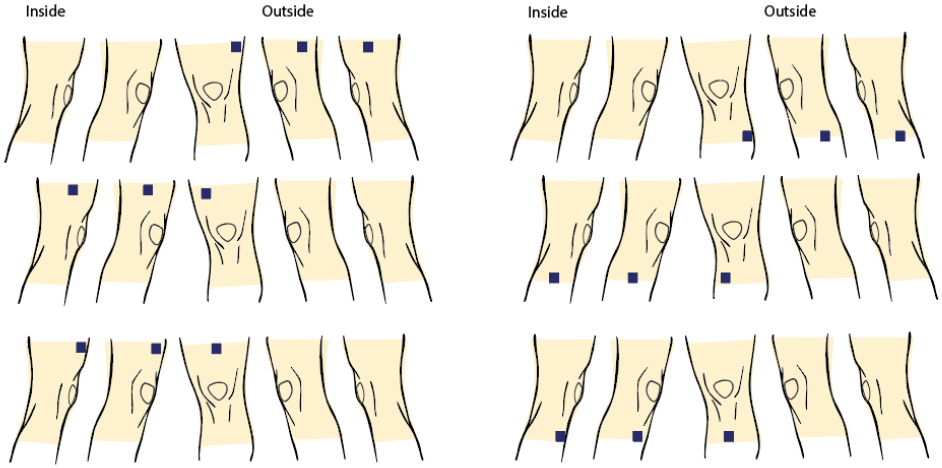

Figure 45: Placement options of hardware

9.2 Wiring with conductive yarn

To replace flexible, insulated copper wires, conductive yarns can be used, which, according to the literature, are an effective, non-invasive way to integrate technology into wearables (Chen et al., 2010). For the NTCs, this is specifically interesting since they are distributed throughout the wearable. Different iterations have been conducted using different yarn types. Also, the transition from the XIAO to the design required multiple iterations to find a stress-free connection.

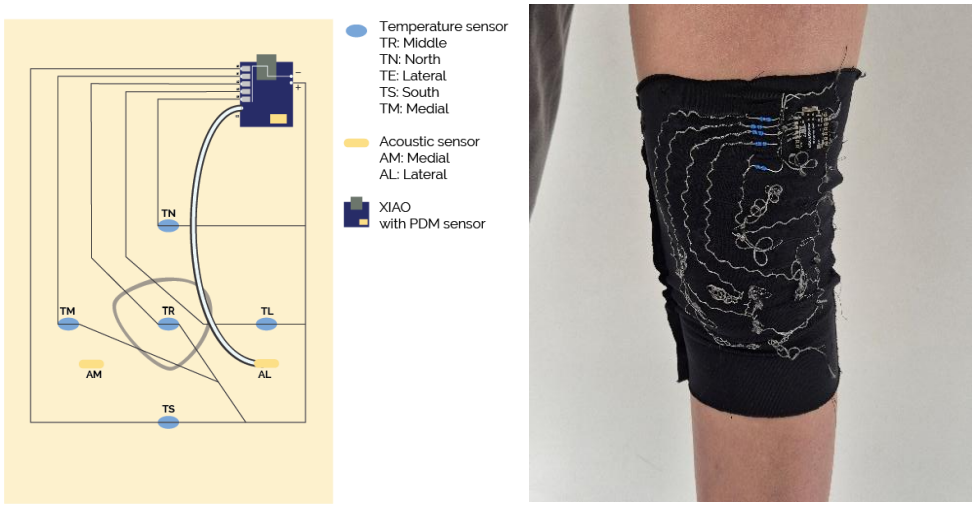

Figure 46: Initial wiring, left: Wiring outline, right: Wiring with conductive yarn

9.2.1 Phase 1: The full sleeve prototype

Initial wiring concepts were explored using a standard sock as a base foundation. This approach provided a low-fidelity platform to test routing options and sewing techniques without using the expensive fabric for the final wearable. For wiring with conductive yarn, note that the yarn was not insulated; therefore, it could not touch other wires, as this would disturb the measured resistance. Therefore, a wiring outline was created (Figure 46).

9.2.2 Phase 2: Adaptation to sensor placement

As the optimal locations for the NTCs shifted, the conductive yarn routing had to be adjusted. Initially, the wiring followed a five-sensor layout. However, following the decision to reduce the system to withhold the NTC on the patella and limit pins on the XIAO to three NTCs, and the finalisation of the hardware housing location, a new wiring overview was developed (Figure 47, p. 90). The wiring solutions were developed around the sensor and hardware locations, rather than adjusting sensor placement to fit easier wiring paths. This ensures that the data collection points remain correct (TW-8).

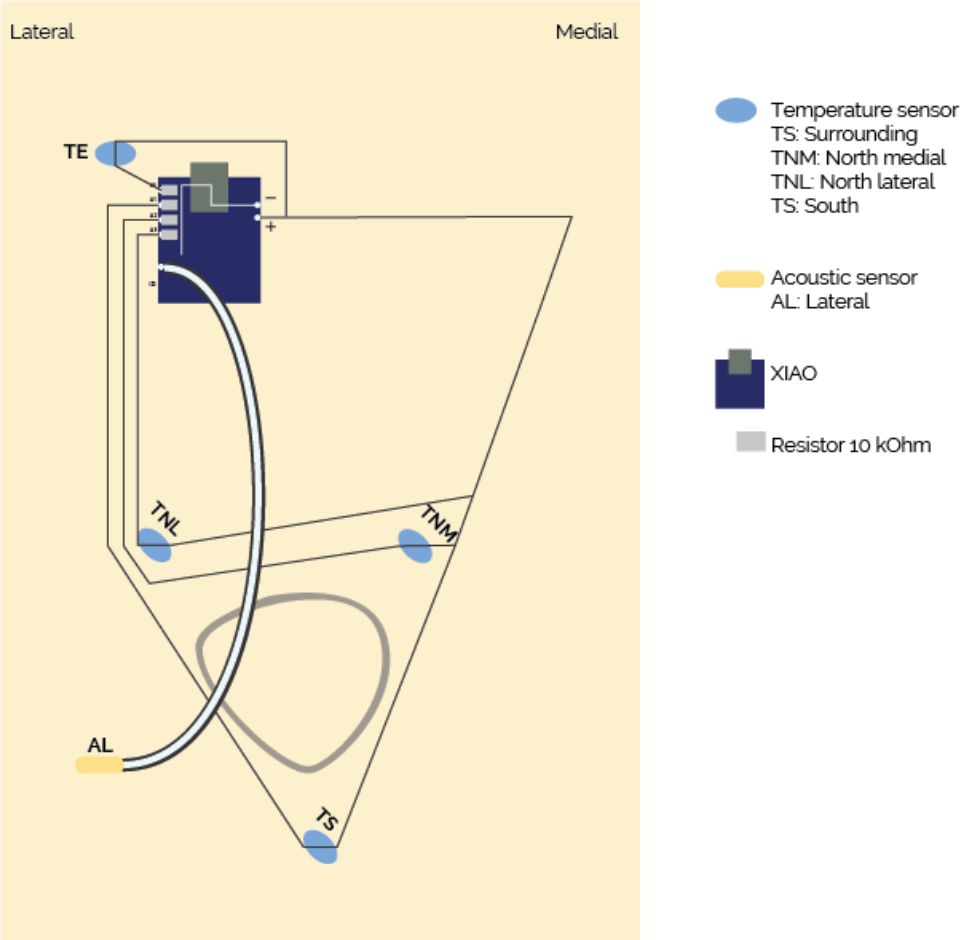

Figure 47: Final wiring outline

9.2.3 Acoustic sensor

In contrast to the temperature sensors, the acoustic sensor was not integrated using conductive yarns. Instead, thin insulated copper wires were used. This decision was driven by two key factors:

Signal integrity and sampling rate

Acoustic measurements require high-frequency sampling, making the data significantly more sensitive to noise than temperature readings. Conductive yarns can introduce variable resistance and interference, which is unacceptable for audio analysis. To ensure the acoustic signal remained accurate and reliable, standard insulated wiring was selected (TR-5).

Mechanical stability

The acoustic sensor is positioned in a region where the microcontroller and the surrounding area do not impose significant elastic requirements. Unlike the knee joint, this area undergoes minimal flexion (bending) during movement. Consequently, the elasticity provided by zigzag-stitched yarns, which is essential for the NTCs surrounding the joint, was not required for this relatively short, static connection.

9.2.4 Choice of conductive yarn for wiring

To use conductive yarns as a replacement for other yarns, the resistance must be very low so data can be transferred easily with minimal noise. Several options, including conductive yarns and copper wiring, were evaluated to find the best fit.

Option 1: Bekaert 9006089 (9 ohm/m) - rejected

The first prototype was built using Bekaert yarn (Figure 48, up; Figure 49, left). However, two significant issues occurred during testing: The thread was quite stiff, making it difficult to sew into the fabric. Also, the fibres frayed easily, causing short circuits between connections. This prevented accurate measurements and was not safe (TR-5, TR-13).

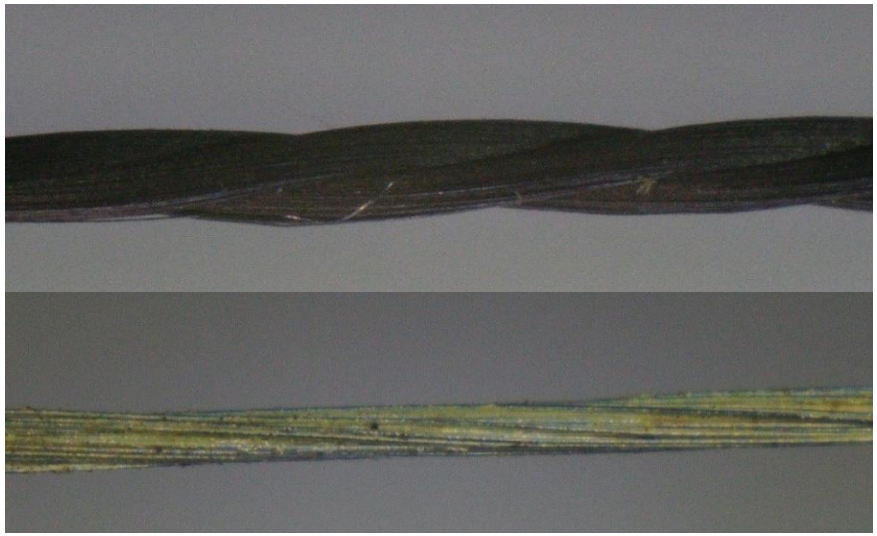

Figure 48: Up: Bekaert, Lower: Liberator Elite; under a microscope

Option 2: Liberator Elite (3.0 ohm/m) - selected

For the second prototype, Liberator Elite (Figure 48, down; Figure 49, right) yarn was introduced. This material performed a lot better. It offered lower resistance, showed minimal fraying, and eliminated the short-circuit issues found in the Bekaert yarn. Another advantage of this yarn was that it could be soldered, ensuring secure connections with sensors and the XIAO.

Figure 49: First prototypes with conductive yarn, Left: Beakaert, Right: Liberator Elite

Option 3: Thin enamelled copper wire - rejected

Very thin copper wire was tested as an alternative to yarn. This could be sown but proved unsuitable because the wire easily broke during movement and handling (UW-2, UR-13). Consequently, raw copper wiring was rejected.

Option 4: Elastic copper ribbon (4-wire) - rejected

An elastic ribbon containing four parallel copper wires was also considered (Figure 50). This option was rejected for two reasons. Routing limitations: the four wires are bundled, preventing individual wires from being routed directly to specific NTC sensors (TR-3, TW-2). And unlike the other yarns, which are sewn into the fabric, this ribbon sits on top of the material. This adds bulk and the possibility of higher temperatures under the wearable (UR-6, UW-13).

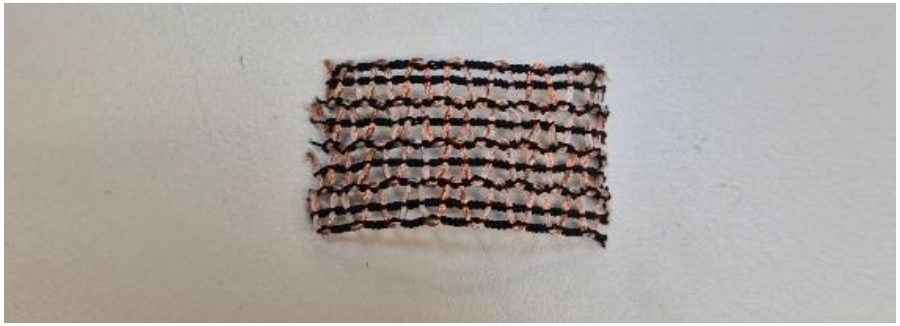

Figure 50: Elastic copper ribbon

Based on these results, Liberator Elite yarn was selected as the best option for wiring connections.

9.3 Connection XIAO to conductive yarn

Several approaches were explored to connect the wearable textile system to the XIAO microcontroller. A recurring challenge across iterations was the combination of stretchable textile materials and rigid hardware connections at the XIAO. Stretching of the fabric introduced mechanical strain on the electrical connections, increasing the risk of wire breakage (UW-2) and unreliable sensor readings (TR-5). The selection and placement of resistors, along with the method of attachment to the XIAO, therefore contributed to achieving robust, compact integration.

9.3.1 Resistor selection and placement

Initially, relatively large resistors were used because they were easier to handle during early prototyping. However, it quickly became apparent that their size negatively affected the compactness of the hardware integration (UW-13). For this project, absolute resistance accuracy was less critical than physical size, as the NTC sensors are intended to detect relative temperature changes rather than absolute values. Any offset introduced by resistor tolerances can be compensated for during sensor calibration.

So, smaller resistors were selected. These were first mounted vertically on the XIAO to reduce the footprint. To further improve compactness and reduce protruding components, the resistors were later placed horizontally. In the final iteration, the resistors were positioned underneath the XIAO, allowing the ground connections to be routed neatly and reducing exposed wiring. This configuration resulted in a compact and mechanically protected hardware assembly (Figure 51, p. 94) (UW-13, TW-1).

9.3.2 Exploration of connection methods

Multiple connection strategies between the conductive yarns and the XIAO were tested across different prototypes (Figure 51).

Connection 1:

The conductive yarns were directly knotted to the XIAO pins. Due to the yarn's fibrous nature, unintended short circuits occurred.

Connection 2:

A thin copper wire was soldered to the XIAO and mechanically twisted together with the conductive yarn. This joint was then sewn into place. While this improved electrical stability, the connection remained mechanically vulnerable.

Connection 3:

The conductive yarn (Liberator yarn) was soldered directly to the XIAO. An insulating layer was added to prevent short circuits caused by loose conductive fibres. This significantly improved electrical reliability.

Connection 4:

A piece of felt was placed behind the XIAO to prevent yarn stretching at the solder joints. However, the felt itself deformed under tension and did not provide sufficient mechanical stability.

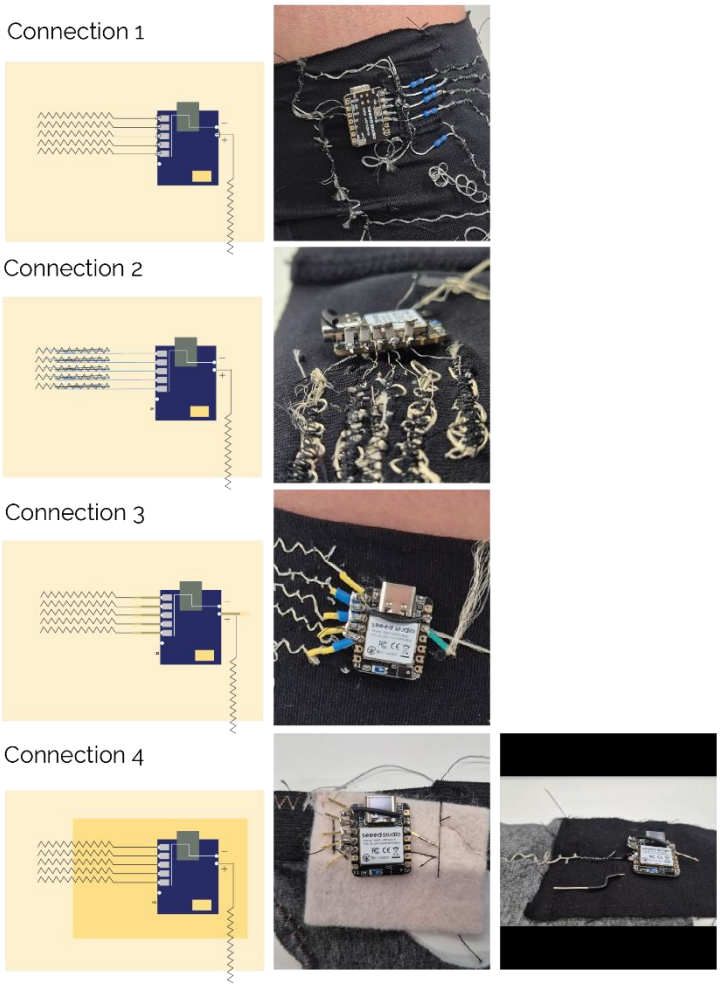

Figure 51: Resistors and XIAO connection to conductive yarn

Final connection solution

The most robust solution was achieved by introducing a small piece of non-stretch 100% cotton fabric behind the XIAO. Approximately 1 cm of this fabric was sewn onto the wearable using a zigzag stitch to allow a gradual transition between stretchable and non-stretchable materials. The XIAO was then sewn onto the non-stretch fabric, and a small insulated wire was soldered to it (Figure 51, p. 94, connection 4, right picture).

This approach successfully reduced mechanical strain on the solder joints, prevented unwanted stretching at the hardware interface, and resulted in a compact, reliable connection suitable for a wearable proof-of-concept (UW-2, UW-13).

Connection yarn to NTC, preventing strain

To ensure mechanical durability and prevent electrical disconnection during movement, a strain-relief approach based on the XIAO connection was mirrored and applied to the NTC sensors. Figure 52 visualises the different components as an exploded view. The integration process is defined in four steps:

1. **Preventing strain:**
   A patch of non-stretch 100% cotton fabric is temporarily attached to the main stretchable body of the wearable. A small hole is cut into this non-stretch layer to house the sensor. The underlying stretch fabric remains intact. This decision was made based on user panel feedback; participants expressed concern about feeling hard components directly against the skin. By leaving the base layer uncut, a soft fabric buffer is maintained for comfort (UW-7).
2. **Connection and soldering**
   Conductive yarn is stitched across the non-stretch patch. The NTC sensor is positioned within the cut aperture, sitting directly underneath the non-stretch layer. The yarn is then cut through at the NTC location, and the sensor terminals are soldered to its ends. In this configuration, the non-stretch fabric absorbs tensile forces, protecting the solder joints from failure during wear (UW-2).

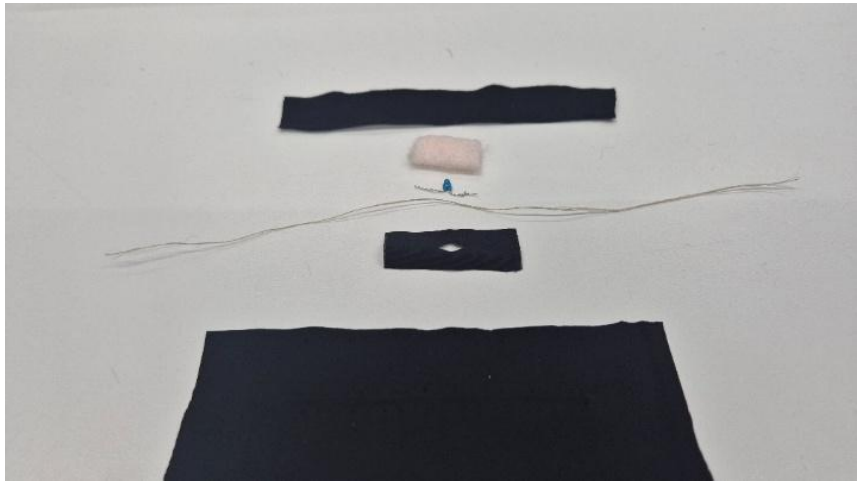

Figure 52: Composition of NTC application without strain

3. **Thermal insulation**
   To ensure the sensor measures skin temperature rather than the ambient air, a layer of wool felt is secured over the back of the sensor. This provides some thermal insulation (TR-10).
4. **Finishing**
   Finally, the entire assembly is covered with a seamless band of stretch spandex-like (80% polyamice, 20% elastane) material. Once secured, all temporary basting stitches are removed. This ensures the final construction is smooth and flexible, eliminating rigid pressure points or rough fabric that could cause irritation (UW-2, UW-7, UR-5).

9.4 Implementation battery and XIAO

For this project, a small available LiPo battery was selected to keep the hardware as compact as possible (UW-13) and maintain wearability. A critical aspect of using LiPo batteries in wearable applications is ensuring adequate protection. LiPo batteries are sensitive to mechanical stress, puncturing, bending, and overheating. Battery damage can lead to reduced performance, swelling, or thermal runaway, posing a safety risk to the user (CM Batteries, 2025). Therefore, both mechanical protection and controlled integration into the wearable are essential (TR-13).

To address this, a focused design sprint was conducted to explore casing and pouch concepts to safely integrate the LiPo battery into the wearable. All iterations are shown in Figure 53, p. 99.

For this design sprint, it was decided to place the battery behind the XIAO. This was decided to protect the battery from external punctures, reduce pressure points on the leg, and keep the hardware as compact as possible (UW-7, UW-13, TR-13).

Concept 1: 3D-Printed casing

The first concept consisted of a full 3D-printed casing (Figure 53, p. 99, concept 1). While this provided sufficient protection, its hard properties reduced comfort during movement by increasing the number of rigid components within the textile system, impacting wearability (UR-2). As a result, this concept was discarded.

Concepts 2 and 3: Textile pouches

Subsequently, several soft pouch-based solutions were explored (Figure 53, p. 99, concepts 2 and 3). The first pouch was made from a relatively thick, non-stretch fabric with a fluffy inner surface. While this material provided some cushioning, it proved difficult to finish cleanly and consistently, resulting in an untidy appearance and reduced seam durability (UR-13).

Next, the same non-stretch (cotton) fabric that had been successfully used for the XIAO connection concept was tested. This fabric provided structural stability and prevented stretching, both of which are important for protecting solder joints and electrical connections. However, the fabric alone did not provide sufficient protection against mechanical impact. To address this, an additional rubber layer was added. This combination provides adequate protection by absorbing minor shocks, distributing pressure across a larger surface area, and preventing direct bending or puncturing of the battery (TR-13). An additional advantage of this solution is that the non-stretch fabric allows for secure electrical connections to be integrated directly onto the pouch. Furthermore, the pouch fit well onto the wearables elastic band. Despite these benefits, the assembly was still relatively bulky (UW-13).

Concept 4: Partial protection

To further reduce bulk, a concept was explored in which only the underside of the LiPo battery was protected, while the top side was covered by the XIAO itself (Figure 53, p. 99, concept 4). This reduced overall thickness and rigidity. However, this approach left the XIAO insufficiently protected, which was considered undesirable given the need to protect all rigid electronic components in a wearable context (TW-1). For this reason, this concept was also not pursued further.

Concept 5: Combined leather and felt pouch

In this iteration, leather was introduced as an internal protective material for its robustness, durability, and resistance to mechanical damage (Figure 53, p. 99, concept 5). A felt storage pouch was developed, with a leather layer integrated at the bottom to protect the LiPo battery from impact and pressure. This configuration provided sufficient mechanical protection while maintaining flexibility and comfort.

In this concept, the XIAO is neatly concealed within the pouch, the overall size remains compact, and the electrical connection is integrated directly onto a non-stretchable material. This effectively combines hardware protection and strain relief in a single solution, addressing multiple requirements simultaneously (UW-13, TW-1, TR-3).

To charge or power the wearable, only the top part of the pouch needs to be opened. This improves accessibility while keeping the electronics protected during normal wear.

Final concept

Later, the SD module was introduced as this was needed for reliable data. This module was mounted under the LiPo battery to keep the hardware as compact as possible (UW-13), thereby adequately protecting the LiPo battery on both sides (TR-13). Concept 3 was revisited, and instead of leather, the anti-stretch 100% cotton fabric was integrated into the felt pouch, as it is much thinner and lighter (UW-6).

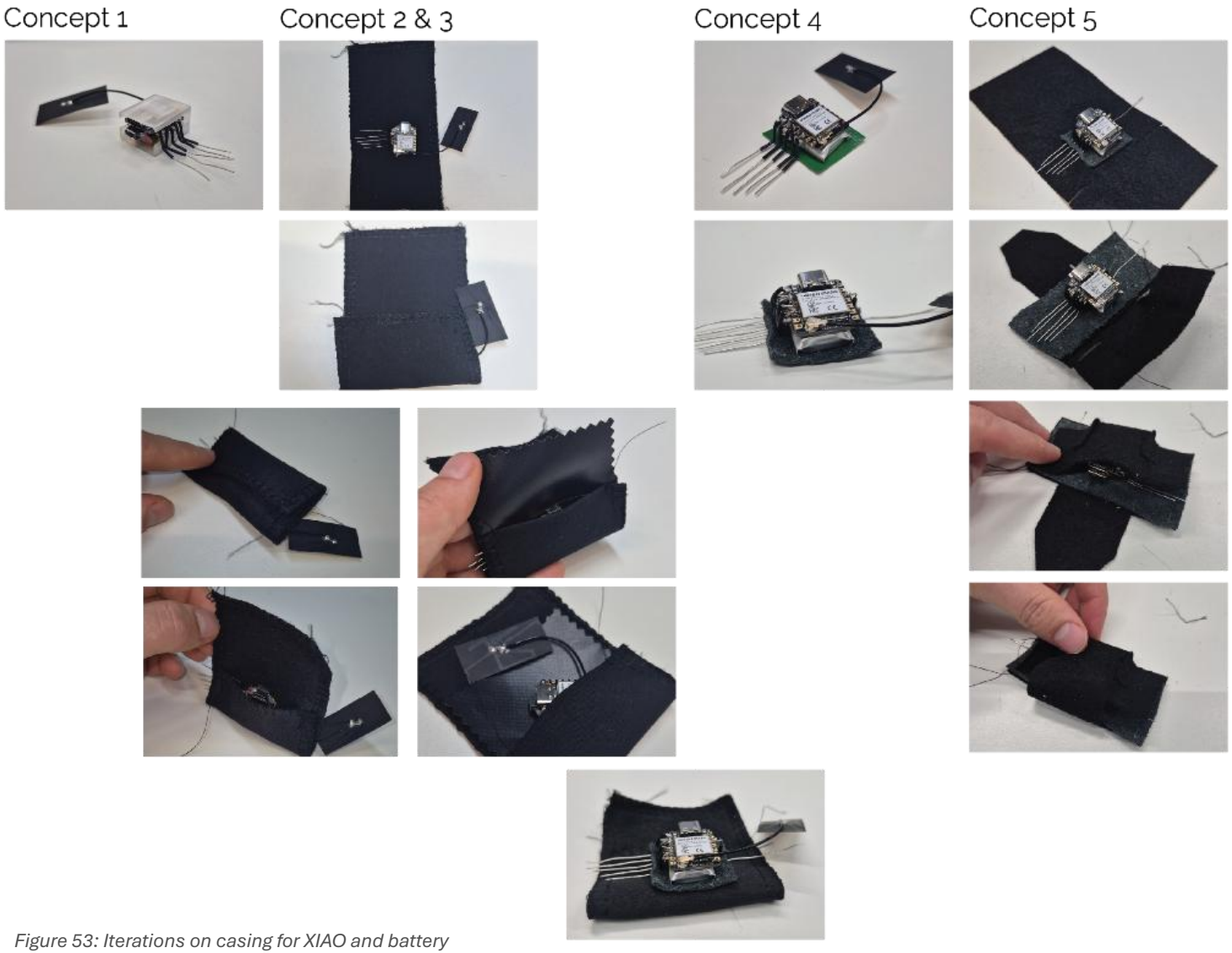

Figure 53: Iterations on casing for XIAO and battery

Relevance for the wearable

Following the selection of electronic and textile components, the final step in the design phase was determining the arrangement and physical integration of the hardware within the wearable (Figure 54). The final integration strategy encompasses the following decisions:

- **Placement:** The main hardware module (microcontroller, battery, and storage) will be positioned on the lateral side of the upper leg. This location minimises interference with the knee's natural range of motion during flexion and extension, while remaining discreet under clothing.
- **Wiring architecture and material:** A definitive wiring diagram has been established to route the connections from the central module to the sensors. For the physical routing, Liberator Elite conductive yarn will be utilised and stitched in a zigzag pattern on the spandex-like material. Providing the necessary flexibility to move with the body without breaking.
- **Mechanical strain relief:** Because the primary sleeve uses elastic fabric (fabric 3, p. 67), a rigid backing is required to prevent the conductive yarn and solder joints from snapping under tension. A piece of non-stretch cotton is implemented directly beneath the hardware zone to isolate the electronics from mechanical strain and stabilise the connections.
- **Hardware protection and comfort:** To ensure user safety, the LiPo battery is physically shielded by the XIAO and the SD card module. Finally, to prevent any hard edges from irritating the skin or getting caught on trousers, the electronic assembly is housed in a felt pouch.

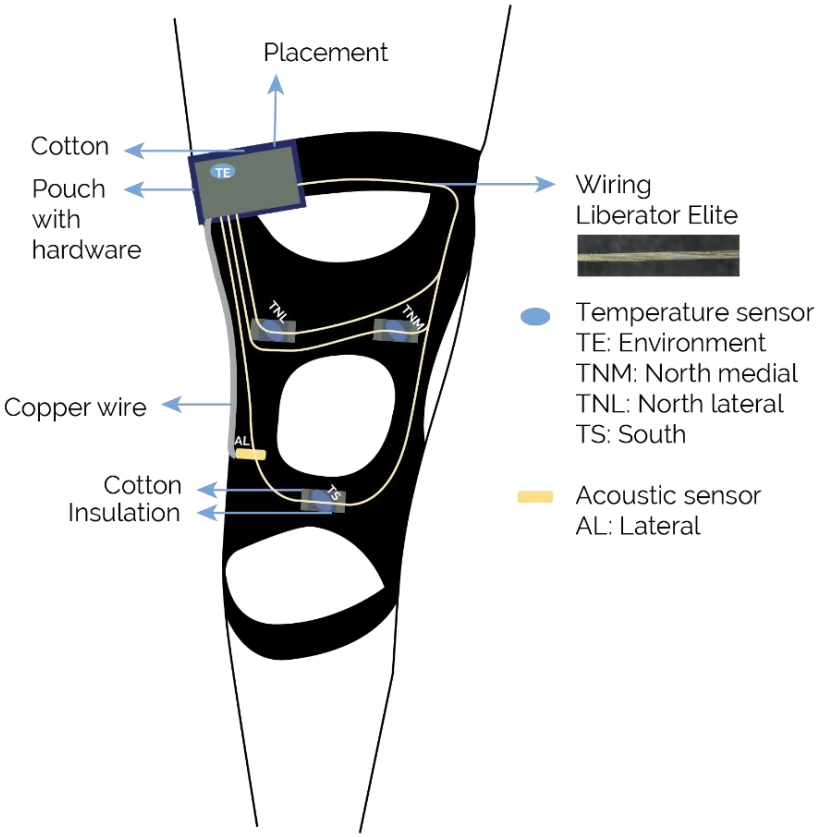

Figure 54: All components integrated in wearable

10 Data analysis

10.1 Data transmission

Throughout the development process, the data transmission method evolved to meet the acoustic sensor's data reliability requirements.

Evolution of connectivity

Initially, data collection was conducted via the Serial Port for quick debugging. Subsequently, Bluetooth Low Energy (BLE) was implemented to enable wireless communication. However, a critical limitation emerged regarding the acoustic sensor. Transmitting high-frequency audio data (sampling rate: 48,000 Hz) via BLE resulted in significant data loss and incomplete files.

To address the data loss, the hardware was upgraded to the Seeed XIAO ESP32-S3, utilising its integrated Wi-Fi capabilities. Furthermore, to mitigate data loss during potential Wi-Fi instability, an SD card module was added to the system. In the final stages of this project, data were written to the SD card module, as this was the most robust way to ensure all data were recorded without loss. The data were more reliable for analysis.

10.2 Visualisation of data

10.2.1 Acoustic sensor

To visualise data from the acoustic sensor, a processing code was developed based on the methodologies established by Toreyin et al. (2016) and Teague et al. (2016). The goal was to transform raw, noisy audio signals into a clean count of acoustic emission events (crepitus). To prevent severe signal clipping and harsh acoustic bursts caused by direct contact or friction, a layer of sponge foam was placed around the MEMS microphone. This serves as a form of integrated mechanical filtering, dampening high-intensity mechanical noise at the source before digital analysis begins.

Exploratory phase and prototyping tools

The initial development phase focused on translating the theoretical framework into functional Python code. Artificial Intelligence (Google Gemini) was used to generate the code structures based on the two papers. While these early iterations did not immediately yield valid diagnostic graphs, they provided insights into how the acoustic data behaves and how it can be visualised.

During this iterative testing, Streamlit (an open-source Python framework) was utilised for rapid prototyping. This enabled

visualisation of the sensor data stream, facilitating evaluation of filter settings and threshold parameters. Although Streamlit was instrumental for internal debugging and analysis during the design phase, it was not selected for the final validation of sound files because Python could generate better graphs. However, it did provide some direction for potential future interfacing.

Algorithm architecture and modifications

The filtering of acoustic data in this project relies on a combination of the methods established by Toreyin et al. (2016) and Teague et al. (2016). As software engineering and advanced signal processing were not the primary focus of this design project, Generative AI was used to bridge the technical gap. By feeding the exact parameters from the literature into the AI, it helped structure and write the Python code required to process the raw audio files.

Methodology implementation

The code followed a specific methodology to isolate relevant joint sounds from background noise:

1. **Normalisation:**
   The signal is first normalised to the range -1.0 to 1.0 a.u. to ensure that detection thresholds remain independent of the recording volume.
2. **Bandpass filtering:**
   A bandpass filter is applied to isolate frequencies between 10-20 kHz. This step is important as it removes low-frequency artefacts such as footsteps and speech, retaining only the high-frequency energy characteristic of crepitus.
3. **Envelope detection and counting:**
   Using the Hilbert transformation, the signal's energy envelope is calculated and smoothed. An adaptive threshold (based on the noise floor's standard deviation) determines when a peak qualifies as a "crack." Finally, a debouncing mechanism (dead time) of 0.10 ms is applied to prevent a single creaking sound from being counted as multiple events.

Verifying the software

To validate the acoustic signal processing, different testing approaches were adopted. The initial phase focused on verifying the software independent of the prototype hardware. For this purpose, a DJI Mic 2 (Figure 55, sampling rate: 48 kHz) was utilised to analyse a pre-recorded WAV file containing confirmed OA knee crepitations, captured in a controlled, silent environment. The results of this analysis are illustrated in Figure 56. The initial test demonstrated a clear distinction of crepitus events within the OA recording. The code used for this graph can be found in Appendix 8.

Figure 55: DJI Mic 2

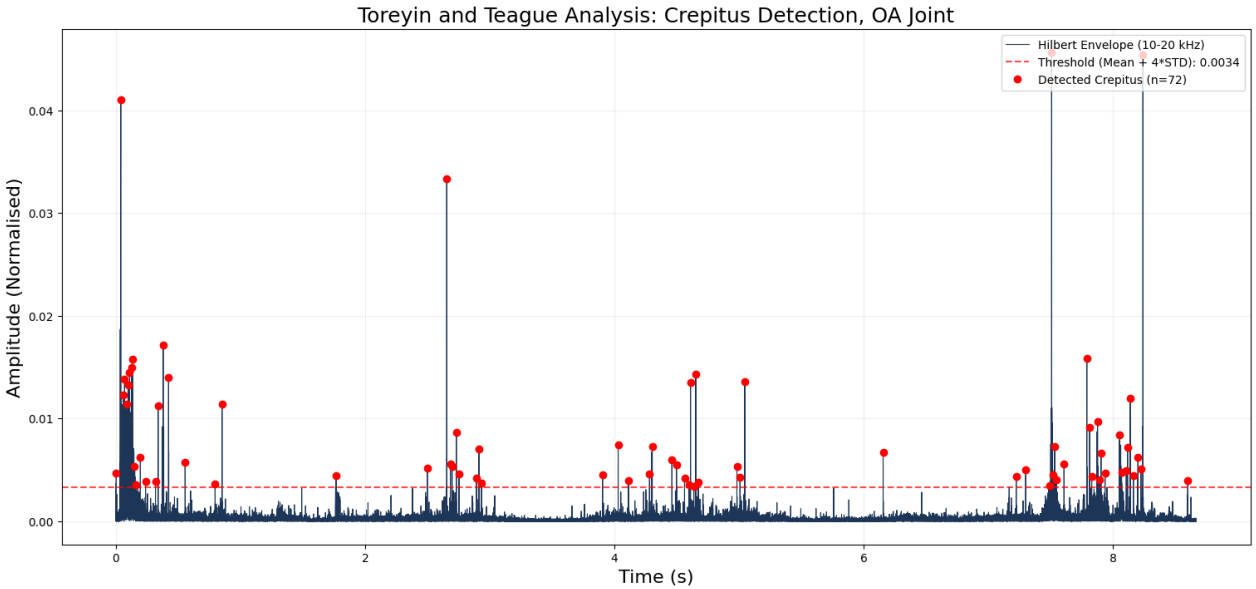

Figure 56: OA knee joint crepitus detection, Toreyin et al. (2016) and Teague et al. (2016) methodology. Showing crepitus events around 0 s, 2.5 s, 4.5 s, and 8 s

Methodology modifications

To further evaluate the algorithm's performance, two additional control recordings were acquired using the DJI Mic 2: acoustic data from a healthy knee (recorded in the same manner as the OA knee) and friction noise generated by trousers rubbing against the microphone mounted on the outside of a prototype while walking. During testing and comparing healthy and OA knee sounds, some modifications were made to the Python code to improve reliability.

Modification of signal normalisation

Standard normalised audio signals scale the peak of any recording to 1.0. During development of the data script, it became clear that this approach was unsuitable for this application.

As in recordings of a healthy knee (which are relatively quiet), standard normalisation could amplify the quiet sound files to the same level as loud crepitus events. To prevent this, the normalisation step was disabled. By analysing the raw energy levels instead, the system compared quiet and high-energy acoustic emissions.

Implementation of a fixed threshold

To distinguish between background noise and physiological events, a "Fixed Threshold" was adopted. Instead of allowing the algorithm to auto-calculate a threshold based on the signal-to-noise ratio of the specific recording, the detection limit is derived from a confirmed OA reference signal. This fixed value is then applied to all incoming data streams. This ensures that an event is registered only if its absolute energy is comparable to known crepitus, thereby filtering out minor artefacts.

Parameter tuning architecture

Recognising that different microphones (e.g., high-fidelity reference microphones vs integrated MEMS microphones) exhibit markedly different sensitivity profiles, the algorithm was designed with tunable parameters rather than hard-coded constants. The system allows for iterative optimisation of:

- The frequency bandwidth: Adjustable low-cut and high-cut filters to target specific acoustic signatures.
- The sensitivity multiplier: A variable factor applied to the standard deviation to fine-tune the strictness of the detection logic.

Comparison of sound files

With these modifications, the tweaking parameters were set as a baseline at 10,000-20,000 Hz and the multiplier at 4. The results of this comparison are shown in Figure 57. This analysis revealed that, without fine-tuning, the algorithm produced a substantial number of false positives in both healthy knee joint and trouser-noise recordings. To improve the signal, an iterative optimisation process was conducted, focusing on three key parameters: Bandpass Low-Cut frequency, Bandpass High-Cut frequency and the Threshold Multiplier (the factor by which the standard deviation is multiplied to set the detection limit).

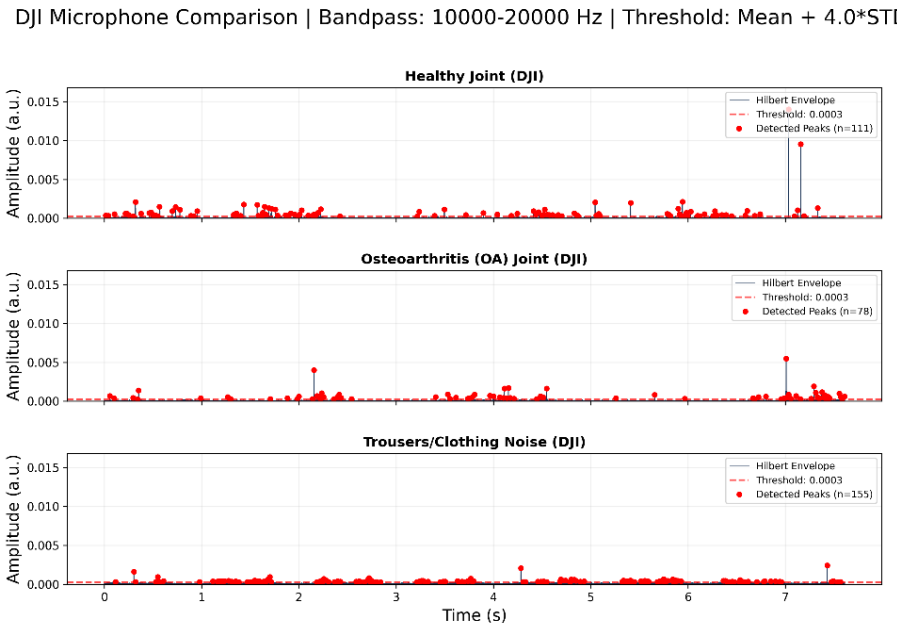

Figure 57: Comparison healty joint, OA joint, and trouser noise, Toreyin et al. (2016) and Teague et al. (2016) methodology (modification) (before tweaking). Showing many false detections of crepitus

This tuning was conducted through an exploratory approach. Various combinations of these parameters were tested to identify the configuration that achieved the best separation between signal and noise. The goal was to maximise the detection of true crepitus events in the OA recordings while minimising false detections in the healthy and clothing-noise datasets. All options tried are listed in Table 8. The comprehensive graphs resulting from these iterations are included in Appendix 8, as is the python code used to analyse the files.

Table 8: Results of exploratory approach, optimising crepitus events on healthy joint vs OA joint vs trousers noise

Trial	Band-pass Low-cut (Hz)	Band-pass High-cut (Hz)	Thres-hold multi-plier	Thres-hold	Detected peaks healthy joint	Detected peaks OA joint	Detected peaks trousers
1	10,000	20,000	4	0.0003	111	78	155
2	10,000	20,000	6	0.0004	69	51	51
3	5,000	20,000	4	0.0014	92	73	104
4	5,000	20,000	6	0.0029	64	50	23
5	3,000	20,000	6	0.0053	19	41	4
6	2,000	20,000	6	0.0079	9	44	4
7	2,000	20,000	5	0.0066	12	53	6
8	1,500	20,000	8	0.0131	3	34	3
9	1,000	20,000	4	0.0093	5	63	9
10	1,000	15,000	4	0.0093	5	63	9
11	100	20,000	4	0.0169	4	56	23
12	600	20,000	3	0.0100	5	75	15

Optimisation results

The data in Table 8, p. 105, shows several correlations between filter settings and detection accuracy. The analysis reveals that the Bandpass Low-Cut frequency and the Standard Deviation Multiplier are the defining factors in differentiating true physiological crepitus from environmental and textile noise.

The relationship between low-Cut frequency and noise sensitivity

A counterintuitive yet logical trend was observed regarding the high-low cut frequency filter (10,000 Hz).

- In Trials 1 and 2 (low-cut: 10,000 Hz), the system registered an extremely high number of false positives for both the healthy joint (n=111) and trouser noise (n=155).
- The energy of the signal in the 10-20 kHz range is very low. Consequently, the calculated detection threshold (based on the OA file's mean energy) decreased to 0.0003. At this frequency range, 10-20 kHz, the energy of the OA file is very low and the energy of the other files, health and trousers, is higher. Although the total energy of the crepitations is higher, this is not the case in this frequency range.
- Lowering the Low-cut frequency to the 1,000-2,000 Hz range included more signal energy, raising the absolute threshold to 0.0093. In this range, the energy of the crepitations is higher, and the threshold will increase as well. At some point, filter out the healthy knee sounds and trouser sounds, which had less energy.

The reintroduction of friction noise at low frequencies

While lowering the filter cutoff improved overall noise rejection, lowering it too much reintroduced artefacts.

- In Trial 11 (Low-cut: 100 Hz), the false detections caused by trousers increased from 9 to 23.
- This could confirm that the mechanical energy of fabric friction is mostly located in the lower frequency spectrum (<1,000 Hz) as indicated by Toreyin et al. (2016). Therefore, a high-pass filter is essential to block these friction artefacts.

Impact of the multiplier

The multiplier functions as a sensitivity tuner.

- Increasing the multiplier (e.g., from 4 to 6) successfully suppresses noise (healthy detections dropped from 111 to 69 in Trials 1 vs 2).
- However, this comes at the cost of sensitivity; valid OA signals are also discarded (OA joint detections dropped from 78 to 51).

The optimal frequency window

Although Toreyin et al. (2016) recommend that a 10-20 kHz bandpass filter is sufficient for eliminating background noise in a clinical setting, these measurements revealed that this range yielded an insufficient signal-to-noise ratio for this comparison of sound files. Due to the low signal energy or noise within this bandwidth, the adaptive threshold decreased. This resulted in a high incidence of false positives, with 155 peaks observed during friction-noise tests. Consequently, a broader bandwidth (1,000-20,000 Hz) was necessary to achieve a threshold (0.0093) that reliably distinguished the electronic noise floor from crepitus events. The data identify a specific operational window in which the signal-to-noise ratio is maximised.

- Trials 9 and 10 (low-cut: 1,000 Hz, Multiplier: 4): Demonstrate the best performance balance.
- OA detection: High sensitivity, 63 events detected.
- Noise rejection: Excellent suppression of healthy knee noise with only 5 events. and minimal trouser interference, only 9 events.

Based on this analysis, configuration #9 is selected as the optimal algorithm for this specific case (Figure 58).

- Selected bandpass: 1,000-20,000 Hz
- Selected multiplier: 4x STD

This configuration yields a threshold of 0.0093 that captures the acoustic signature of OA, distinguishing it from both the silence of a healthy joint and the frictional noise of clothing, providing the most reliable basis for the proof-of-concept. However, it is important to emphasise that the optimal filter parameters derived in the previous section were established using a DJI Mic 2. Because acoustic sensitivity, frequency response, and noise floors vary significantly across hardware components, these settings serve as an optional baseline. Future iterations utilising different microphones (e.g., the integrated MEMS) will

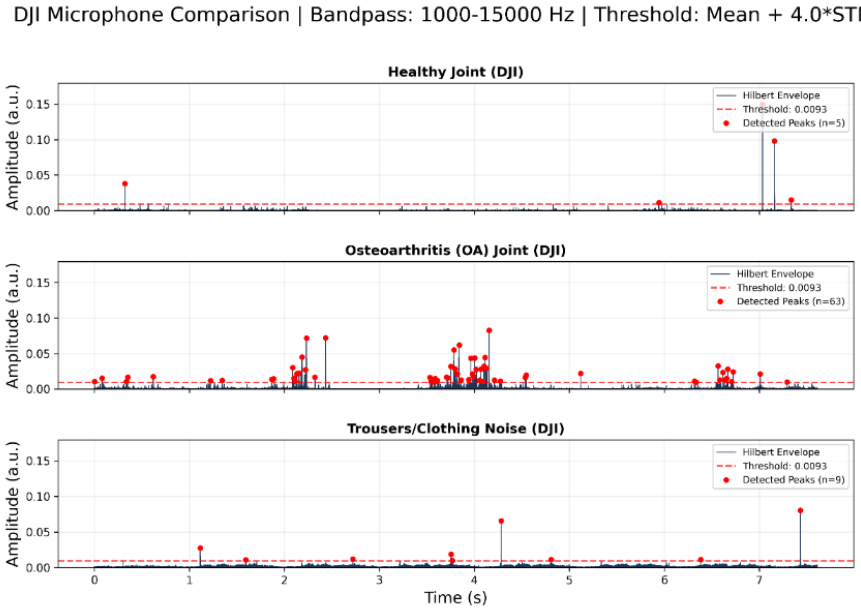

Figure 58: DJI microphone comparison, healthy joint, OA joint, trouser noise (DJI microphone). Toreyin et al. (2016) and Teague et al. (2016) methodology (modification) (after tweaking). Showing clear crepitations in the OA in comparison with the other files

require a dedicated recalibration to account for hardware-specific characteristics. However, with this test, the methodology is validated and can be used in the validation phase. An addition is later made, namely the handling of artefacts (outlier removal).

Addition of outlier removal

During the analysis of the acoustic graphs, another issue was identified: isolated energy spikes. These extreme peaks were significantly louder than any physiological joint sound. Upon investigation, it was thought that these were mechanical artefacts and were likely caused by uncontrolled physical impacts, such as the wearable accidentally tapping or moving over the microphone.

These mechanical impacts pose a problem for the algorithm. Because their absolute energy is so high, they can lift the standard deviation of the entire file, rendering the dynamic threshold calculation inaccurate and masking the true, subtle crepitus signals. To ensure the robustness of the final data methodology, two additional filtering steps were implemented in the Python script specifically to handle these outliers before the final event counting took place:

1. **Amplitude clipping:** An upper limit was established. If an acoustic event exceeds a specific, extremely high amplitude threshold, it is immediately classified as a mechanical impact rather than a physiological joint sound (crepitus). These extreme outliers are clipped or removed from the dataset to prevent them from corrupting the threshold multiplier calculations.
2. **Event duration filtering:** Mechanical impacts against a hard casing often have a different acoustic "decay time" compared to the internal friction of a joint. By evaluating the width (duration) of the energy envelope, the algorithm can filter out spikes that are unnaturally short or excessively long, further isolating the true OA crepitations.

Note: While these outlier-removal techniques were experimentally integrated during this development phase, they were fully activated and utilised during the final validation tests with the integrated wearable hardware to ensure the accuracy of the final results.

10.2.2 Temperature sensor

Exploratory phase

The first phase of data visualisation was characterised by an iterative and exploratory approach. As this project utilised Python for data analysis, the workflow involved rapid prototyping to determine the most effective methods for processing sensor data. While the resulting graphs were often unstructured and contained extraneous raw data, they provided critical insights into the systems' behaviour. A summary of these early visualisations and the takaways are provided in Appendix 9.

Despite the visual limitations of the early graphs, several key findings emerged:

- Thermal fit: NTC sensors require optimal contact with the skin to prevent fluctuating readings (TR-9).
- Signal smoothing: Raw data shows significant noise ("spikes"). Without smoothing techniques, such as a moving average, the data remained too unstable for analysis (TW-4).
- Hardware integrity: Short circuits were identified as a major source of data corruption, emphasising the need for robust insulation.
- Calibration: A one-point calibration method using a hotplate was used as an effective strategy for aligning the NTC sensors. However, this is not used in the final wearable, as relative data are currently acquired.

Refined temperature algorithm

To address the noise issues identified during the exploratory phase, a filtering algorithm was implemented. This process ensures that the final visualised data is stable and readable:

1. Sampling: The microcontroller samples the analogue inputs continuously.
2. Pre-processing: A 1-second (1,000 ms) average is calculated on the chip.
3. Transmission: Only this average value is transmitted to the data analysis platform.
4. Post-processing: Python interprets the incoming stream and applies a secondary 60-point moving average to smooth out remaining trends for visualisation.

Relevance for the wearable

The signal processing depends on the sensor:

- **Acoustic processing:** The raw audio first undergoes bandpass filtering to eliminate low-frequency mechanical artifacts, A Hilbert transform is then applied to extract the signal's energy envelope. True crepitus events are identified using a detection threshold calibrated from an OA reference sound file. To ensure accuracy, a 0.10 ms debouncing mechanism prevents double-counting of prolonged sounds, while amplitude clipping actively removes extreme peaks and their surrounding durations caused by external mechanical impacts.
- **Temperature processing:** The XIAO calculates an average of 1 second, furthermore a 60-second moving average filter is applied to the thermistor data to smooth out minor noise spikes and reveal the underlying trend.

Deliver

The Deliver phase presents the final project outcomes, which are divided into three distinct prototype models:

- **Works-like prototype**: A functional proof-of-concept designed to capture objective physiological data from the knee.
- **Feels-like prototype**: A non-functional physical model created to test ergonomics, fit, and physical comfort.
- **Looks-like prototype**: Visualisations illustrating the intended aesthetics and form factor of the final product.

These three models are used to evaluate the design across three validation pillars:

- Feasibility (technical implementation): Validated using the works-like prototype to test the sensor architecture, hardware integration, and software functionality.
- Desirability (user needs): Assessed using both the feels-like and looks-like prototypes. This involves physical comfort trials with healthy subjects wearing the feels-like model, alongside concept validation interviews with two OA patients to gauge overall wearability and aesthetic acceptance.
- Viability (clinical relevance): Evaluated by presenting the overall concept and collected data to a medical expert, confirming the value of the wearable for future OA research.

11 Final prototype: Lola

11.1 Works-like prototype

All components from the development phase are integrated into the final wearable (Figure 59 and Figure 60, p. 113). This works-like prototype is not how the final wearable would look from the outside. However, all technical aspects are in place, and data can be collected to test technical feasibility. The final name of this wearable is Lola, meaning Long-term Osteoarthritis Logging Assistant, indicating its use and features.

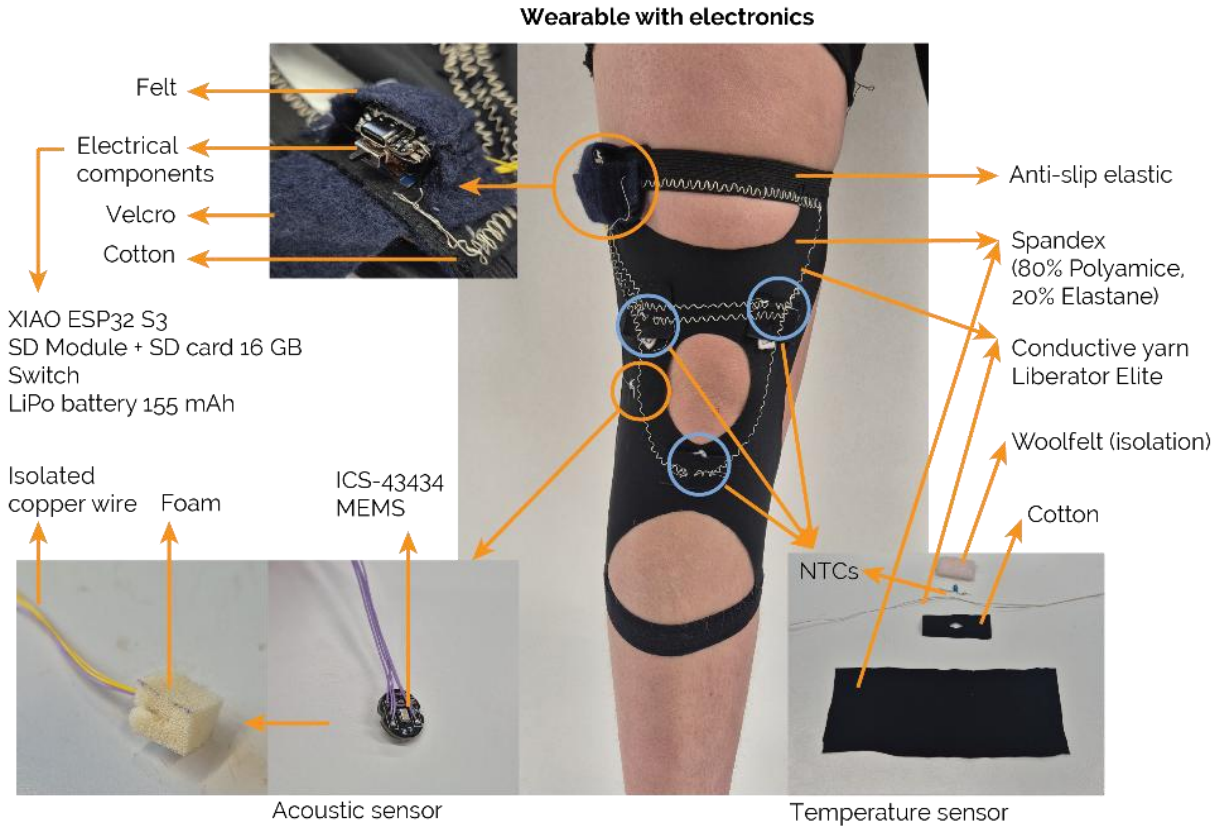

Figure 59: Wearable with electronics, and described parts

Figure 60: Final wearable with electronics

11.1.1 Hardware

The hardware consists of a XIAO ESP32 S3, a LiPo battery of 155 mAh, 3.7 V, an micro SD card module, 4 NTCs, and a 43434 MEMS breakout board, conductive yarn Liberator Elite, and Conductive isolated copper wires.

In addition to the hardware, fabrics are needed to prevent strain. For the NTC and XIAO, additional cotton is used, along with some wool felt for insulation. The connection, diagram, is shown in Figure 61. The corresponding pin-to-pin connections are listed in Table 9. The code for this final wearable is provided in Appendix 10.

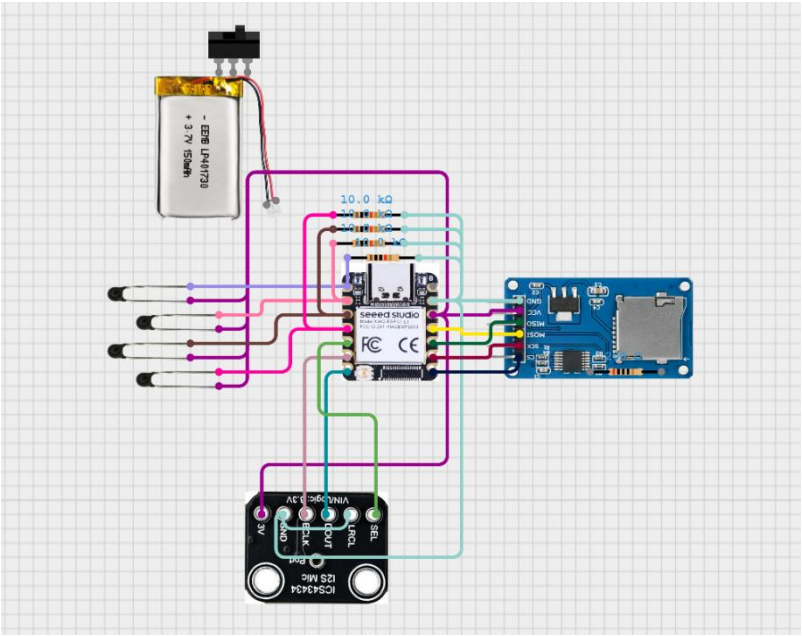

Figure 61: Connection diagram XIAO to NTCs to MEMS to SD module

Table 9: Pin-to-pin connection

Part	Pin	ESP32 Pin
MEMS	SCK (Serial clock)	GPIO 6
	WS (Word select / LR)	GPIO 5
	SD (Serial data)	GPIO 43
	VCC	3.3V
	GND	GND
	L/R	GND
SD MODULE	CS (Chip select)	GPIO 44
	SCK (Clock)	GPIO 7
	MISO	GPIO 8
	MOSI	GPIO 9
	VCC	3.3 V
	GND	GND
NTCs	1	A0
	2	A1
	3	A2
	4	A3

11.1.2 Design

The design consists of 2 anti-slip elastics with a spandex-like material between them, forming a base for other components, such as NTCs and MEMS. This spandex material consists of 80% PA (polyamide) and 20% EA (elastane). The casing is made of felt and cotton to prevent strain and protect the wearable. Velcro is used for the casing closure.

11.1.3 Integration of hardware

The conductive Liberator Elite yarn is stitched on the spandex material. From the outset, the casing is attached, enabling seamless integration. The yarn is stitched in zigzag for elastic wiring. Then the hardware is placed in the casing and soldered to the yarns. With the switch on the XIAO, the connection to the LiPo battery can be turned on and off.

Data storage and transmission

The system utilises for dual redundancy, with both acoustic and temperature data written directly to the SD card as the primary storage method. To ensure seamless data transfer to the SD card and proper operation of the acoustic sensor without blocking the processor, FreeRTOS was utilised on a dual-core architecture. The workload is divided into separate, parallel tasks: Task 1 (core 1) handles the high-frequency acoustic data collection (48 kHz) and places it into a memory queue. Task 2 (core 0) manages NTC temperature sampling and SD card writing.

Because writing data to the SD card is relatively slow and can cause data loss if accessed continuously, the system uses a chunking strategy. Data from the queue is buffered and physically written to the SD card in batches of 50 packets, resulting in approximately one save operation per second.

File management

The system operates on a session-based recording protocol. Upon initialisation, the firmware automatically scans the SD card and generates a new numbered raw binary file (e.g., /storage0.bin, /storage1.bin, etc.) for the current session. This automated naming convention prevents the accidental overwriting of previous measurements. Furthermore, because the system relies on the continuous, one-second saving routine, the active file remains stable. This ensures that even if the wearable is abruptly powered off, data corruption is prevented and the session is safely preserved.

Data retrieval and integrity

To avoid wireless transmission bottlenecks and ensure lossless extraction of the heavy audio files, the system utilises an offline data retrieval method. All session data is stored locally on a 16 GB micro-SD card. Following a recording session, the SD card is physically removed from the wearable and accessed via a computer. The raw binary file is then processed using a custom Python script provided in Appendix 11. This script automatically parses the integrated dataset and separates it into two distinct formats: the high-frequency acoustic data is extracted and saved as a standard .wav audio file, while the synchronised temperature data is exported as a .csv file for further clinical analysis.

To prevent byte-shifting errors and ensure robust data extraction, a frame-synchronisation technique is implemented in the firmware. Every individual data packet written to the SD card is prefixed with a static 16-bit synchronisation word (0xAAAA). When the Python script parses the raw binary file, it continuously verifies this marker. If a hardware interruption or buffer overflow causes a temporary loss of bytes, the script uses this synchronisation word to realign the data stream. This fail-safe mechanism guarantees that the high-frequency acoustic data and the temperature readings remain perfectly synchronised and uncorrupted throughout the entire recording session.

LED indicator's

Since the prototype operates as a wearable without a display system, status is communicated via a single programmable LED on the microcontroller unit. To ensure that the user, whether a researcher or a patient, can verify the wearables status without external software, a clear visual feedback language was implemented. The wearable provides real-time feedback on three states:

1. Recording (normal operation): A slow, rhythmic blink confirms that the acoustic and thermal data are successfully being written to the SD card. This blinking indicates that the measurement is active.
2. Storage error (troubleshooting): A rapid, stroboscopic flash alerts the user to a storage failure. This indicates that the SD card is either missing, improperly inserted, or not formatted correctly (FAT32). The system will automatically retry initialisation until a valid card is detected. At this stage, the XIAO is in 'sleep,' so little battery power is consumed. It is recommended to recharge the LiPo battery in this stage.
3. System freeze (critical failure): A solid, non-blinking light indicates a hardware or software deadlock. This prompts the user to perform a manual reset via the physical button.

The second LED on the XIAO indicates whether it is charging if a LiPo battery is attached and a USB-C is connected. If the red LED is blinking, the battery is charging; if it is off, it is fully charged and

ready to use. If the red LED is on without blinking, no LiPo battery is connected, and the switch has to be put to the other side, to enable charging.

11.1.4 Software

Acoustic signal processing methodology

To systematically isolate relevant physiological joint sounds (crepitus) from environmental and mechanical background noise, an acoustic signal processing pipeline was developed. The raw audio data is processed through an algorithm consisting of four phases:

Signal conditioning and pre-processing

- **No normalisation:** no amplitude normalisation was applied. Applying standard normalisation to quiet recordings (such as a healthy knee) would artificially amplify the electronic noise floor to the level of actual crepitus, inevitably creating false positives.
- **Bandpass filtering:** The raw audio signal is passed through a bandpass filter. This critical step eliminates low-frequency mechanical artefacts, such as footsteps or general body movement, retaining only the high-frequency energy characteristic of joint friction.

Envelope extraction

- **Hilbert transformation:** To analyse the true acoustic power of the crepitus, a Hilbert transform is applied to the filtered signal. This calculates the signal's energy envelope, converting the rapidly oscillating audio waveform into a clear, measurable amplitude curve over time.

Event detection and thresholding

- **Fixed thresholding:** A fixed detection threshold was implemented. This threshold is derived directly from a confirmed OA reference signal. This baseline ensures that only high-energy physiological events trigger a count, actively ignoring minor background fluctuations.
- **Debouncing:** To prevent a single, prolonged creaking sound from being erroneously registered as multiple separate events, a temporal debouncing mechanism (a 'dead time' of 0.10 ms) is applied immediately after a peak is detected.

Outlier removal:

- **Amplitude clipping**: Extremely loud peaks are removed; these are mechanical impacts from outside the body and not medical crackling sounds (crepitations).
- **Amplitude clipping duration:** around the loud peaks it can be determined how long of the audio file will be cut out.

Tuning architecture

- Recognising that different microphones possess unique sensitivity and noise profiles, the software architecture was designed with adjustable parameters. This allows tuning of frequency bandwidths, sensitivity multipliers, amplitude clipping, and event-duration filtering. This flexibility is useful for finding the right parameters for the algorithm to reject transient mechanical impacts and find possible crepitations.

Temperature processing

Also, the raw data from the temperature sensors were specifically visualised to see physiological trends and mitigate environmental interference.

- **Moving average filter:** Unlike acoustic crepitus, physiological temperature changes occur gradually. However, raw thermistor data, when visualised directly, appears as a spiky line due to noise or minor fluctuations. To clean the signal and highlight the underlying physiological trend, a 60-second moving average filter was applied to the data. This technique effectively smooths the thermal curve.
- **Environmental contextualisation:** To ensure the validity of the skin temperature readings, an outward-facing environmental sensor was integrated into the wearables casing. This sensor continuously tracks ambient temperature trends. By plotting this environmental baseline alongside skin temperature, the system can contextualise the data, enabling the distinction between a genuine physiological joint flare-up and external thermal influences (e.g., the user entering a heated room or going outside).

11.2 Feels-like prototype

All ergonomic and material design choices from the development phase are integrated into this physical model (Figure 62 and Figure 63, p. 120). This feels-like prototype does not contain functional electronics for data collection. However, all structural and textile aspects are in place, allowing the wearable to be evaluated for physical comfort, fit, and general wearability (desirability). Hardware placement and volume were simulated using 3D-printed components.

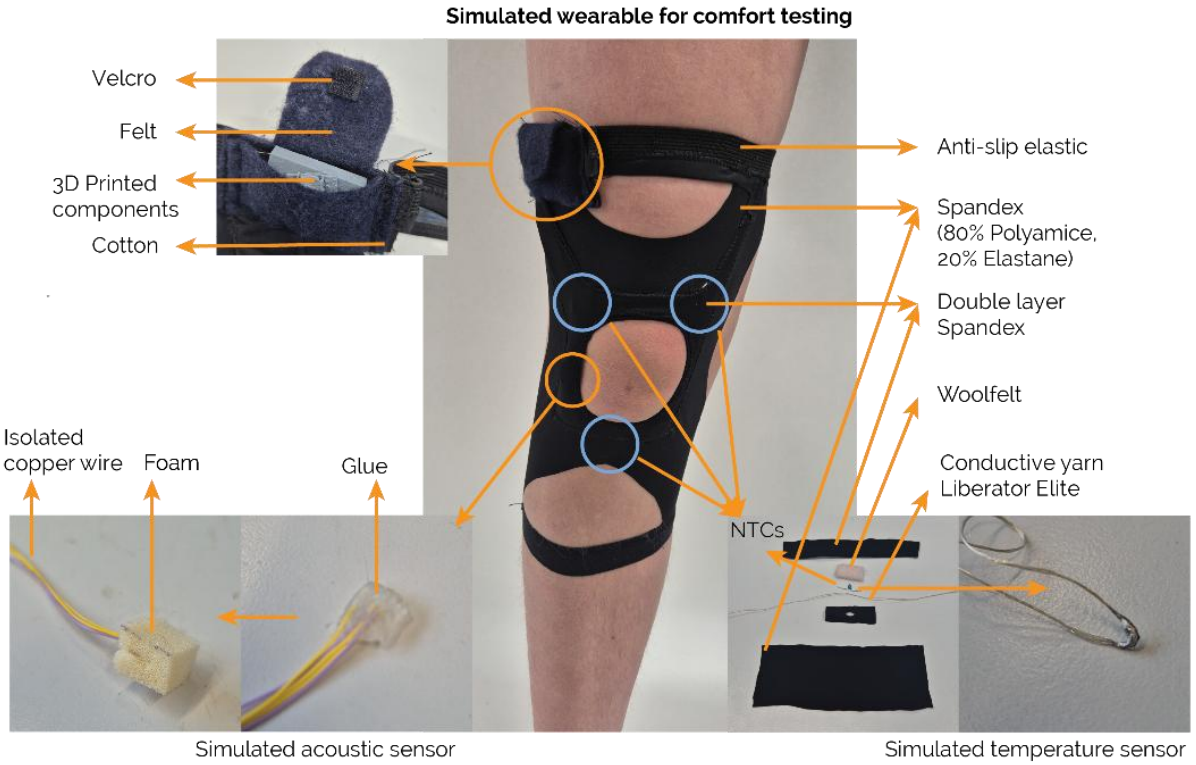

Figure 62: Feels-like model, with described parts

Figure 63: Final feels-like model

11.2.1 The design

The final physical design of the wearable is centred around comfort and the natural anatomy of the knee. While the works-like prototype validated the technical functionality, this physical model demonstrates the actual fit, material integration, and overall wearability.

- **Cut-outs:** To meet the requirements for thermal comfort and heat dissipation, an open design was chosen. The patella (kneecap) is left entirely uncovered, serving as an intuitive visual anchor during donning. Additionally, the popliteal region (knee hollow) is left open to prevent the fabric from pinching or chafing, and to avoid excessive sweating during full knee flexion.
- **Material selection:** The main body of the wearable is constructed from a lightweight, breathable stretch fabric. Instead of resembling a thick, insulating orthopaedic brace, this material provides an airy fit. It provides sufficient compression to keep the sensors securely in place (preventing vertical migration) while remaining soft enough to avoid feeling like a burdensome medical wearable.
- **Hardware integration & aesthetics:** The rigid technical components (such as the microcontroller and battery) are entirely concealed from view. They are housed in a soft, enclosed pouch on the lateral (outer) side of the upper thigh. This positioning not only protects the electronics but also prevents hard edges from pressing directly into the user's skin. Furthermore, the underlying wiring and sensors are neatly integrated beneath an additional protective layer of fabric, resulting in a safe and visually clean final product.

11.3 Looks-like renders

All visual and aesthetic design choices from the development phase are translated into these looks-like renders (Figure 64). Unlike the physical prototypes, this iteration provides a better representation of the final wearable, developed with AI-assisted visualisations based on the feels-like prototype. These renders were specifically created to accurately reflect the aesthetics, material textures, and refined finish of a modern medical consumer wearable. By providing realistic visual representations of the possible end product, these renders enable effective communication of the product's identity and the collection of reliable stakeholder opinions on its overall visual desirability.

Figure 64: Looks-like model, made with AI based on the proof-of-concept

Additional integration aspects

While the primary focus of this project was validating the core sensing technology and physical hardware, preliminary concepts for the broader product ecosystem were also developed. To evaluate the wearables seamless integration into daily life, several system aspects, such as sizing strategies, data connectivity, and digital interfaces, were visualised through 'looks-like' renders. Rather than representing final design decisions, these visualisations served as a discussion tool during the validation sessions with OA patients and clinical experts. The qualitative feedback gathered from these concepts will directly inform the final recommendations for future implementation.

- **Physical integration and sizing strategy:** To ensure optimal sensor contact across different body types, a sizing system (S-XL) is proposed, where the fastening sleeve is matched to the patient's specific thigh and calf circumference.
- **Connectivity:** A store-and-forward architecture is proposed. Data is stored locally on the wearable throughout the day and automatically transmitted only when connected to a designated Wi-Fi network (e.g., during overnight charging).
- **Digital interface:** The user interface is split between a patient-facing mobile app and a professional clinical dashboard.
    - *Patient app (context and engagement):* Designed to prevent medical anxiety, this app translates complex data into a simplified "Joint Health Score." Crucially, it gathers

data through manual symptom logging (e.g., subjective pain levels) and automatic activity tagging (via connections with platforms such as Apple Health or Strava). This contextual data allows the system to distinguish healthy exercise signals from possible flare-ups.

- *Clinical dashboard (diagnostics):* Designed for medical experts, this web portal provides access to high-resolution raw data. It allows the clinician to remotely monitor disease progression and focus solely on critical events without the need to review hours of baseline data.

12 Validation tests

The objective of this chapter is to verify whether the proof-of-concept meets the requirements set out in the definition phase. To provide a comprehensive assessment, the validation is structured around: Feasibility (technical Performance), Desirability (user acceptance and comfort tests), and Viability (price estimations). The validation utilises the three prototype iterations developed.

- **For feasibility (the "works-like" prototype):** All quantitative measurements for validation, acoustic filtering and temperature analysis were performed using the functional proof-of-concept. This hardware provides the necessary raw data to validate the integrated sensors. Data was gathered from one healthy individual (the researcher) and one individual with undiagnosed crepitations.
- **For desirability (the "feels-like and looks-like" model):** Comfort and user requirements were tested with the feels-like prototype, to ensure feedback was not biased by exposed electronics. These initial physical tests were conducted with healthy users (fellow students). To further evaluate visual acceptance and desirability among the target audience, a qualitative validation session was conducted with two patients with OA using the looks-like renders.
- **For viability**: The data of the works-like wearable is used, and cost estimations were based on the works-like wearable. These results were shown to expert M. van Middelkoop.

For some tests with the acoustic sensor and for the temperature sensor, trousers were worn. A picture of the trousers worn in these tests is shown in Figure 65.

Figure 65: Trousers worn for testing

12.1 Feasibility

Feasibility is tested in two ways: first, tests and analyses are conducted on the acoustic sensor, after which the same is done for the temperature sensor.

12.1.1 Acoustic sensor data validation

Test Setup

With the baseline algorithm established, a validation test evaluated the integrated acoustic sensors and algorithm. Two subjects participated: one healthy control and one with undiagnosed knee crepitus (non-diagnosed OA). Both completed a standard lower-body exercise protocol (Appendix 12).

Furthermore, the sit-to-stand exercise was also measured with trousers on for both individuals to assess the impact of clothing on exercise measurements. This approach gives an indication of the feasibility of daily monitoring while wearing trousers.

For these analyses, the baseline detection threshold was calibrated using the acoustic data from the non-diagnosed OA individual performing the exercises without trousers, providing a clean reference for crepitus peaks. The healthy individual's data was then compared to this reference to evaluate differences.

Using adjustable software parameters, an iterative optimisation process was conducted to determine the optimal parameters for the wearables integrated microphone under dynamic motion. Based on these trials, the optimal signal-to-noise ratio for this hardware configuration was determined to be a 1,500-20,000 Hz bandpass filter, combined with a standard deviation multiplier of 10.0, yielding an absolute threshold of 0.0157. Furthermore, an outlier threshold of 0.30% was implemented, and an event duration filter of 0.1s was applied to mitigate impact noise. 3 graphs were made with the acquired data.

1. Comparison of a non-diagnosed OA individual vs a healthy individual, with all exercises done as described in Appendix 12. (Figure 66, p. 126).
2. Comparison of a non-diagnosed OA individual vs a healthy individual with only the sit-to-stand exercise to zoom in on one. And get a better understanding of how crepitations behave (Figure 67, p. 127).
3. Comparison of a non-diagnosed OA individual vs a healthy individual, both sit-to-stand, with and without trousers (Figure 68, p. 128).

Codes for all three graphs can be found in the Appendix 12.

Results

The first set of results (Figure 66) shows increased acoustic activity during physical exertion compared to periods of rest. Also, the system successfully quantified a difference between the two subjects throughout the protocol. The non-diagnosed OA individual registered a total of 784 detected peaks, whereas the

healthy individual registered only 110 peaks. This overarching contrast demonstrates that the wearable can distinguish symptomatic knees from healthy joints.

Activity analysis

A detailed review of the different exercise phases reveals that the frequency of detected acoustic events is dependent on the specific type of motion and the load placed on the joint:

Activities such as walking and stair climbing yielded a dense cluster of high-amplitude peaks for both individuals. While the non-diagnosed OA subject still exhibited a higher peak density, the healthy subject also triggered numerous events during these phases. This showed that these movements introduce substantial mechanical artefacts (possible causes are heel-strike vibrations or fabric friction) that exceed the detection threshold, making it difficult to isolate true physiological crepitus from environmental noise during regular walking in this wearable.

The most distinct and reliable diagnostic differences were observed during controlled exercises. During the 'sit-to-stand' and 'Leg extensions' phases, the healthy individual registered

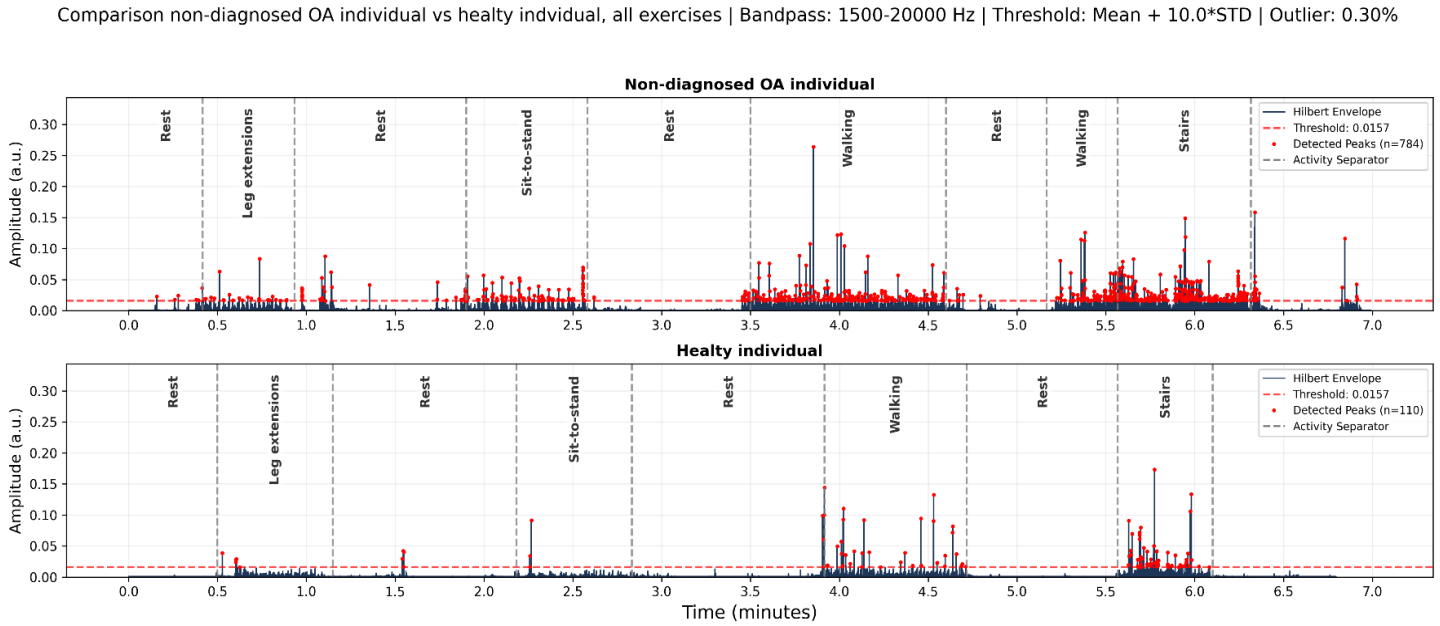

Figure 66: Comparison of a non-diagnosed OA individual vs a healthy individual, with all exercises done as described in Appendix 12. Showing the difference in crepitus detection for both individuals and the differences in crepitus detection during different activities.

almost zero acoustic events. In contrast, the non-diagnosed OA individual displayed a continuous, clear pattern of crepitus exactly corresponding to the flexion and extension of the knee under load.

Isolating one exercise

The sit-to-stand exercise alone showed greater detail in how acoustic emissions in the knee of the non-diagnosed OA individual behaved. Because this specific, controlled knee-joint movement provided a clean acoustic amplitude, it revealed a distinct, repeatable wave pattern. This is not observed in the healthy individual's data, thereby making the physiological difference between the two subjects clear. The non-diagnosed OA individual showed 182 crepitus peaks, which were thought to synchronise with the exercise's up-and-down (sit-to-stand) motion. In stark contrast, the healthy individual registered 7 peaks over the exact same time frame.

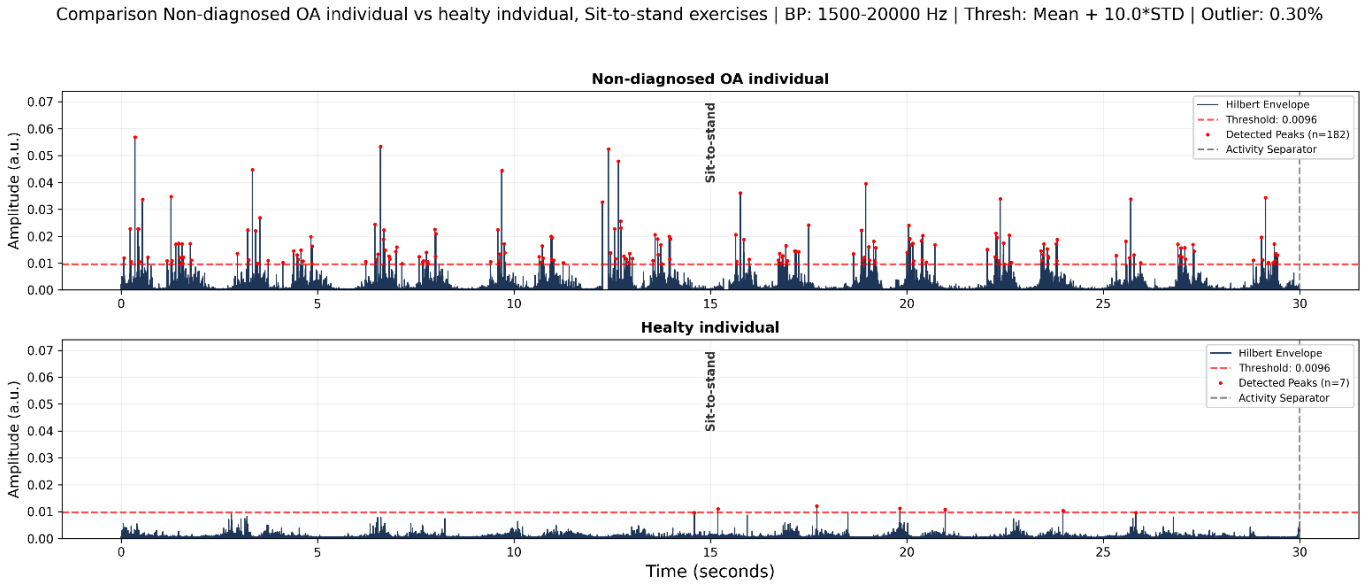

Figure 67: Comparison of a non-diagnosed OA individual vs a healthy individual with only the sit-to-stand exercise to zoom in on one. And get a better understanding of how crepitations behave. Showing clear crepitus ''waves'' for the non-diagnosed OA individual.

Comparing trousers and no trousers

To evaluate wearability in daily life, a 4-way comparison was conducted during a 20-second 'sit-to-stand' test to isolate the acoustic impact of wearing long trousers versus shorts (no trousers) (Figure 68).

The data clearly demonstrate that fabric friction introduces a lot acoustic artefacts. This results in many empty spaces in the graph because outliers were observed and removed.

- **Without trousers:** The baseline data remains extremely clean. The OA individual registered 127 peaks, while the healthy individual registered only 3 peaks.
- **With trousers:** The total peak count increased for both users. The OA individual jumped to 287 peaks, and, the healthy individual jumped from 3 to 100 peaks. This indicates that the microphone is sensitive to the sound of fabric rubbing against the acoustic sensor, triggering false positives.

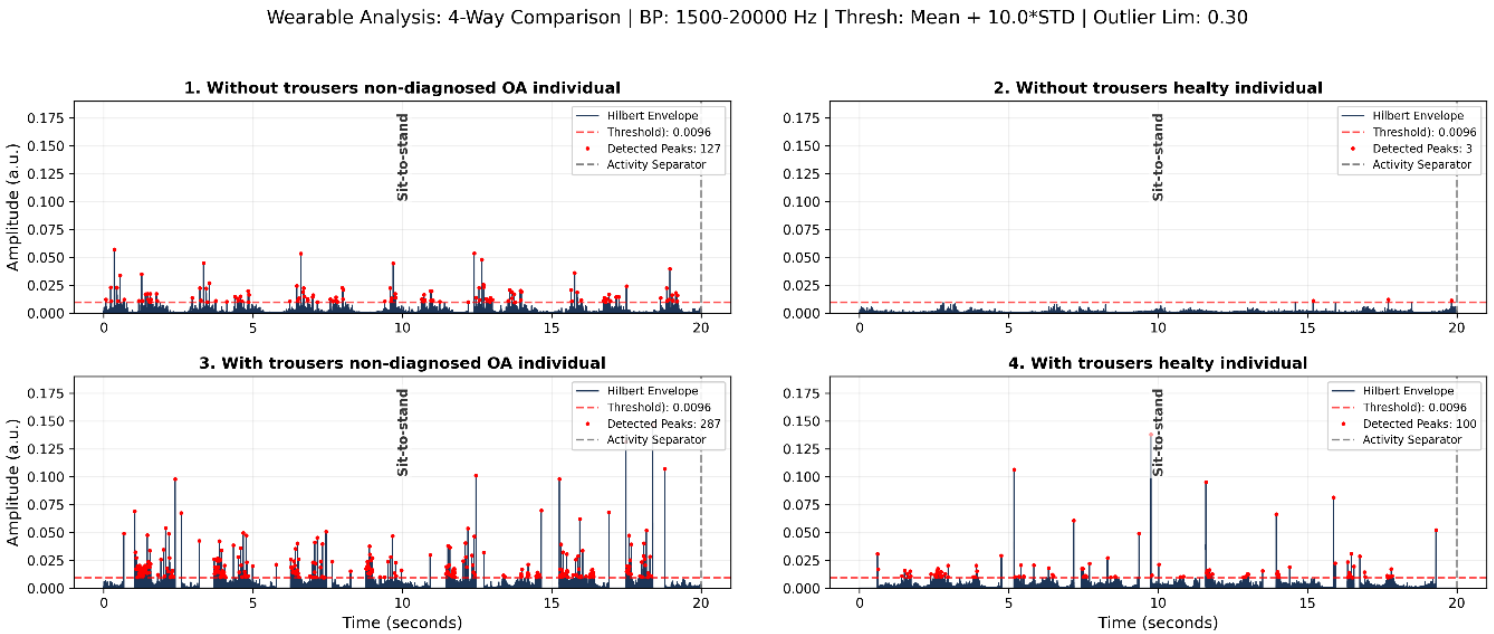

Figure 68: Comparison of a non-diagnosed OA individual vs a healthy individual, both sit-to-stand, with and without trousers. Showing that wearing the wearable under trousers indicat significant noise.

Interpretation of the data

When looking at the results from all exercises, the isolated exercises, and the clothing tests, several conclusions can be drawn regarding the wearables diagnostic capability:

1. Proof-of-concept validated: The acoustic sensor and the developed Python filtering algorithm successfully and consistently differentiated a symptomatic (crepitus) knee from a healthy knee. The large difference in peak counts (e.g., 182 vs 7 during controlled exercises) demonstrates that the hardware configuration can capture physiological joint sounds.

2. The 'Sit-to-stand': The data explicitly show that continuous monitoring (like walking) is currently not yet suitable for accurate, clear crepitus counting due to mechanical noise (such as taps on the microphone by fabric friction or heel strikes). To achieve reliable data, clinical tests could first focus on controlled, loaded articulations. The sit-to-stand exercise produced a rhythmic, clear acoustic signature of the OA joint, while the healthy joint remained completely silent.

3. The clothing barrier: The 4-way comparison revealed that fabric rubbing against the microphone casing generates high-frequency friction noise that the current algorithm cannot distinguish from crepitus (resulting in more false positives for the healthy individual and for the non-OAA crepitus individual).

Implication for future use: For accurate medical assessments, the wearable could be worn with shorts, or further research is needed to reduce mechanical noise. Future iterations could explore different microphone housings to damp external fabric friction, enabling accurate readings even under standard trousers. Additionally, advanced data filtration is needed to remove artefacts.

Discussion

The acoustic validation gave key insights into the wearables function, but several limitations remain:

- **No clinical diagnosis:** The non-diagnosed OA individual exhibited audible crepitus, but had no formal OA medical diagnosis. Furthermore, a sample size of one is sufficient for a proof-of-concept. However, it is too small to draw statistically significant clinical conclusions.
- **Data analysis constraints:** This project's scope is rooted in industrial design. The analysis relied on fundamental signal processing. The researcher is not a specialised data analyst. Distinguishing complex clothing friction from actual joint crepitus with 100% accuracy will require an expert in data analysis or advanced, data-driven algorithms. This could include Machine Learning trained on large clinical datasets.

- **Clothing artefacts:** When worn under trousers, the fabric rubbing against the microphone created severe acoustic artefacts and false positives that the current algorithm could not fully filter out. These artefacts will also differ per type of trousers.
- **Continuous vs active monitoring:** Continuous movement (like walking) introduces much noise. Therefore, with the current software, the wearable is better suited for short, controlled exercises (such as a daily sit-to-stand routine) than for passive 16-hour monitoring.
- **Non-calibrated acoustic sensor:** The MEMS microphone used in this wearable is a sensor that is not accurately calibrated; no unit can be given to the values given from the data. To still be able to compare results, arbitrary units are used.

Conclusion

Acoustic validation demonstrates the wearables technical feasibility to monitor joint crepitus. During controlled, loaded movements such as the sit-to-stand exercise, the system accurately differentiated a symptomatic knee from a healthy one (with 182 vs 7 peaks). However, walking currently introduces significant mechanical artefacts that disrupt the data. The same applies to clothing that is worn during measurements. Therefore, while the proof-of-concept is effective for isolated, active measurements, achieving reliable 16-hour passive monitoring will require further research into how to minimise these impacts or filter these artefacts from the data.

12.1.2 Temperature sensor validation

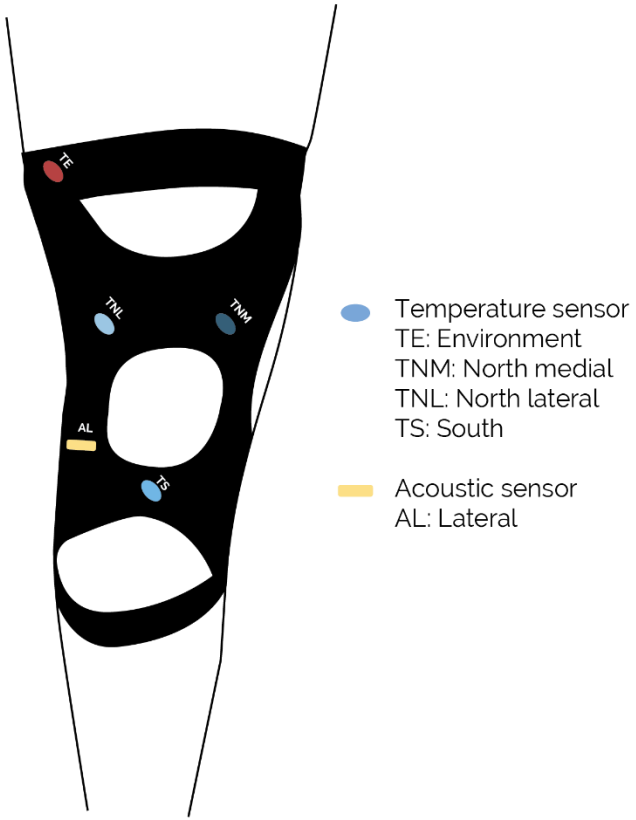

Figure 69: Placement of NTCs

Temperature test setup

To test the temperature sensors, 3 tests have been executed with the works-like prototype. These tests were executed with a healthy individual (the researcher). The corresponding code used to develop the graphs can be found in Appendix 13. A reminder of the final placement of the temperature sensors is shown in Figure 69.

Note: No calibration was performed, as the relative temperature change was the focus and absolute values would not affect the results.

The tests were conducted as follows:

Test 1: Motion impact assessment (done without (test 1a) and with trousers (test 1b))

- Conditions: Tested wearing shorts and long trousers.
- Objective: To determine if the physical motion of walking influences the temperature readings (e.g., due to air flow or sensor shifting) independent of physiological changes.
- Procedure:
  - Acclimatisation phase: 5 minutes (indoors sitting).
  - Activity phase: 8 minutes (walking inside).
  - Recovery phase: 5 minutes (indoors sitting).

Test 2: Ambient temperature influence (done with trousers)

- Conditions: Tested wearing long trousers.
- Objective: To assess the impact of external weather conditions and the sensor's ability to remain stable when transitioning between indoor and outdoor environments. And what the impact of such a temperature change is.
- Procedure:
  - Acclimatisation: 7 minutes (indoors sitting).
  - Transition: 1 minute (walking to the exit).
  - Exposure: 2 minutes (outdoors walking).
  - Transition: 1 minute (walking back to workstation).
  - Recovery: 7 minutes (indoors sitting).

Test 3: exercise-induced heat generation (done without trousers)

- Conditions: Tested wearing shorts.
- Objective: To measure the sensor's sensitivity to physiological skin temperature increases caused by physical exertion (simulating active use).
- Procedure:
  - Baseline: 5 minutes (indoors sitting).
  - Exertion: 10 minutes (sports/active movement).
  - Cooldown: 10 minutes (indoors sitting).

Test 1a without trousers

The aim of this test was to isolate the effect of physical motion on temperature data, excluding the insulating effect of clothing. The subject wore short trousers, leaving the wearable directly exposed to ambient air (Figure 70).

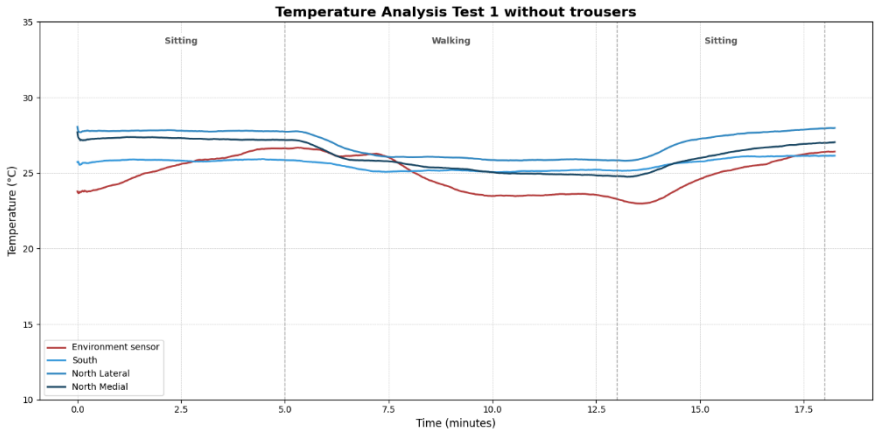

Figure 70: Results test 1a without trousers

Phase 1: Acclimatisation (0-5 min)

During this phase, the skin temperature sensors remained stable. In contrast, the environment sensor (red) displayed a warm-up curve.

Phase 2: Walking inside (5-13 min)

Upon the start of walking (t = 5 min), a distinct cooling effect was observed across all sensors:

- Skin sensors: All three skin contact sensors showed a temperature drop of approximately 2.0-2.5 °C.
- Environment sensor: was influenced more by the flowing wind since it was not insulated, allowing this NTC to cool off more.

This uniform decrease indicates a cooling effect. Since the sensors were uncovered, the airflow generated by walking cooled both the skin surface and the wearable casing, overpowering any heat generated by the skin.

Phase 3: Recovery (13-18+ min)

Immediately after the subject returned to a sitting position (t = 13 min), the cooling ceased.

- All sensors showed a rapid recovery. The skin sensors trended back towards their original values.

Conclusion of test 1a without trousers

The data shows that airflow is a dominant factor. Movement causes a significant drop in measured temperature due to convection, thereby masking any potential rise in skin temperature associated with muscle activity. Also, it looks like the environment sensor takes longer to find a stabilised temperature.

Test 1b with trousers

This test, identical to the previous one, was performed while wearing trousers over the wearable. The objective was to evaluate the impact of clothing on ambient air cooling observed in the previous test (Figure 71).

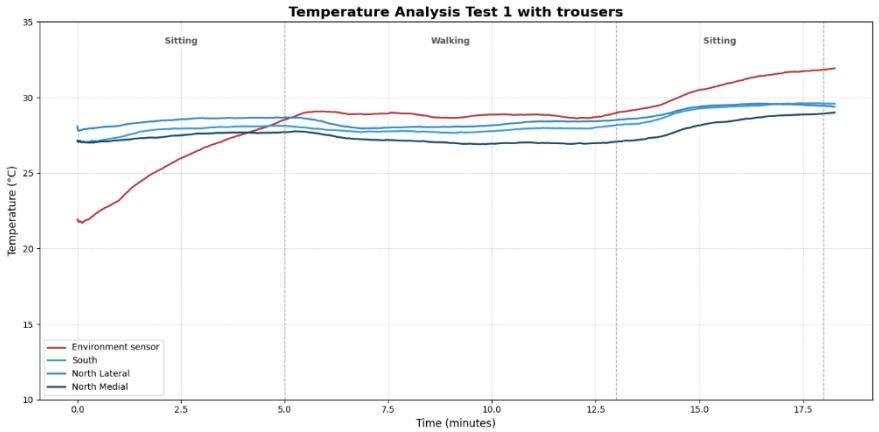

Figure 71: Results test 1b with trousers

Phase 1: Acclimatisation (0-5 min)

Unlike in the open-air test, the environmental sensor showed a larger temperature increase during the first stage. This is most likely because the temperature under the trousers is warmer.

- The skin temperature readings were stable but trended slightly upwards. The warming effect of the environmental sensor was greater than in comparison with the test without trousers. This

steeper curve could indicate that the trousers are isolating, keeping your legs warm.

Phase 2: Walking (5-13 min)

The most critical observation occurred during the walking phase.

- Stability: In contrast to the uncovered test, no big temperature drop was observed. While the previous test showed a ~2.5 °C drop due to airflow, the skin sensors remained quite stable during this test.
- Damping effect: The trousers effectively acted as a windbreaker, shielding the sensors from the ambient airflow generated by the walking motion. The convective cooling effect was neutralised by the fabric layer.

Phase 3: Recovery (13-18 min)

Upon returning to a sedentary position, a heating effect was observed.

- Heat build-up: Both the skin sensors and the environment sensor showed a continuous rise. Which is expected as exercise increases skin temperature.
- Thermal lag: Unlike the uncovered test, where temperatures stabilised quickly, the enclosed environment sensor continued to heat up.

Conclusion of test 1b with trousers (comparison)

While wearing trousers successfully eliminates wind/motion artefacts (preventing the false "cooling" drops), it also introduces a thermal offset. The clothing traps heat, causing the sensors to read higher temperatures after a walk.

Test 2 with trousers

This test aimed to evaluate the impact of transitions between a controlled indoor environment and a colder outdoor environment while wearing long trousers (Figure 72). The outdoor temperature was about 2 °C.

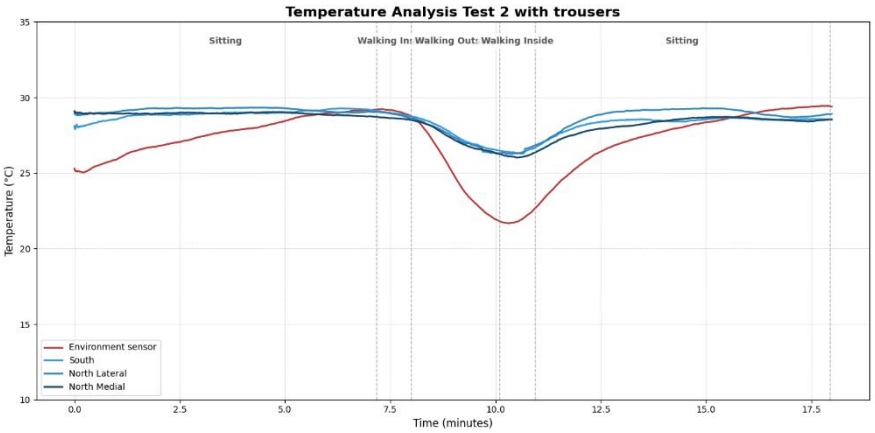

Figure 72: Results test 2 with trousers

Phase 1: Acclimatisation (0-7 min)

During the initial indoor sedentary phase, the environment sensor's behaviour was unchanged.

Phase 2: Transition and exposure (7-11 min)

At t=7 min, the subject walked outside. and a significant thermal event was recorded:

- Environment sensor: Reacted sharply to the cold outdoor air. The temperature dropped by approximately 7.5 °C, indicating that the trousers' fabric does not provide complete thermal isolation.
- Skin Sensors: Showed a drop in temperature following the environment sensor. This confirms that the cold external temperature physically cooled the skin surface and the wearable casing.
- This shows that big temperature changes, such as going outside, can be visualised and accounted for (when it is colder outside than inside).

Note on thermal lag: The graph shows that the lowest temperature occurs slightly after the walking outside phase marks, indicating thermal lag. It takes 1-2 minutes for the cold to fully penetrate the fabric and isolation.

Phase 3: Recovery (11-18 min)

Upon returning indoors and sitting down (t=11 min), the re-heating process began.

Conclusion of test 2 with trousers

This test demonstrates a correlation between the environment sensor and the skin sensors during temperature transitions. Although the environmental sensor is shielded by trousers, it detects the ingress of cold air. Crucially, the drop in skin

temperature was accompanied by a large drop in the environmental sensor reading.

- Implication: This validates the potential for algorithmic compensation. If the algorithm observes a simultaneous drop in skin temperature alongside the environmental sensor, it can classify the event as environmental influence rather than a physiological flare-up (which typically causes a rise in skin temperature). This, however, depends on the temperature outside. For this, the weather data could also be integrated in an improved analysis.

Test 3 without trousers

The objective of this test was to isolate the physiological heat production associated with physical exertion (active muscle use). To minimise the influence of trapped air, the subject wore shorts, leaving the wearable exposed (Figure 73).

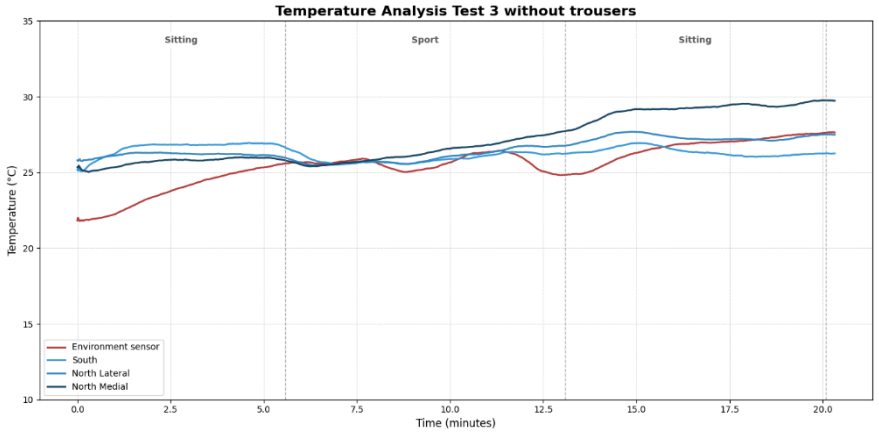

Figure 73: Results test 3 without trousers

Phase 1: Baseline (0-5.5 min)

During the initial acclimatisation, the sensors displayed the same pattern as in the sensors' stabilisation of test 1a.

Phase 2: Sport (5.5-13 min)

Upon the start of physical activity (squats/active movement), a trend was observed compared to the walking test without

trousers (test 1a). A cooling effect is observed, possibly due to the airflow, after which the temperature increases.

This indicates that the heat produced by the active leg muscles and the knee joint overwhelmed the convective cooling of the air. The internal heat generation was actively transferred to the skin surface.

Phase 3: Cooldown (13-20 min)

The most significant physiological response occurred after the exertion ceased. Instead of immediately cooling down, specifically the north medial skin temperature continued to rise sharply.

Thermal lag: This rise highlights the thermal inertia of the biological tissue. Heat generated deep within the muscles and joint capsule takes time to conduct to the skin surface.

Conclusion and literature context

The data of test 3 confirms that physical exertion increases local skin temperature, specifically in the medial knee region. This aligns with clinical findings, such as those by Marziani et al. (2023), who demonstrated that exercise induces significant thermal changes in the knee joint.

This indicates that the wearable is sufficiently sensitive to detect physiological warming (inflammation/activity) distinct from environmental heating. The fact that the temperature continued to rise during the cooldown (phase 3) can be a ‘’marker" that distinguishes it from a simple environmental fluctuation (which would drop immediately). However, this could also have been seen as a flare-up, indicating the need for analysis to determine what a flare-up is, could help.

Discussion

While the thermal validation provided critical insights into sensor behaviour and environmental influences, several limitations must be acknowledged when interpreting these results for future development:

- **Anatomical differences:** The tests were conducted on a single subject. Bodies vary significantly. The thickness of fat and muscle layers varies across body types. Resulting in different outcomes. This is not yet considered in these tests.
- **Clothing variability (loose vs. tight fit):** The tests involving clothing were performed using relatively loose-fitting trousers. Different fabrics (e.g., denim versus breathable sportswear) and fits (e.g., tight leggings) will alter the temperature around the knee. Tight clothing might press the environmental sensor more firmly against the skin or restrict airflow entirely, altering the results observed in these tests.
- **Lack of advanced data processing:** The current conclusions are based on visual analysis of average temperature trends. As this project focused on hardware integration and proof-of-concept validation, advanced data filtering (such as machine learning, sensor fusion, or baseline-correction algorithms) was not applied. A professional data analyst or software engineer is required to check or write robust algorithms that automatically filter out movement artefacts and environmental influences.
- **Exercise vs. pathology:** Test 3 successfully measured heat generated by physical exertion in a healthy knee. Because the tests were not conducted during an active clinical OA flare-up, the exact thermal signature of inflammation versus exercise remains a hypothesis that requires validation in a formal clinical trial.
- **Short test duration:** The test scenarios lasted approximately 20 minutes each. Continuous daily monitoring (16+ hours) involves long-term baseline shifts, such as the body's natural rhythm, hormonal temperature fluctuations, and extended periods of inactivity (e.g., sitting at a desk for hours), which these short-burst tests did not capture.

Conclusion

The series of thermal validation tests demonstrates that the integrated NTC sensors are sensitive and can capture subtle temperature changes on the skin surface. However, the data clearly show that continuous thermal monitoring in real-world, wearable settings is complex due to external and internal thermodynamic factors.

The tests highlight two primary conclusions:

- Trousers play a critical role in data stability. Without trousers, cooling (airflow from walking) could mask physiological heat generation. Trousers effectively neutralise this wind artefact

but introduce a thermal offset by trapping body heat, raising the baseline temperature during activity.

- The necessity of contextual data: The sensors successfully detected physiological warming (thermal lag) caused by physical exertion (test 3) and drops caused by outdoor exposure (test 2). However, an exercise-induced temperature spike could resemble an OA flare-up. Furthermore, environmental drops closely mimic changes in sensor contact. Therefore, raw temperature data alone is insufficient for OA monitoring. To make this data clinically relevant, the system requires compensation (using the environment sensor to account for weather changes) and activity tracking (using an IMU to distinguish between a sports session and an unprovoked inflammatory flare-up).

To accurately detect flare-ups, these factors need to be considered, and a way to describe a flare-up and how it translates into temperature needs to be found.

12.2 Desirability

The desirability is tested in two ways: first, tests with the feels-like model were done to validate comfort. Second, tests were conducted using the looks-like model to include patients' views.

12.2.1 Comfort design validation feels-like prototype

To validate the desirability and user requirements, a qualitative test trial was conducted using the looks-like model. The primary objective was to assess the user requirements and wishes as defined in the Define phase.

The test setup

5 participants were asked to wear the looks-like model for 4 hours, as this was the time required for the wearable to be comfortable and provide a reliable indication of full-day wear. This duration was sufficient to reveal pressure points, skin irritation, or discomfort. Beforehand, participants were not informed of potential discomfort to prevent priming bias; any feedback on comfort or irritation was elicited spontaneously.

Participants were instructed to wear the wearable during their regular daily activities without restrictions. After 4 hours, a structured interview was conducted to evaluate specific comfort criteria. The full questionnaire is provided in Appendix 14. To analyse a potential correlation between body type and wearable stability (e.g., potential slipping), anthropometric measurements (thigh and calf circumferences as described by Figure 74) were recorded for each participant.

Note: for this test, participants were asked to wear loose trousers so the wearable could be put on more easily without removing the trousers altogether; only the pants had to be rolled up.

Figure 74: Anthropometric measurements

Table 10: Participants of comfort tests

Participant	Gender	Thigh circumference in cm	Calf circumference in cm
1	Women	41	36
2	Women	44	37
3	Man	43,5	37.5
4	Man	44	35.5
5	Women	42	40

Results

A 4-hour wear test was conducted with 5 healthy participants (3 females, 2 males; thigh circumference ranging from 41–44 cm, and calf circumference from 35.7–40 cm, Table 10). The qualitative feedback and quantitative stability measurements were clustered into four key evaluation criteria:

General comfort and tactile adaptation

Overall, the wearables impression was positive. Participants described the main fabric as lightweight, unobtrusive, and breathable. Crucially, all five participants experienced rapid tactile adaptation; they reported completely forgetting they were wearing the wearable within 10 to 30 minutes of engaging in daily tasks. The open-hole design at the back of the knee allowed unhindered joint flexion. Furthermore, the wearables slim profile proved successful for daily integration, as it could be worn comfortably and discreetly under both loose and tighter trousers without chafing or severe visible outlines.

Stability and pressure points

While the main body of the textile was comfortable, the elastic bands introduced some challenges.

- **Skin irritation:** All 5 participants reported that the elastics were the most prominently present, which also resulted visually in mild red marks on the skin after the 4-hour period, though without severe irritation.
- **Slipping:** The vertical stability varied among participants. While three users experienced minimal migration (ranging from 1 cm on the lower elastic to 4 cm on the upper elastic), two users experienced noticeable downward slipping (with one instance of a 12 cm drop). Participants indicated that the top elastic band had insufficient grip compared to the bottom anti-slip band, making the top section feel less secure.

Usability and donning

The donning process was generally fast, taking participants between 15 and 30 seconds. Once they understood how the wearable worked, this went faster. The patella cutout and the hardware casing served as an effective, intuitive visual cue for correct top/bottom orientation. However, because the stretch fabric is extremely thin and lightweight, some users initially felt overly cautious, fearing they might tear the material or put their foot through the wrong holes.

Aesthetics and perceived quality

Aesthetically, the wearable was received as a sporty, cool, and modern product rather than a medical device, with users appreciating the black colour scheme. However, multiple users noted that the unrefined edges and still "flubbery" side panels detracted from the overall sense of quality.

Discussion

While the 4-hour wear test provided valuable ergonomic insights, two main limitations should be considered when interpreting the results:

- **Healthy subjects:** The five participants were healthy individuals without joint stiffness or reduced fine motor skills, which is common in patients with OA. Consequently, the positive "ease of donning" results (15–30 seconds) are not representative of the actual target demographic (OA patients).
- **Clothing constraints:** During the test, all participants wore relatively loose-fitting trousers. This does not reflect the full spectrum of everyday clothing. Testing the wearable under tighter garments could yield different results regarding visual discretion, fabric rolling, and potential pressure points caused by the hardware casing.

These limitations emphasise the necessity of conducting future wear tests directly with OA patients, ensuring that realistic mobility challenges and a wider variety of daily clothing are factored into the evaluation.

Conclusion

In conclusion, the 4-hour wear test validates the wearables comfort and positive human experience. The lightweight, breathable, and open-hole design successfully achieves comfortable wearability, discreet integration under clothing, and rapid tactile adaptation, allowing users to completely forget they are wearing the wearable within 30 minutes. Furthermore, the sporty, non-medical aesthetic was well-received, proving that the wearable is desirable for everyday use.

However, the test also clearly identifies a limitation in the current feels-like prototype. The elastic bands fail to provide consistent vertical stability, leading to downward slipping for some users. Ultimately, while the baseline comfort and visual identity are successful, future iterations must focus on improving the way the wearable is donned and on replacing the top elastic band with a more secure, adjustable closure system to ensure consistent stability and durability across various sizes, which may reduce redness and irritation around the elastics.

Key takeaways for future iterations

- **Closure redesign:** The elastic bands fail to provide reliable vertical stability and cause mild skin irritation. The design could transition to an adjustable closure system (such as a wrap-around with velcro as a closure mechanism) to secure the wearable, hopefully preventing slipping, and eliminating red marks from seams.
- **Material refinement:** To improve the perceived quality and prevent the fabric from feeling fragile or "flubbery" during donning, future iterations should investigate seamless edge-finishing techniques.
- **Visual cues for orientation:** The patella cutout and the hardware casing are successful, intuitive indicators for the correct top/bottom alignment. These visual cues should be preserved in future designs to ensure fast and easy donning.
- **Aesthetic validation:** The lightweight, breathable black fabric successfully balances a sporty look with discretion under clothing. This non-medical aesthetic encourages daily adoption and should remain the foundation of the wearables visual identity.

12.2.2 User validation looks-like visualisations, with OA patients

To evaluate the overall desirability of the concept, a qualitative online validation session was conducted with two patients diagnosed with OA (one male, one female). This semi-structured interview specifically assessed their willingness to use the design long-term, their aesthetic acceptance of the design, and any potential physical or psychological barriers to adoption. The validation session was systematically structured into the following phases:

1. Introduction and context: Explanation of the hypothesis (relationship between crepitus/inflammation and OA) and the purpose of the wearable.
2. First impression: Inventory of concerns prior to seeing the design.
3. Reveal: Presentation of the design with 3D renders via a PowerPoint, asking the respondent to share their “first thoughts” without explaining the functionality.
4. In-depth interview: Specific questions focused on comfort, the 16-hour scenario, visibility under clothing, attachment and a possible user interface (app).
5. Reflection: A concluding question about the ideal situation to reveal hidden desires.

Notes were taken during the session. The setup is in Appendix 15, along with the rough notes.

Results

The feedback highlighted insights specific to the end users, categorised into four key themes:

Motivation and visual acceptance

The patients were willing to wear the wearable long-term (up to 16 hours a day) if it delivers clear medical benefits. Pain prevention serves as the primary motivator; if the wearable can actively predict joint overload, users are committed to adopting it. Aesthetically, the sporty black design was preferred over "skin-coloured" alternatives, which were deemed visually unappealing. Furthermore, wearing the wearable under clothing was not considered an issue. Drawing comparisons to continuous glucose monitors for diabetes, the patients noted that visible bumps from the hardware casing are fully acceptable if the wearable is functional and non-irritating.

Usability and donning barriers

The most significant critique centred on the physical donning process. The current 'slip-on' sleeve design was identified as a major barrier for the OA patients, who frequently experience joint stiffness, reduced balance, and limited mobility. Patients expressed distinct concerns about their feet or toes getting caught in the cut-outs during application. To address this, they recommended transitioning to a 'wrap-around' design utilising

velcro or other closure systems to ensure accessible, stress-free donning.

Stability and ergonomic adjustability

While the visual renders appeared comfortable, patients raised practical concerns regarding gravity and material behaviour. They feared the concentrated weight of the hardware casing might cause the wearable to slip downward during walking. To mitigate this, they suggested positioning the casing lower on the leg. Additionally, a wrap-around solution was favoured because it allows for dynamic adjustability throughout the day, accommodating natural leg swelling or fabric stretching.

Data interaction and load management

Regarding a digital interface (app), users desired filtered, actionable insights. They specifically want to understand the correlation between major physical activities and subsequent joint overload to aid in daily activity management. While users are willing to manually input subjective pain scores after significant activities, they stressed that the system should not require input for minor, routine movements.

Discussion

The qualitative validation session with osteoarthritis (OA) patients provided crucial insights into user acceptance, but the following limitations must be acknowledged:

- **Small sample size:** The session was conducted with only two OA patients. While their feedback was detailed and valuable for this stage of prototyping, the small sample size limits the generalizability of the conclusions to the broader, diverse OA demographic.
- **Non-physical evaluation (render bias):** Because the validation was conducted online using 3D looks-like renders, participants could only evaluate the visual desirability and conceptual usability of the wearable. Since they did not physically hold or wear a prototype, their specific concerns regarding weight distribution (the casing slipping) or donning difficulties remain valid thoughts but lack physical verification.
- **Hypothetical acceptance:** The patients expressed a high willingness to wear the wearable daily, but this was strongly conditioned on the premise that the wearable can accurately predict pain or help with research. This value-driven acceptance is currently hypothetical and can be fully validated once a functional wearable demonstrates its reliability in a real-world clinical trial.

These limitations highlight the need for future physical wear tests specifically involving the OA target group, combining both the feels-like comfort and the works-like data validation in one integrated prototype.

Conclusion

All in all, it can be concluded that the target group (OA patients) is open to integrating the wearable into their daily lives, provided the ultimate “reward” is sufficiently high. Patients are willing to wear the wearable for long periods (up to 16 hours a day) and accept a casing outline or slight adjustments to their clothing if the wearable helps them prevent pain or support research. The acceptance of the product therefore stands or falls with its predictive medical added value; for this target group, pain reduction outweighs aesthetic or minor physical objections.

Key takeaways for future iterations

- **Closure redesign:** The slip-on sleeve must be replaced with an adjustable wrap-around mechanism, with, for example, velcro as a closing mechanism to accommodate for the reduced mobility of OA patients. Further, linking to the comfort testing where redness occurred, it is thought that these adjustments could help since the wearables tightness can be adjusted and personalised.
- **Hardware placement:** The electronics casing should be lowered or redistributed to lower the centre of gravity, which could further improve downward slipping.
- **Value proposition:** The digital ecosystem must focus on predictive load management, helping users prevent pain, rather than merely tracking data passively.
- **Aesthetic direction:** Maintain the black, functional "medical-sporty" look and actively avoid skin-mimicking colour palettes.

12.3 Viability

The viability assessment began with the creation of a comprehensive Bill of Materials (BOM). The financial model and the data acquired during the feasibility phase were presented to M. van Middelkoop for validation.

12.3.1 Bill of materials

The bill of materials is based on all components used in the works-like the prototype. However, two different acoustic sensors have been selected. The preferred sensor for later stages is smaller and more flexible but quite expensive. The cheaper option is larger but more affordable. Therefore, both are included for price considerations. The complete BOM is in Appendix 16.

The total cost for the wearable with the budget acoustic sensor is 74.29 Euros.

The total cost of the wearable with the preferred acoustic sensor is 130.19 Euros.

Note: For this cost estimation, only direct material costs (Bill of Materials) are considered. Expenses related to manufacturing, assembly labour, and operational overhead have not been included in this calculation.

12.3.2 Expert validation

The prepared questions and notes taken during the expert interview can be found in Appendix 17

The expert validated the technical foundation as a promising starting point. However, an estimated unit cost of around €250 (including production) requires a substantial budget for large clinical trials (e.g., €7,500 for a 30-wearable sample size). The expert concluded that the wearables financial viability is directly tied to its cost-benefit ratio within the healthcare system. If future iterations, supported by pattern-recognition algorithms for acoustic data, can successfully correlate sensor readings with subjective pain reports to predict early flare-ups, the wearable will easily earn back its initial investment through reduced healthcare interventions. The expert noted that a validation study might be needed to test whether temperature and acoustic data can also be evaluated subjectively, for example, by asking whether patients experience higher temperatures and crepitations throughout the day and whether they perceive pain. Furthermore, it was emphasised that a data analyst must thoroughly review the current dataset. The outcomes of these specific steps will ultimately determine whether further financial investment in the wearables development is justified.

13 Evaluation of requirements

This chapter evaluates the list of requirements and assesses the degree to which they have been fulfilled, and identifies remaining challenges and concerns shown in Table 11 and Table 12 on p. 149 and 150. Also, where needed, a recommendation is given for further iterations.

Table 11: User requirements evaluation and recommendations

User requirement (must)	Achieved/ Partially achieved/ Remaining concern	Scope	Rationale	Recommendation
UR-15 Freedom: The design allows for full functional knee flexion (up to 120°). With no mechanical support.	Achieved	**PoC** **Final**	During the 4-hour wear test, the main fabric stretched seamlessly and conformed to the knee's curvature. Participants experienced a full, unhindered range of motion due to the open-hole design at the back of the knee.	
UR-16 Adaptation: The user is unaware of the wearables physical presence after 60 minutes of wear.	Achieved	**PoC** **Final**	During the 4-hour wear test, all 5 participants experienced rapid tactile adaptation, reporting that they completely forgot they were wearing the wearable within 10 to 30 minutes of engaging in daily tasks.	
UR-17 Stability: The wearable shifts vertically by less than 1 cm after 4 hours of wear.	Remaining concerns	**PoC** **Final**	During the 4-hour test, vertical stability varied significantly among participants. While some experienced minimal migration, others experienced noticeable downward slipping (up to a 12 cm drop) due to the concentrated weight of the hardware casing and insufficient grip of the top elastic band.	Transition to an adjustable wrap-around strap system to ensure a secure, personalised fit. Additionally, apply a wider, stronger anti-slip silicone lining to both the top and bottom bands to prevent rolling and slipping.
UR-18 Weight: The wearable total weight does not exceed 100g.	Achieved	**PoC** **Final**	The electronic wearable weighs 30 grams.	Keep weight as low as possible
UR-19 Skin integrity: No visual redness or tissue damage after 4 hours of wear.	Remaining concern	**PoC** (For the Final, this will be 16 hours)	During the 4-hour comfort test, all 5 participants exhibited mild red marks around the upper and lower elastic bands, possibly due to using a single size for varying leg circumferences.	This can be solved by adding soft, velcro-adaptive straps. Individuals can adjust the wearable to their own size, reducing redness or stability issues.
UR-20 Thermal: Skin temperature under the wearable does not exceed the surrounding skin temperature by more than 2 °C at rest.	Partially achieved	**PoC** (For the Final, this needs to be reconsidered)	Although no tests were done specifically on the thermal degree. Participants in the comfort tests do not report additional warmth around the knee and state that the wearable is breathable.	Further research could be done on skin temperature.
UR-21 Biocompatibility: All skin-contact materials are hypoallergenic and do not cause skin reactions.	-	**Final** (No research is conducted on allergic reactions)		
UR-22 Hygiene/washability: The textile component of the wearable is machine-washable at 30°C without loss of structural integrity, provided the electronic module is removed.	-	**Final** (For now, out of scope)		
UR-23 Independence: An individual can correctly don the wearable independently, without external assistance, within 2 attempts.	Partially achieved	**PoC** (For the Final, individuals have to become OA patients)	Healthy users intuitively used the patella cut-out and the hardware casing as top/bottom visual cues. However, a concern is that in future iterations, the casing could be moved to the lower leg to prevent slipping, which will remove this natural 'top' indicator.	Integrate clear, visual indicators (e.g., a printed arrow or subtle texture difference) to guide orientation when the hardware casing is repositioned.
UR-24 Donning/doffing: The wearable can be put on correctly in 60 seconds and taken off in 30 seconds.	Partially achieved	**PoC** **Final**	During the wear test, 5 healthy users donned the wearable in 15–30 seconds. However, qualitative validation with 2 OA patients highlighted that the 'slip-on' sleeve design would not suffice for the target group, as fine motor skills are difficult.	Implement an open, wrap-around closure system. This removes the need to pull the wearable over the foot, eliminating the need for fine motor skills and flexibility.
UR-25 Concealability: The wearable fits under loose-fitting trousers.	Achieved	**PoC** (For the Final, it should fit under all sorts of trousers)	The 4-hour test confirmed the wearable fits comfortably and discreetly under different loose-fitting trousers. Furthermore, OA patients indicated that a slightly visible outline from the hardware casing is acceptable, compared to widely accepted continuous glucose monitors.	
UR-26 Discretion: The wearable makes no audible noise during walking. Also, no light goes through the trousers.	Achieved	**PoC** **Final**	The physical materials produce no audible friction noise to bystanders, and the fabric and trousers adequately shield the internal LED.	When integrating later, consider making the LED blink only to indicate when it's on or off. During the day, no light is seen.
UR-27 Shape retention: Materials do not deform or lose elasticity for 30 usage cycles.	Achieved	**PoC** (For the Final, more cycles must be achieved)	Throughout the technical and comfort validation phases, the prototype was donned, stretched, and doffed more than 30 times by multiple users without critical structural failure or loss of elasticity in the main fabric.	For long-term clinical trials, the use-cycle requirement should be increased to withstand months of daily wear and machine washing (requiring a detachable hardware module).
UR-28 Duration: Overall comfort remains valid for at least 4 hours of continuous wear.	Achieved	**PoC** (For Final comfort remains valid for 16 hours)	No participant notes the wearable uncomfortable after a 4 hour wear.	

Table 12: Technical requirements evaluation and recommendations

Technical requirement (must)		Achieved/ Partially achieved/ Remaining concern	Scope	Rationale	Recommendation
TR-1	**Continuous operation:** The hardware module operates reliably for a continuous 2-hour period during standard daily activities without failure.	Partially achieved	**PoC** (Final: continuous operation)	During controlled testing, the casing remained intact. However, during the 4-hour comfort test, participants reported that the casing bumped into tables (Participant 5). This indicates that the shock-absorbing properties required to protect the electronics during sustained daily collisions might need improvement.	The casing needs to be improved depending on the final hardware volume.
TR-2	**Assembly:** Electronic components and PCB footprints are suitable for manual soldering and handling.	Achieved	**PoC** (Final: this is not needed as automated fabrication is available)	All electronic components (XIAO, NTCs, SD module) were successfully assembled and hand soldered.	Transition to Surface Mount Technology (SMT) on a custom Printed Circuit Board (PCB) or a flexible PCB (FPC) to reduce volume, eliminate manual soldering errors, and enable scalable industrial fabrication.
TR-3	**Wiring flexibility:** Internal wiring connecting the PCB to the distributed sensors can withstand bending up to 120° without signal loss.	Achieved	**PoC Final**	The integrated conductive yarn ensures that the wearable remains flexible, allowing for 120 degrees of flexion.	
TR-4	**Data export**: Raw acoustic and thermal data can be analysed.	Achieved	**PoC Final**	Raw sensor data was successfully exported, processed and filtered via custom Python scripts, which applied basic filtering to visualise the thermal and acoustic data in readable, timestamped graphs.	
TR-5	**Data reliability and storage:** Data is accurate, reliable, and stored without loss.	Achieved	**PoC Final**	The proof-of-concept was equipped with a 16 GB microSD card. This storage amount was deemed sufficient for 48 hours in Chapter 8.5: Addition of SD card module. To ensure signal quality and prevent data corruption by avoiding dropped bytes, a custom packet structure was implemented. Each data block is prefixed with a Sync Word (0xAAAA) and a Sequence Number. This small synchronisation word has negligible storage and enables post-processing software to automatically detect and repair stream misalignments, ensuring that a single write error does not corrupt the entire recording session.	For the final wearable, it is recommended to use a store-and-forward strategy. where the wearable collects data throughout the day and, while charging, sends it via Wi-Fi to an app that doctors can access.
TR-6	**Acoustic placement:** The acoustic sensor is positioned below the centre of the patella on the medial or lateral side.	Achieved	**PoC Final**	The acoustic sensor is placed directly below the centre of the patella on the lateral side.	
TR-7	**Sampling rate:** For reliable data, the acoustic sampling frequency is at least 44.1 kHz.	Achieved	**PoC Final**	The acoustic sensor has a sampling rate of up to 48 kHz.	
TR-8	**Thermal range & accuracy:** The sensor captures 25-40 °C with a 1 °C resolution/accuracy.	Achieved	**PoC Final**	The integrated 10 kΩ NTC operates between -80 °C and 150 °C with an accuracy tolerance of ±0.9%. Mathematical conversion confirms a hardware measurement error of only ±0.225 °C. Data analysis confirmed 99.9% of acquired data fell well within the 1 °C resolution target.	
TR-9	**Physical fit:** For reliable data, the wearable provides a tight, skin-fit around the temperature sensors.	Achieved	**PoC Final**	The NTCs are integrated in places where skin contact can be retained.	
TR-10	**Insulation:** Thermal insulation is required over the temperature sensors.	Partially achieved	**PoC Final**	A layer of thermal insulation was integrated over the NTCs. However, the thermal validation tests (test 1 & 2) revealed that external environmental factors (such as wind or trousers) still significantly influence the readings, indicating that the current insulation is not yet fully optimised.	Conduct dedicated thermodynamic testing to determine the optimal thickness and material (e.g., neoprene or closed-cell foam) for the insulation patches, balancing protection against ambient air with the risk of creating artificial heat pockets.
TR-11	**Ambient reference:** An outward-facing, uninsulated external sensor continuously measures the ambient environmental temperature.	Achieved	**PoC Final**	An ambient sensor has been added to the wearable. So external factors can be visualised in the data.	
TR-12	**Battery life:** The battery supports at least 2 hours of continuous data logging.	Achieved	**PoC** (Final: 16-20 hours)	A power analysis of the 155 mAh LiPo battery, with continuous SD logging, yielded a theoretical 2.5 hours. During controlled endurance testing, the prototype achieved a continuous runtime of 1 hour and 55 minutes, safely enabling the 30-minute validation sessions.	To achieve the 16+ hour requirement for the final product, upgrade to a 1200 mAh battery (offline-first strategy) and implement IMU-based event-driven logging to conserve power.
TR-13	**Safety:** The battery is enclosed in a rigid, puncture-resistant casing and includes a Battery Management System for overcharge and thermal protection	Achieved	**PoC Final**	The LiPo battery is adequately protected, and the XIAO prevents overcharging.	
TR-14	**Recording feedback:** It must be explicitly clear to the user when the wearable is active and logging data.	Achieved	**PoC Final**	An onboard LED on the XIAO microcontroller provides basic visual confirmation when the wearable is actively logging data.	Ensure the LED only illuminates during setup or error states to prevent light bleeding through clothing during daily use, maintaining user discretion.

Overall, the evaluation of the user requirements, technical requirements, and wishes demonstrates that the Proof-of-concept (PoC) successfully validates the sensor functionality and baseline wearability. However, analysing the partially achieved and unachieved criteria reveals three critical areas that must be addressed before the wearable can be fully adopted as a daily medical wearable by OA patients:

1. **Ergonomics and accessibility:** The current 'slip-on' design could pose a physical barrier for patients with reduced mobility. Furthermore, the elastic bands create localised pressure points (mild redness) and do not consistently prevent the wearable from slipping down during active use.
2. **Hardware robustness and volume:** The casing is vulnerable to daily impacts (e.g., bumping onto furniture) and requires further improvement to be completely unobtrusive and comfortable under tight clothing.
3. **Power and data management for longitudinal use:** Transitioning from short-term proof-of-concept testing to continuous, full-day monitoring (16+ hours) requires an extended battery life.

These specific limitations form the foundation for the next design iteration. The actionable solutions to overcome these challenges, such as transitioning to a wrap-around closure, developing a custom PCB with casing, and implementing a store-and-forward data strategy, are discussed in the recommendations chapter.

14 Discussion

14.1 Final conclusion

To directly answer the design question formulated at the start of this project: **Yes, it is feasible to design a wearable proof-of-concept that technically validates non-invasive temperature and acoustic sensing at the knee for osteoarthritis patients.**

The development and evaluation of this prototype successfully demonstrated that the sensing technology can be integrated into a non-invasive, textile-based wearable. The custom acoustic signal processing algorithm proved capable of differentiating between a healthy joint and a symptomatic OA joint, most notably during controlled, loaded articulations such as the sit-to-stand exercise, where it detected distinct physiological crepitus. Similarly, the thermal sensors established a foundational method for capturing localised joint temperature, and the looks-like renders demonstrated that a wearable monitoring concept is generally well received by the target demographic.

However, while the technical validation of the sensor technology is a success, the current proof-of-concept is not yet a fully autonomous, market-ready clinical wearable. The testing phases revealed challenges. Continuous monitoring and clothing friction introduce mechanical artefacts that currently disrupt the acoustic data. Furthermore, the hardware casing requires further development, and the system's power management must be optimised for long-term use.

Ultimately, this project successfully achieved its goal: building and validating the foundational hardware, software, and physical wearable required to measure OA symptoms around the knee. To evolve this proof-of-concept into a robust, seamless, and patient-friendly medical wearable, extensive further development is required. The specific technical, ergonomic, and strategic next steps to achieve this are comprehensively outlined in the recommendations chapter on the next page.

14.2 Recommendations

14.2.1 Feasibility

Power consumption

To elevate the wearable from a short-term proof-of-concept to a wearable continuous, full-day monitoring (a minimum of 16 hours, with a 4-hour buffer), selecting the appropriate battery capacity is critical. The battery must provide sufficient energy to sustain continuous data collection while remaining small and lightweight.

To make an informed recommendation for this battery selection, a comprehensive power analysis was conducted (Table 13). The hardware's energy consumption was evaluated across various operational states to determine the most efficient data management strategy. The tested states included:

- Active SD card writing with continuous Wi-Fi transmission.
- No SD card module with continuous Wi-Fi transmission.
- No SD card programmed with continuous Wi-Fi transmission.
- No SD card programmed and Wi-Fi disabled.
- Active SD card writing with Wi-Fi disabled.

Corresponding code can be found in Appendix 18.

Table 13: Power consumption analysis

Time/Unit	SD writing/ Wi-Fi	No SD in the module/ Wi-Fi	No SD programmed/ Wi-Fi	No SD programmed/ No Wi-Fi	SD writing/ No Wi-Fi
- / Milli-Ampere (mAh)	140	100	100	40	60
10 min / (mAh)	23	16	16	7	10
1 hour (calculated) (mAh)	138	96	42	60	60
20 hours (calculated) (mAh)	2,760	1,920	1,920	840	1,200

Results

The analysis demonstrated that continuous data streaming via Wi-Fi is power-intensive and limits the wearables operational lifespan. Therefore, to work for 20 hour daily usage without an excessively bulky battery, it is recommended to adopt an offline-first data strategy.

Store and forward architecture

During daily use, the wearable should write only the collected sensor data to the onboard SD card, keeping the Wi-Fi module disabled. Data transmission and cloud synchronisation via Wi-Fi should be restricted to periods when the wearable is removed and connected to an external power source (e.g., during overnight charging). Based on this optimised power profile (active SD writing / No Wi-Fi), calculations show that a 1,200 mAh LiPo

battery is required to reliably achieve the 20-hour operational target while maintaining a manageable footprint for the user of approximately 65 × 35.5 × 5.2 mm.

Split cell battery

To improve wearability, a split-cell battery can be considered. Replacing the single rigid battery with two smaller 600 mAh cells to reduce bulk and better conform to the leg's natural curvature.

Movement integration

It is important to note that the current 1,200 mAh battery calculation assumes the worst-case scenario: continuous logging of both acoustic and thermal data. However, significant power optimisations can be achieved in future iterations by integrating a low-power motion sensor (e.g., an accelerometer or IMU) and turning the acoustic sensor on only when movement is detected. In addition, the low-power NTC sensor would remain active, continuously logging long-term thermal trends.

Stiffness detection and swelling monitoring

Furthermore, beyond power optimisation, integrating IMU's or other sensors that can detect movement offers substantial clinical value. Joint stiffness, particularly morning stiffness and a reduced range of motion, is also a symptom of OA. By continuously tracking knee kinematics, such as flexion angles, angular velocity, and overall patterns, an IMU could provide objective, quantitative data on this stiffness throughout the day. Consequently, incorporating a motion sensor would not only extend the wearables operational lifespan through event-driven logging but also lift its diagnostic potential by capturing another critical mechanical indicator of OA progression alongside crepitus and temperature.

Furthermore, as demonstrated by Ma et al. (2025), the integration of sensors to monitor joint swelling is another relevant parameter for OA management.

Custom PCB

The current prototype uses a XIAO ESP32S3 development board with an SD card breakout module. To achieve the required comfort and form factor, future iterations may transition to a custom Printed Circuit Board (PCB). The physical footprint can be reduced:

- Microcontroller: The ESP32-S3 chip (21 × 17.5 mm) can be mounted directly on the PCB.
- Storage: The bulky breakout board is replaced by a dedicated MicroSD slot (approx. 15 × 15 mm).

By positioning the microcontroller and SD slot efficiently, the total electronic footprint is estimated to fit within a 35 × 25 mm area (approximately the size of a postage stamp).

Improved casing

While the felt pouch casing was sufficient for proof-of-concept testing, it is not robust enough for unconstrained daily use. To transition from a functional prototype to a reliable medical wearable, the hardware enclosure will require further upgrades to match the improved hardware.

Sensor calibration

Currently, no acoustic and temperature sensors are calibrated. If they are calibrated, higher-quality raw data can be converted into standardised units, ensuring clinical validity.

Acoustic sensor recommendations

Given the severe acoustic interference caused by clothing and ambulatory movement, addressing mechanical artefacts will be the primary focus in future iterations. To formulate actionable solutions, the validation of some results was discussed with technical expert J.P.R. Thevenot. If J.P.R. Thevenot made a recommendation, a [2] is placed behind the heading.

Re-evaluating the monitoring strategy (continuous vs episodic)

Given the current limitations, future research must determine the optimal monitoring protocol. It may be more effective to shift from continuous, passive 16-hour monitoring to controlled, episodic assessments (e.g., performing a standardised sit-to-stand test twice a day without trousers). While this approach improves data reliability by eliminating friction artefacts entirely, it introduces a behavioural barrier (requiring active undressing and testing). Future studies must validate patient preferences regarding user compliance and align the chosen strategy with the specific data requirements of the medical research.

Hardware and material optimisation

To passively reduce noise before it even reaches the sensor, several physical redesigns are recommended based on expert feedback:

- **Friction-reducing materials [2]:** J.P.R. Thevenot highlighted that foam, now around the acoustic sensor, may not provide adequate acoustic dampening. Future iterations should conduct controlled rubbing tests using interface materials with varying tackiness and friction coefficients to identify the least "noisy" textile or silicone cover. Additionally, baseline noise generated by the user's specific type of trousers should be minimised or standardised during testing.

- **Microphone embedding [2]:** A physical isolation surrounding the microphone could be designed to better shield the component from external mechanical shocks.

Advanced data processing

To filter out the remaining noise, the software architecture must be upgraded:

- **Spectrogram analysis [2]:** is suggested by J.P.R. Thevenot, future data analysis should incorporate spectrogram plotting to gain deeper visual insights into the distinct frequency signatures of fabric rubbing versus physiological crepitus.
- **Adaptive noise cancellation:** Utilising an outward-facing reference microphone, Adaptive Noise Cancellation or Spectral Subtraction algorithms can be applied to actively subtract clothing noise from the primary joint recording.
- **Machine learning & on-board processing:** Transition from basic thresholding to Machine Learning models trained to distinguish specific friction patterns. Furthermore, basic signal filtering should be performed locally on the microcontroller (edge computing) to reduce data transmission and extend battery life.
- **Threshold adaptation:** In the methodology for detecting crepitations in the current proof-of-concept, the threshold value for detecting crepitations is statically determined based on the non-OA crepitations of individuals' data. However, this is not sufficient for future daily monitoring of osteoarthritis patients. Because both joint sounds and ambient sounds vary across patients in practice, further research is needed into personalised calibration and adaptive algorithms to achieve a reliable product.

Data privacy

Currently, the proof-of-concept records and stores raw audio files for analysing joint sounds. While this was useful for initial testing, it poses a privacy risk for a daily-wear wearable, as ambient sounds or private conversations could be recorded and reconstructed. To resolve this in a consumer-ready product, future iterations must implement computing protocols. Instead of saving raw audio files to an SD card, the microcontroller should process the acoustic signal in real-time, extract only the relevant numerical data (such as peak amplitude, frequency, and event timestamps), and immediately overwrite the audio. Furthermore, by logging only the mathematical features of the crepitus rather than the audio itself, the original sound cannot be recreated, thereby guaranteeing patient privacy and ensuring compliance with medical data regulations.

Thermal insulations

Further research is needed to determine the optimal insulation level for the NTCs in the wearable. Balancing protection against ambient air with the risk of creating artificial heat pockets.

14.2.2 Desirability

Wrap-around closure system

The current 'slip-on' sleeve design poses a physical barrier for OA patients with reduced mobility and joint stiffness and carries a risk of toes getting caught in the fabric cutouts. The next iteration must transition to an open, wrap-around design. This allows users to place the wearable directly onto the knee and secure it without pulling it over the foot.

Sizing and skin-friendly adjustability

To accommodate the diverse body types within the user group and prevent the slipping observed during the 4-hour test, the wearable should adopt a standardised sizing system (S, M, L) combined with adjustable straps. To address concerns about velcro causing skin irritation, the design must utilise skin-friendly velcro, placed exclusively on the exterior of the wearable, with a soft, seamless fabric backing (underlay) to ensure the rigid fasteners never make contact with the user's skin.

Optimised weight distribution

To counteract gravity-induced downward slipping caused by the hardware casing, the weight distribution should be optimised. Heavy or rigid components (such as the battery and microcontroller) should be relocated to the lower part of the leg, towards the upper calf, where the natural anatomy and the bottom anti-slip band provide more stability.

Hygiene

Because the wearable is intended for daily, long-term use (up to 16 hours a day), hygiene is critical. The design must feature a detachable electronic core. By housing the sensors and hardware in a removable, water-resistant module, the textile sleeve can be easily separated and hand-washed without damaging the technology.

Digital interfacing

Although the development of a functional User Interface (UI) fell outside the scope of this hardware-focused proof-of-concept, a clear digital strategy is essential for the final product vision. To bridge the gap between daily data collection and clinical interpretation, a dual-platform architecture is proposed: a patient-facing mobile application and a separate dashboard for clinicians and researchers.

Patient portal: The goal of the patient application is to gather subjective context to enrich the objective sensor data.

- **Symptom logging:** The app serves as a digital diary where patients can log subjective experiences such as pain intensity, stiffness, and perceived swelling. This allows researchers to correlate specific signal spikes (e.g., a temperature rise) with the patient's felt experience.
- **Activity and sports integration:** To distinguish between exercise-induced heat/crepitus and pathological flare-ups, the app must capture activity context. This can be achieved through:
  - **Manual tagging:** A simple interface to toggle "Exercise Mode."
  - **Ecosystem integration:** Connectivity with existing fitness platforms (e.g., Apple Health, Strava) to automatically timestamp physical activity.
- **Patient feedback:** While patients will not have access to the complex raw data, the app should provide simplified insights or "gamified" adherence statistics to maintain user engagement and motivation.

Researcher dashboard: The professional portal is designed for in-depth analysis and remote monitoring.

- **Raw data access:** Unlike the patient UI, clinicians have full access to the raw data (acoustic waveforms and temperature gradients) for detailed medical assessment.
- **Automated analysis tools:** To prevent information overload, the dashboard could feature built-in diagnostic algorithms. These tools will automatically flag anomalies, highlighting periods of statistically significant temperature increase or abnormal acoustic activity. This allows the medical professionals to focus on critical events rather than reviewing hours of data.

14.2.3 Viability

To ensure the wearable transitions successfully from a technical proof-of-concept to a viable, scalable medical product, future phases must prioritise clinical validation and environmental responsibility.

Clinical correlation study

Before investing in advanced software development or large-scale hardware manufacturing, a validation study is required. This study will not use the wearable prototype. Instead, the parameters could first be evaluated subjectively: patients should be asked to self-report their perceived pain, as well as their perceived localised knee temperature and joint sounds (crepitus). This subjective patient data must then be analysed to show clear OA flare-ups. Proving a strong, reliable correlation between what the patient subjectively feels or hears and the actual physical occurrence of a flare-up, only if this is the case, further development makes sense.

Sustainability

While environmental sustainability was excluded from the scope during the initial proof-of-concept phase to prioritise functional validation, it is a critical factor for commercial viability. Before transitioning to mass production, a comprehensive Life Cycle Assessment must be conducted. This assessment should evaluate the ecological footprint of the chosen electronics, batteries, and textiles, specifically identifying areas where material use can be reduced, modularity can be improved to facilitate easier recycling, and more sustainable manufacturing processes can be implemented.

14.3 Personal reflection

Looking back over the past six months, I realise how much I have learned throughout this process. When starting this project, I already had experience with textiles and sewing, so I expected the challenges to be mostly in programming and data interpretation. Developing skills in Arduino and Python had always interested me, but I had not found the time in previous projects. This graduation project was the perfect opportunity to focus on these skills. The learning curve was steep, but I learned a lot through trial and error, using Google Gemini to help write scripts and get the electronics working.

Building the prototypes and assembling the wearable, were the parts I enjoyed most. The biggest obstacle in this project was interpreting and visualising the data. In the Integrated Product Design programme, the focus is on the design process rather than detailed quantitative data analysis. As a result, mastering this skill and converting raw sensor data into clear, accurate graphs took me much time and effort.

The most important lesson I learned is insight into my own work method. I tend to act quickly, make fast decisions, and keep momentum. However, this project taught me that speed is not always possible or needed. I learned that accuracy and patience are crucial. Paying attention to small details is necessary to turn a creative idea into a reliable proof-of-concept.

All in all, I enjoyed working on this project, which gave me a lot of knowledge and independence, skills that I will certainly use in practice!

References

Alfieri, F. M., De Oliveira Vargas E Silva, N. C., Santos, A. C. a. D., & Battistella, L. R. (2020). Cutaneous temperature and pressure pain threshold in individuals with knee osteoarthritis. Reumatologia/Rheumatology, 58(5), 272–276. https://doi.org/10.5114/reum.2020.100195

Amers, E. L., Orme, B. V., Torun, H., Wood, D., Shi, Y., Nettleton-Parker, J., & Dodd, L. E. (2024). Conformable, wearable embroidered temperature sensors for Real-Time monitoring in extreme environments (p. 6). https://doi.org/10.3390/engproc2023052006

Arfaoui, A., Bouzid, M. A., Pron, H., Taiar, R., & Polidori, G. (2012). Application of Infrared Thermography as a Diagnostic Tool of Knee Osteoarthritis. Journal of Thermal Science and Technology, 7(1), 227–235. https://doi.org/10.1299/jtst.7.227

Artrose | ReumaNederland. (n.d.). https://reumanederland.nl/reuma/vormen-van-reuma/artrose

Artrose Gezond. (2025, September 12). Knieartrose - Artrose Gezond. https://artrosegezond.nl/knieartrose/

Batteries, C., & Batteries, C. (2025, October 31). Advanced Lithium Polymer Battery Safety Guide. CM BATTERIES. https://cmbatteries.com/nl/advanced-lithium-polymer-battery-safety-guide/

Bekaert. (n.d.). Metal fiber technology for smart textiles [Video]. Bekaert. https://www.bekaert.com/en/products/basic-materials/textile/e-textiles-/conductive-fibers-and-yarns-for-smart-textiles

Billings, J., Gee, J., Ghulam, Z., & Abdullah, H. A. (2024). Smart Compression Sock for Early Detection of Diabetic Foot Ulcers. Sensors, 24(21), 6928. https://doi.org/10.3390/s24216928

B. L. Pugliese, V. Civeriati, A. S. Tenforde, D. Demarchi and P. Bonato, "Detecting Exercise-Induced Temperature Distribution Changes at the Knee Using a Wearable Array of Thermistors," in IEEE Access, vol. 13, pp. 106759-106770, 2025, doi: 10.1109/ACCESS.2025.3581491.

keywords: {Temperature measurement;Temperature sensors;Thermistors;Biomedical monitoring;Temperature distribution;Monitoring;Cameras;Skin;Particle measurements;Graphical user interfaces;Digital health;heat distribution index;inflammation;knee osteoarthritis;thermistor array;wearable sensors},

Boeijen, A., Daalhuizen, J., & Zijlstra, J. (2020). Delft Design Guide : Perspectives - Models - Approaches - Methods. https://research.tudelft.nl/en/ publications/delft-design-guide-perspectives-models-approaches-methods

Brito, C. J., Miarka, B., García-Pastor, T., Pérez, D. I. V., Marins, J. C. B., & Sillero-Quintana, M. (2020). Osteoarthritis subjects have differentiated lower extremity thermal skin response after the concurrent acute training session. Journal of Thermal Analysis and Calorimetry, 145(5), 2467–2475. https://doi.org/10.1007/s10973-020-09827-0

Chen, W., Dols, S., Oetomo, S. B., & Feijs, L. (2010). Monitoring body temperature of newborn infants at neonatal intensive care units using wearable sensors (pp. 188–194). https://doi.org/10.1145/2221924.2221960

Cho, Y., Jeong, S., Kim, H., Kang, D., Lee, J., Kang, S., & Kim, J. (2021). Disease-modifying therapeutic strategies in osteoarthritis: current status and future directions. Experimental & Molecular Medicine, 53(11), 1689–1696. https://doi.org/10.1038/s12276-021-00710-y

De Marziani, L., Boffa, A., Angelelli, L., Andriolo, L., Di Martino, A., Zaffagnini, S., & Filardo, G. (2023). Infrared Thermography in Symptomatic Knee Osteoarthritis: Joint Temperature Differs Based on Patient and Pain Characteristics. Journal of Clinical Medicine, 12(6), 2319. https://doi.org/10.3390/jcm12062319

De Marziani, L., Boffa, A., Orazi, S., Andriolo, L., Di Martino, A., Zaffagnini, S., & Filardo, G. (2023). Joint Response to Exercise Is Affected by Knee Osteoarthritis: An Infrared Thermography Analysis. Journal of Clinical Medicine, 12(10), 3399. https://doi.org/10.3390/jcm12103399

De Marziani, L., Zanasi, L., Roveda, G., Boffa, A., Andriolo, L., Di Martino, A., Zaffagnini, S., & Filardo, G. (2024). Symptoms and joint degeneration correlate with the temperature of osteoarthritic knees: an infrared thermography analysis. International Orthopaedics, 49(1), 101–108. https://doi.org/10.1007/s00264-024-06376-1

De Oliveira Vargas E Silva, N. C., Anjos, R. L. D., Santana, M. M. C., Battistella, L. R., & Alfieri, F. M. (2020). Discordance between radiographic findings, pain, and superficial temperature in knee osteoarthritis. Reumatologia/Rheumatology, 58(6), 375–380. https://doi.org/10.5114/reum.2020.102002

Denoble, A. E., Hall, N., Pieper, C. F., & Kraus, V. B. (2010). Patellar Skin Surface Temperature by Thermography Reflects Knee Osteoarthritis Severity. Clinical Medicine Insights Arthritis and Musculoskeletal Disorders, 3, CMAMD.S5916. https://doi.org/10.4137/cmamd.s5916

Faisal, A. I., Majumder, S., Scott, R., Mondal, T., Cowan, D., & Deen, M. J. (2020). A simple, Low-Cost Multi-Sensor-Based smart wearable knee monitoring system. IEEE Sensors Journal, 21(6), 8253–8266. https://doi.org/10.1109/jsen.2020.3044784

Fraden, J. (2016). Handbook of modern sensors: physics, designs, and applications. Choice Reviews Online, 53(10). https://doi.org/10.5860/choice.195891

Garmin. (n.d.). Forerunner® 255 Music. Retrieved from https://www.garmin.com/nl-NL/p/780196/#specs

GBD Compare. (n.d.). Institute for Health Metrics and Evaluation. https://vizhub.healthdata.org/gbd-compare/

Gefen, A. (2008, October). How much time does it take to get a pressure ulcer? Integrated evidence from human, animal, and in vitro studies. *PubMed*. Retrieved from https://pubmed.ncbi.nlm.nih.gov/18927481/

Halmandge, A. M., Malik, R., Sarawagi, R., & Sharma, J. (2024). Comparison of MRI Osteoarthritis Knee Score with Clinico-Radiological Grading. Indian Journal of Radiology and Imaging - New Series/Indian Journal of Radiology and Imaging/Indian Journal of Radiology & Imaging, 35(01), 073–080. https://doi.org/10.1055/s-0044-1789230

Home | Sensemodi. (n.d.). Sensemodi. https://www.sensemodi.com/

Hunter, D. J., & Bierma-Zeinstra, S. (2019). Osteoarthritis. The Lancet, 393(10182), 1745–1759. https://doi.org/10.1016/s0140-6736(19)30417-9

Hunter, D. J., McDougall, J. J., & Keefe, F. J. (2008). The Symptoms of Osteoarthritis and the Genesis of Pain. Rheumatic Disease Clinics of North America, 34(3), 623–643. https://doi.org/10.1016/j.rdc.2008.05.004

Karpiński, R., Prus, A., Jonak, K., & Krakowski, P. (2024). Vibroarthrography as a Noninvasive Screening Method for Early Diagnosis of Knee Osteoarthritis: A Review of Current Research. Applied Sciences, 15(1), 279. https://doi.org/10.3390/app15010279

Katz, J. N., Arant, K. R., & Loeser, R. F. (2021). Diagnosis and Treatment of Hip and Knee Osteoarthritis. JAMA, 325(6), 568. https://doi.org/10.1001/jama.2020.22171

Knight, J. F., & Baber, C. (2005). A Tool to Assess the Comfort of Wearable Computers. Human Factors the Journal of the Human Factors and Ergonomics Society, 47(1), 77–91. https://doi.org/10.1518/0018720053653875

Knipe, H. (2020). MRI Osteoarthritis Knee Score (MOAKS). Radiopaedia.org. https://doi.org/10.53347/rid-74955

Kohn, M. D., Sassoon, A. A., & Fernando, N. D. (2016). Classifications in Brief: Kellgren-Lawrence Classification of Osteoarthritis. Clinical Orthopaedics and Related Research, 474(8), 1886–1893. https://doi.org/10.1007/s11999-016-4732-4

Korzelius, E. K. (2013). Gewrichts slijtage: veerkrachtig door het leven. AnkhHermes.

Kovats, A., Jones, M. D., Azzi, A., Ho, D. S. F., Ram, A., & Thom, J. M. (2024). Exercise on Crepitus in Knee Osteoarthritis: A Systematic Review and Meta-Analysis. Journal of Clinical Exercise Physiology, 13(4), 112–122. https://doi.org/10.31189/2165-6193-13.4.112

Leroux, F. (2025, March 9). Why Garmin's smartwatch battery life is so much better compared to Android watches. Android Police. https://www.androidpolice.com/why-do-garmin-batteries-last-so-much-longer/

Lo, G. H., Strayhorn, M. T., Driban, J. B., Price, L. L., Eaton, C. B., & Mcalindon, T. E. (2017). Subjective Crepitus as a Risk Factor for Incident Symptomatic Knee Osteoarthritis: Data From the Osteoarthritis Initiative. Arthritis Care & Research, 70(1), 53–60. https://doi.org/10.1002/acr.23246

Loeser, R. (2009). Aging and osteoarthritis: the role of chondrocyte senescence and aging changes in the cartilage matrix. Osteoarthritis and Cartilage, 17(8), 971–979. https://doi.org/10.1016/j.joca.2009.03.002

Lugoda, P., Costa, J. C., Oliveira, C., Garcia-Garcia, L. A., Wickramasinghe, S. D., Pouryazdan, A., Roggen, D., Dias, T., & Münzenrieder, N. (2019). Flexible Temperature Sensor Integration into E-Textiles Using Different Industrial Yarn Fabrication Processes. Sensors, 20(1), 73. https://doi.org/10.3390/s20010073

Ma, Z., Fang, L., Fang, C., Chen, F., Xing, S. P., Chai, B., Zheng, Z., & Wang, S. J. (2025). Intelligent wearable system design for personalized knee motion and swelling monitoring in osteoarthritis care. Cell Reports Physical Science, 6(3), 102438. https://doi.org/10.1016/j.xcrp.2025.102438

Majumder, S., Mondal, T., & Deen, M. (2017). Wearable Sensors for Remote Health Monitoring. Sensors, 17(1), 130. https://doi.org/10.3390/s17010130

McKnight, M., Agcayazi, T., Ghosh, T., & Bozkurt, A. (2018). Fiber-Based Sensors. In Elsevier eBooks (pp. 153–171). https://doi.org/10.1016/b978-0-12-811810-8.00008-7

NICE. (2022, October 19). Overview | Osteoarthritis in over 16s: diagnosis and management | Guidance | NICE. https://www.nice.org.uk/guidance/ng226

Niedermann, R., Wyss, E., Annaheim, S., Psikuta, A., Davey, S., & Rossi, R. M. (2013). Prediction of human core body temperature using non-invasive measurement methods. International Journal of Biometeorology, 58(1), 7–15. https://doi.org/10.1007/s00484-013-0687-2

Onajite, E. (2013). Understanding Sample Data. In Elsevier eBooks (pp. 105–115). https://doi.org/10.1016/b978-0-12-420023-4.00008-3

Parry, E., Ogollah, R., & Peat, G. (2019). ‘Acute flare-ups’ in patients with, or at high risk of, knee osteoarthritis: a daily diary study with case-crossover analysis. Osteoarthritis and Cartilage, 27(8), 1124–1128. https://doi.org/10.1016/j.joca.2019.04.003

Pazzinatto, M. F., De Oliveira Silva, D., Faria, N. C., Simic, M., Ferreira, P. H., De Azevedo, F. M., & Pappas, E. (2018). What are the clinical implications of knee crepitus to individuals with knee osteoarthritis? An observational study with data from the Osteoarthritis Initiative. Brazilian Journal of Physical Therapy, 23(6), 491–496. https://doi.org/10.1016/j.bjpt.2018.11.001

Petrigna, L., Amato, A., Roggio, F., Trovato, B., & Musumeci, G. (2024a). Thermal threshold for knee osteoarthritis people evaluated with infrared thermography: a scoping review. Journal of Thermal Biology, 123, 103932. https://doi.org/10.1016/j.jtherbio.2024.103932

Pinskerova, V., Samuelson, K. M., Stammers, J., Maruthainar, K., Sosna, A., & Freeman, M. a. R. (2009). The knee in full flexion. Journal of Bone and Joint Surgery - British Volume, 91-B(6), 830–834. https://doi.org/10.1302/0301-620x.91b6.22319

Polanský, R., Soukup, R., Řeboun, J., Kalčík, J., Moravcová, D., Kupka, L., Švantner, M., Honnerová, P., & Hamáček, A. (2017). A novel large-area embroidered temperature sensor based on an innovative hybrid resistive thread. Sensors and Actuators a Physical, 265, 111–119. https://doi.org/10.1016/j.sna.2017.08.030

Queiroga, F., Cross, M., Thomas, M. J., March, L., Epstein, J., & Guillemin, F. (2023a). A scoping review of patient self-report measures of flare in knee and hip osteoarthritis (OA): A report from the OMERACT flares in OA working group. Seminars in Arthritis and Rheumatism, 63, 152281. https://doi.org/10.1016/j.semarthrit.2023.152281

Reuma Nederland. (2025, March 13). Wat gebeurt er in je gewricht bij artrose? Artrose | Reuma.nl. https://www.reuma.nl/over-reuma/vormen-van-reuma/artrose/wat-gebeurt-er-in-je-gewricht-bij-artrose

RS PRO Thermistor, 10kΩ Resistance, NTC Type, 2.4 x 63.5mm | RS. (n.d.). https://nl.rs-online.com/web/p/thermistor-ics/0151237?gb=s

Schiphof, D., Van Middelkoop, M., De Klerk, B., Oei, E., Hofman, A., Koes, B., Weinans, H., & Bierma-Zeinstra, S. (2014). Crepitus is a first indication of patellofemoral osteoarthritis (and not of tibiofemoral osteoarthritis). Osteoarthritis and Cartilage, 22(5), 631–638. https://doi.org/10.1016/j.joca.2014.02.008

Selfe, J., Hardaker, N., Whitaker, J., & Hayes, C. (2007). Thermal imaging of an ice burn over the patella following clinically relevant cryotherapy application during a clinical research study. Physical Therapy in Sport, 8(3), 153–158. https://doi.org/10.1016/j.ptsp.2007.04.001

Soukup, R., Hamacek, A., Mracek, L., & Reboun, J. (2014). Textile based temperature and humidity sensor elements for healthcare applications (Vol. 143, pp. 407–411). https://doi.org/10.1109/isse.2014.6887634

Stoppa, M., & Chiolerio, A. (2014). Wearable Electronics and Smart Textiles: A Critical Review. Sensors, 14(7), 11957–11992. https://doi.org/10.3390/s140711957

Teague, C. N., Heller, J. A., Nevius, B. N., Carek, A. M., Mabrouk, S., Garcia-Vicente, F., Inan, O. T., & Etemadi, M. (2020). A wearable, multimodal sensing system to monitor knee joint health. IEEE Sensors Journal, 20(18), 10323–10334. https://doi.org/10.1109/jsen.2020.2994552

Teague, C. N., Hersek, S., Toreyin, H., Millard-Stafford, M. L., Jones, M. L., Kogler, G. F., Sawka, M. N., & Inan, O. T. (2016). Novel methods for sensing acoustical emissions from the knee for wearable joint health assessment. IEEE Transactions on Biomedical Engineering, 63(8), 1581–1590. https://doi.org/10.1109/tbme.2016.2543226

Thomas, M. J., Guillemin, F., & Neogi, T. (2022). Osteoarthritis Flares. Clinics in Geriatric Medicine, 38(2), 239–257. https://doi.org/10.1016/j.cger.2021.11.001

Thomas, M. J., Yu, D., Nicholls, E., Bierma-Zeinstra, S., Conaghan, P. G., Stoner, K. J., Neogi, T., Parry, E. L., & Peat, G. (2019). Short-Term Recovery Trajectories of Acute Flares in Knee Pain: A UK-Netherlands Multicenter Prospective Cohort Analysis. Arthritis Care & Research, 72(12), 1687–1692. https://doi.org/10.1002/acr.24088

Togawa, T. (1985). Body temperature measurement. Clinical Physics and Physiological Measurement, 6(2), 83–108. https://doi.org/10.1088/0143-0815/6/2/001

Toreyin, H., Jeong, H. K., Hersek, S., Teague, C. N., & Inan, O. T. (2016). Quantifying the consistency of wearable knee acoustical emission measurements during complex motions. IEEE Journal of Biomedical and Health Informatics, 20(5), 1265–1272. https://doi.org/10.1109/jbhi.2016.2579610

Yao, Q., Wu, X., Tao, C., Gong, W., Chen, M., Qu, M., Zhong, Y., He, T., Chen, S., & Xiao, G. (2023). Osteoarthritis: pathogenic signaling pathways and therapeutic targets. Signal Transduction and Targeted Therapy, 8(1). https://doi.org/10.1038/s41392-023-01330-w